Studies on Extraction and Purification of Rebaudioside-A and Dehydration of Aloe Vera Gel

A Thesis

Submitted in Partial Fulfilment of the Requirements

for the Degree

of

DOCTOR OF PHILOSOPHY

By

Arijit Das

Department of Chemical Engineering

Indian Institute of Technology Guwahati

Assam, India

June 2016

This work is dedicated to my parents for their love, support, and patience which motivated me to carry out this research work

Content

Declaration

I hereby declare that the work embodied in this thesis entitled **'Studies on Extraction and Purification of Rebaudioside-A and Dehydration of Aloe Vera Gel'** is the outcome of my investigations carried out under the supervision of **Dr. Chandan Das** and **Dr. Animes Kumar Golder**, Department of Chemical Engineering, Indian Institute of Technology Guwahati, Assam, India, for the award of the degree of Doctor of Philosophy. This work has not been submitted elsewhere for any degree to the best of my knowledge and belief.

Date:

Place: Guwahati

Arijit Das
(Roll No. 10610703)
Department of Chemical Engineering
IIT Guwahati
Guwahati-781 039, Assam, India

भारतीय प्रौद्योगिकी संस्थान गुवाहाटी
Indian Institute of Technology Guwahati

भारतीय प्रौद्योगिकी संस्थान गुवाहाटी
गुवाहाटी ७८१ ०३९, असम, भारत
Indian Institute of Technology Guwahati
Guwahati 781 039, Assam, India

CERTIFICATE

It is certified that the thesis entitled "**Studies on Extraction and Purification of Rebaudioside-A and Dehydration of Aloe Vera Gel**", being submitted to the **Indian Institute of Technology Guwahati** by **Arijit Das** (Roll No. 10610703) for the award of the degree of **Doctor of Philosophy** in **Chemical Engineering**, is a bona fide record of research work carried out by him under our guidance and supervision. This work has not been submitted elsewhere for any degree or diploma.

Dr. Chandan Das
Associate Professor
Department of Chemical Engineering
Indian Institute of Technology Guwahati
Gwahati-781 039, Assam, India
Coordinating Supervisor

Dr. Animes Kumar Golder
Associate Professor
Department of Chemical Engineering
Indian Institute of Technology Guwahati
Guwahati-781 039, Assam, India
Co-Supervisor

भारतीय प्रौद्योगिकी संस्थान गुवाहाटी
Indian Institute of Technology Guwahati

Acknowledgements

Starting from the very first day at IIT Guwahati till the completion of my Doctoral degree, I will cherish all the wonderful moments that I was blessed with. As we all know, time flies by in the blink of an eye. I can still very well remember the drizzling morning of my first day in this beautiful campus. The high hills with foggy peaks, the Mighty Bramhaputra, the greenery, chirps of various birds and insects made me fall in love with the campus at the very beginning. Wherever I go in the coming days, these memories will always remain close to my heart. IIT Guwahati, my first home for the last six years, has provided me the platform to achieve my goals and make my dreams come true. I am indeed thankful to IIT Guwahati for giving me the chance to meet so many delightful persons, without their presence I would not have been here today. It is really difficult to express my gratefulness in a just few words, but here, is my modest attempt.

At the very beginning, I would like to thank my supervisors, Dr. Chandan Das and Dr. Animes Kumar Golder, for giving me the opportunity to work under their guidance. I am highly grateful for their continuous support, valuable suggestions, constructive criticism and most importantly, for providing a homely environment in my working place. Every day, the morning lab-visit started with the inspiring enquiry by Golder sir, “What is going on, Arijit?” which boosted me to work sincerely throughout the day. Das sir always advised to learn something out of the concise-concepts and also to implement them in various aspects of the research-work.

I also extend my sincere gratitude to my doctoral committee members, Prof. Kaustubha Mohanty, Dr. Vaibhav V. Goud and Prof. Pranab Kumar Ghosh for their valuable suggestions at various stages, which enabled me to work better. I again thank Prof. Mohanty sir for inspiring me regarding both professional and personal matters.

I would like to thank the staff members of the Chemical Engineering Department, specially, Dr. Lukumani Borah, Mr. Jayanta Kumar Mout, Mr. Balen Chandra Mahanta, Mrs. Ritumoni Kalita, Mr. Harsaraj Biswanath, Mr. Pankaj Sekhar Baruah, Mr. Deep Jyoti Sinha and Mr. Sailen Das for their help and cooperation in my entire PhD tenure. I am grateful to the staffs of Central Instruments Facility of IIT Guwahati for providing the analytical facility of my research.

I sincerely thank my lab mates cum friends Mahesh bhai, Vijay ji, Giri da, Raj kumar, Sujoy, Suman, Venkata, Kibrom and Amit Baran, for providing a healthy and cheerful work environment. I thank Mahesh bhai, Vijay ji and Giri da for showing sympathetic behavior towards my problems. I am also thankful to my senior research scholars, Dr. Debasish Ghosh, Dr. Somen Jana, and Dr. Soumya Sasmal for their useful tips, friendly behavior and assistance.

Moving ahead of research, I would like to thank a priceless person of my life, Prasanta, a friend cum brother. Your support, opinion and, inspiration in every critical junction are the only thing which gave me strength to move ahead. I won't ever forget the love, care and affection I got from you. I will always cherish the moments spent with you. Next, I owe my gratitude to Rimel, for her charming presence and encouragement. Life would have been absolutely different if I had not met with her.

I treasure my friendship with Saptarshi, Sabyasachi, Chitrita, Anirban, Dilip, Hanif, Amit, Soumyadeep, Abu, Manab da, Rakesh, Aniket, Turjya, Vinay, Digar, Sanjib da, Avik, Kamal, Santhi Raju, Manish, Sankar, Suman, Medhi, Ashim, Anil, Romen, Afsana, Shailendra, Rajeev, Raju and many more to be listed. Special thanks to Abhradip and Diptadeep for assisting me in some part of my experimental works.

I am also obliged to express my humble regards and respect to my parents, my grandmother, who is no more with us and my *mama* and *mami* for their blessing and moral

support. Special thanks to my elder sister and Sanjib da for performing my responsibilities while I was away from home.

At last, I thank the Almighty for blessing me what I am today with such wonderful parents and friends.

Arijit Das

भारतीय प्रौद्योगिकी संस्थान गुवाहाटी
Indian Institute of Technology Guwahati

Abstract

This work comprises of two parts. In the first part, extraction and purification of rebaudioside A from 'Stevia' leaves were studied using water as a green solvent. The second part covered the dehydration of aloe vera gel using hot air, microwave, and hybrid drying techniques.

Stevia rebaudiana (Bertoni) is a medicinal herb which contents eight sweet-tasting glycosides. Among which rebaudioside-A (Reb-A) is the most predominant, having the sweetening potential of about 450 times as compared to the sucrose solution (0.4 % w/v). Reb-A is proposed as a future alternative to sugar. But the challenges lie in its extraction and purification processes due to its lesser quantity in the leaves.

The present work studied the extraction of Reb-A using water as a green solvent. The effect of extraction parameters, namely, extraction time, leaves to water ratio, and temperature on Reb-A recovery was investigated. It was noted that at higher leaves to water ratio, the extraction efficiency of Reb-A was reduced with the progress of extraction time. Reb-A decomposition was comparable with the enhancement of its recovery at a higher temperature. Response surface methodology (RSM) was applied to optimize the extraction process along with the Artificial Neural Network (ANN) modeling. The optimum extraction time was found as 51 min for a leaves to water ratio of 2.36 % at 71°C by which 73.12 % Reb-A recovery was achieved.

Membrane based separation study using ultrafiltration (UF) membrane for the purification of Reb-A in both batch and cross-flow setups was performed. The selection of UF membrane was made in terms of its transient flux decline and Reb-A recovery. The effects of transmembrane pressure drop (TMP) and feed flow velocity on color, clarity, total solids, purity, and selectivity were investigated in detail in the cross-flow ultrafiltration. TMP drop of 414 kPa and *Re* number of 1667 were found to be most suitable operative conditions

with the selectivity of 0.45 and flux value of 5.86×10^{-6} $m^3m^{-2}s^{-1}$ for 30 kDa UF membrane. The Hermia's fouling models modified by Field for cross flow membrane set up were tested to the entire range of flux decline data and the cake filtration showed the best fitting (R^2=0.96-0.98) under the whole operating conditions.

Aloe vera (*Aloe barbadensis* Miller) is a perennial herb which is nowadays a prime concern of many researchers for its intense immune-therapeutic benefit. The process of dehydration of aloe vera gel often fails to retain its physico-chemical properties in the dried aloe vera gel. This part of the works proposes microwave-assisted drying (MWAD) and hybrid drying processes of aloe vera gel instead of a single prolonged drying method. The performance of MWAD and four proposed hybrid drying processes, *i.e.*, centrifugation followed by freeze drying (CFFD), microwave followed by freeze drying (MWFFD), centrifugation followed by HAD (CFHAD) and microwave followed by hot air drying (MWFHAD) had been evaluated in terms of its carbohydrate and protein contents, and functional properties of dried aloe vera gel. Among all drying techniques, CFFD, and CFHAD showed the highest carbohydrate and protein retention of 91.8, 82.3 % and 90.9, 85.6 %, respectively.

Further, in MWAD, the influence of three independent parameters, namely, microwave power, gel quantity and drying time on moisture ratio was investigated. A 'two level' face-centered central composite design (FCCD) developed a multivariate regression model to evaluate their effects on the moisture ratio. The optimal MWAD condition was established as 49.82 W g^{-1} power density and 5.78 min of drying time corresponding to the moisture ratio of 0.15. An ANN model of 3-5-1 neural network architect with the 'Levenberg-Marquardt backpropagation' algorithm showed the best prediction of the output response. Finally, eight drying kinetic models were tested to study the behavior of MWAD of aloe vera gel. Two term model was the best fitted with the effective moisture diffusivities

ranges from 2.025×10^{-6} to 7.087×10^{-6} m^2 s^{-1} and, the drying efficiency was found to vary from 50.8 to 68.7 %.

Keywords: Stevia extract; Rebaudioside-A; Solvent extraction; Ultrafiltration; Permeate flux; Response Surface Methodology; Artificial Neural Network; Fouling models; Aloe vera gel; Dehydration processes; Microwave-assisted drying; Hybrid drying techniques; Physico-chemical properties; Kinetics models; Moisture diffusivity; Drying efficiency

Abbreviation

AAD	Absolute average deviation
ANN	Artificial neural network
CCCD	Circumscribe central composite design
CCD	Central composite design
CF	Cake filtration
CFFD	Centrifugation followed by freeze drying
CFHAD	Centrifugation followed by hot air drying
CPB	Complete pore blocking
d.m	Dry matter
DI	Deionized
FAC	Fat adsorption capacity
FD	Freeze drying
HAD	Hot air drying
HMW	High molecular weight
IPB	Intermediate pore blocking
LMW	Lower molecular weight
MR	Moisture ratio
MWAD	Microwave-assisted drying
MWCO	Molecular weight cut off
MWFFD	Microwave followed by freeze drying
MWFHAD	Microwave followed by hot air drying
PES	Polyethylene sulfone
Re	Reynolds number
Reb-A	Rebaudioside-A
RMSE	Root mean square error
RSM	Response surface methodology
SPB	Standard pore blocking
TMP	Trans-membrane pressure
TS	Total solids
WRC	Water retention capacity

Nomenclature

A	Optical absorbance
A_s	Peak area for stevioside from the standard solution
A_x	Peak area of steviol glycoside for the sample solution
D_{eff}	Effective diffusion coefficient ($m^2\ s^{-1}$)
D_H	Hydraulic diameter (m)
f_x	Ratio of the formula weight of steviol glycoside to the formula weight of stevioside
J	Permeate flux ($m^3\ m^{-2}\ s^{-1}$)
J_0	Initial permeate flux ($m^3\ m^{-2}\ s^{-1}$)

J_{lim}	Limit value of the permeate flux attained in steady-state conditions ($m^3\ m^{-2}\ s^{-1}$)
k_2	Complete pore blocking model constant (s^{-1})
k_s	Standard pore blocking model constant ($m^{-0.5}\ s^{-0.5}$)
G	Cake filtration model constant ($s\ m^{-2}$)
m	Gel quantity (g)
P	Microwave power (W)
R^2	Regression coefficient
$\mathcal{R}$	Leaves to water ratio (g per 100 mL water)
t	Extraction time (min) or Drying time (min)
T	Temperature (°C)
V	Volumetric flow rate ($m^3\ s^{-1}$)
W	Amount of leaves in the sample solution (mg)
W_s	Amount of stevioside in the standard solution (mg)
X_{w0}	Initial moisture content (g water/g d.m.)
X_{we}	Equilibrium moisture content (g water/g d.m.)
X_{wt}	Moisture content at time 't' (g water/g d.m.)

Greek Symbol

η_d	Microwave drying efficiency (%)
μ	Viscosity ($g\ cm^{-1}\ s^{-1}$)
ρ	Density ($kg\ m^{-3}$)
σ	Intermediate pore blocking model constant (m^{-1})

List of Figure Captions

List of Table Captions

CHAPTER 1

Introduction, Literature Review, and Objectives

This chapter briefly describes the fundamental information of two medicinal plants, viz., stevia and aloe vera. It concisely illustrates an overview of their origin, main components, structures, properties, medicinal importance, various analytical and separation techniques, drawbacks of conventional processes for commercial production, major research areas, and global market demands. This discussion finally leads towards the state of the art aims and objectives for the present work.

CHAPTER 1

Introduction, Literature Review, and Objectives

1.1 Background

The importance of medicinal plants has been realized and acknowledged since the ancient period. The Indian *Atharvaveda* and the Egyptian *Ebers Papyrus* documented quite details on the herbal medicines and their uses. There are several hundred of medicinal plants which have been used for thousands of years as a remedy of various diseases. The medicinal plants are mostly the rich sources of phenolic, polyphenolic, alkaloid, quinone, terpenoid, lectins, and polypeptide compounds which are effective alternatives to antibiotics, chemicals, and vaccines (Harikrishnan et al., 2011; Maundu et al., 2001). In addition, the medicinal plants are a good source of a wide variety of nutrients (Chang, 2000). The herbal medicinal treatment is believed to be used for the recovery of diseases in the human body without any side effect. It happens through balancing the qualities and synergistic planning and formulation of the medicinal herbs. Their role cannot be confined to mere the curation of diseases, but they are also consumed daily basis for fitness of the human body. In Ayurveda, it is rightly called as the elixirs of life.

There is an increasing demand for the herbal medicinal treatment. The majority of the population in developing countries depends on the traditional system of medicine for their primary healthcare. Today, the World Health Organization (WHO) has estimated that in Africa continent 80 % of the population still uses traditional remedies, including plants, as their primary health care tools (WHO, 2002). Due to the increasing trend towards the use of an alternative system of medicine, several researchers across the world have been engaged in research and documentation of various aspects of these natural medicinal plants. In India,

numerous researchers have been published the ethno-botanical studies in the last few decades (Jain and Puri, 1984; Bhandary et al., 1995; Rajan et al., 2002; Yabesh et al., 2014).

A diverse range of medicinal plants is available including aloe vera (*aloe barbadensis*), almond (*Terminalia catappa*), caraway seed meal (*Carum carvi* L.), cinnamon (*Cinnamomum zeylanicum*), garlic (*Allium sativum*), ginger (*Zingiber officinale*), ginseng (*Panax ginseng*), green tea (*Camellia sinensis* L.), Arabic coffee bean (*Coffee Arabica*), stevia (*Stevia rebaudiana*), neem (*Azadirachta indica*), guava (*Psidium guajava*), olive tree leaf (*Olea europaea*), papaya (*Carica papaya*), peppermint (*Mentha piperita*), amla (*Phyllanthus emblica*), ashwagandha (*Withania somnifera*), kalmegh (*Andrographis paniculata*), turmeric (*Curcuma longa* L.), tulsi (*Ocimum sanctum*) and many more (Hai, 2015). The medicinal components may be found in the whole or parts of the plants. The common parts are leaves, roots, seeds, flowers, and fruits.

Nowadays, an enhanced consumption of sugars has resulted in several nutritional problems. The adverse effects of prolonged consumption of sugar are severely testified worldwide (Caroline, 2004; Brown et al., 2008). The demand for a sweetener which is natural, non-toxic, sugar-like taste, low caloric, heat, and pH stable has been investigated for decades. To meet all these demands, investigators have come with an herby medicinal plant, ‘stevia’, a plausible alternative to sugar. Aloe vera also has been explored nowadays for the profound immune-therapeutic benefit. The high rehydration properties make it use extensively in cosmetic industries (Femenia et al., 2003). The present chapter details the properties, constituents, medicinal benefits, research scenario and market demand of stevia and aloe vera.

1.2 Sugar, sugar substitutes and stevia

1.2.1 Adverse effects of sugar consumption

An enhanced consumption of added sugar in the processed foods and beverages is the single worst ingredient in the modern diet. It can have harmful effects on metabolism and, contribute to all sorts of diseases. It contains quickly digested calories with no nutrients, no protein, no essential fats and no enzymes. The main adverse effect of sugar is the decay of teeth as it provides easily digestible energy for the harmful bacteria in the mouth (Touger-Decker and van Loveren, 2003). The consumption of sugar causes other severe diseases like non-alcoholic fatty liver disease (Ouyang et al., 2008), type II diabetes (Basu et al., 2013), obesity (Bray et al., 2004), heart attack (Johnson et al., 2007) and, finally sugar can be addictive for a lot of people.

According to WHO, 422 million adults are victims of diabetic globally. One in three adults over 18 years is overweight and, one among them is obese (http://www.who.int/diabetes/en, Dt. 27.04.2016). In India, more than 62 million people are diabetic currently (Joshi and Parikh, 2007; Kumar et al., 2013). Diabetes is rapidly gaining the status of a potential epidemic in India. In 2000, India already reached with the highest number of diabetes mellitus individual (31.7 million) followed by China (20.8 million) and United States (17.7 million). It is expected that the number of diabetic patients is going to reach 79.4 million in India by 2030 (Wild et al., 2004).

The necessity of an alternative to sugar has been imperative over the decades. Almost every single sweetener has been investigated as a possible alternative to sugar. In the following section, a brief discussion has been presented on the merits and demerits of sugar substitutes.

1.2.2 Sugar substitutes

A sugar substitute is a food additive that duplicates the effect of sugar in taste, usually with a less food energy. Some sugar substitutes are natural and some are synthetic. Those are not natural, in general, are referred to as artificial sweeteners. An important class of sugar substitutes is known as high-intensity sweeteners. These are the compounds with sweetness that is many times that of sucrose, the common table sugar. As a result, much less amount of sweetener is required and, the energy contribution is often negligible.

In this regard, it will be noteworthy that the human tongue responds to a range of different substances, registering them as various tastes. The tongue is covered with tiny clusters of chemical sensors, called taste buds. It is the geometric shape of incoming molecules that determines how they taste. In sugar, a dual set of hydrogen atoms poking out from their surface like a prong, ready to bond with receptors in the tongue, causing a taste of sweetness. These two hydrogen atoms are between 2.5 and 4 angstroms apart. For an example, saccharin and sucrose have an entirely different molecular structure but having the same prongs with similar spacing, leading to a similar taste sensation of sugar.

1.2.2.1 Artificial sweeteners

The majority of market available sugar substitutes are artificially-synthesized. There are ongoing controversies over whether the use of artificial sweetener poses health risks or not.

Saccharin: Saccharin is the common name for benzoic sulfinide, a sweet substance providing no nutritive value. It is 300 to 500 times sweeter than sucrose and, is often used to improve the taste of toothpaste, dietary foods, and dietary beverages. The bitter aftertaste of saccharin is often minimized by blending it with other sweeteners. Saccharin is unstable

when heated but, it does not react chemically with other food ingredients (Larry and Greenly, 2003). The studies in the 1970s revealed the potential risk of saccharin for bladder cancer in rats. It was banned in Canada in 1977. In the USA, a warning label was added on the package. In 2001, the requirement of a warning label was lifted after a study showed that rats develop bladder cancer from saccharin due to a function but not relevant to human beings as our urine composition is different. Most other countries also permit saccharin, but restrict the levels of use, while other countries have outright for banning it.

Aspartame: It was discovered in 1965. It is an odorless, white crystalline powder that is derived from two amino acids, aspartic acid, and phenylalanine. It is about 200 times sweeter than sugar and, can be used as a tabletop sweetener. When cooked or stored at high temperatures, aspartame breaks down into its constituent amino acids. This makes aspartame undesirable as a baking sweetener. It has become one of the most controversial artificial sweeteners due to its connotations with side effects such as headaches, brain tumors, brain lesions, and lymphoma (Roberts et al., 1997).

Sucralose: Sucralose is a chlorinated sugar and, is about 600 times sweeter than sugar (Larry and Greenly, 2003). It has no nutritive value and, is eliminated from the body in the same form in which it was ingested. Sucralose is the only artificial sweetener that maintains its sweetness when heated. So, it can be used in baking. Sucralose is currently used in soft drinks, hot chocolate, fruit drinks, maple syrup, and apple sauce.

Sorbitol: Sorbitol is also known as glucitol. It is a sugar alcohol used in sugar-free candies and other diet foods. It is found naturally in some fruits and berries but generally is produced through chemical processing. Though sorbitol has some nutrient value but it also is

known for numerous side effects including abdominal pain and intestinal difficulties. So, the products containing sorbitol should be used in moderation.

Lead acetate: Lead acetate is an artificial sugar substitute made from lead. The use of lead acetate as a sweetener eventually produced lead poisoning in any individual ingesting it habitually. Lead acetate was banned as a food additive throughout most of the world after the high toxicity of lead compounds has become apparent.

Cyclamate: It was discovered in 1937 and, is around 30 times sweeter than sucrose. It is heat stable and, poses synergistic sweetening power with other sweeteners. Only a small percentage of cyclamate is metabolized. Cyclamate was implicated as a possible carcinogen and, banned in the United States in 1970. However, more than 50 countries still use it as a sweetening agent (Larry and Greenly, 2003).

1.2.2.2 Natural sweeteners

Natural sweeteners contribute the taste of sugar and, are of less caloric. There are several natural sweeteners such as curculin, glycyrrhizin, mannitol, mabinlin, isomalt, stevia, etc. For the most of the natural sweeteners, the sweetness capacity is less than sucrose. They often do browning reaction (honey, agave nectar, date sugar and molasses) and, cannot withstand low pH.

Curculin: Curculin is a sweet protein that has been discovered and isolated in 1990 from the fruit of *Curculigo latifolia*, originated from Malaysia. It is around 550 times sweeter than sucrose. Like most of the proteins, curculin is susceptible to heat. At a temperature of

50°C, it starts to degrade and, lose the 'sweet-tasting' and 'taste-modifying' properties. So, it is not good for use in hot or processed foods.

Glycyrrhizin: It is around 50 times sweeter than sucrose. Glycyrrhizin has the medicinal values as it inhibits liver cell injury and, it could retain fluid with other side effects.

Mannitol: Mannitol is a white, crystalline solid that looks and tastes like sucrose. Its sweetening potential is half of the sucrose.

Mabinlin: It is a protein which is extracted from the seed of Chinese plant Mabiniang. Mabinlin is 100-400 times sweeter than sucrose.

Stevia: Stevia is an herbal plant of *Asteraceae* family, originated from the high rain forest of Brazil and Paraguay. It is used by their native people 'Guarany' as a traditional sweetener for decades. Eight diterpene glycosides in stevia leaves are responsible for its high sweetness. The glycosides present in stevia leaves are stevioside, rebaudioside A (Reb-A), rebaudioside B, rebaudioside C, rebaudioside D, rebaudioside E, steviolbioside and dulcoside A. Out of these, stevioside and rebaudioside-A are the most predominant sweetening components. Stevioside and Reb-A are around 300 and 450 times sweeter than sucrose (Kinghorn, 2002). Stevia based sweeteners show good stability towards microbial activity, heat, and pH treatments. No significant degradation is detected in carbonated beverages (Chang and Cook, 1983).

1.2.3 Why stevia emerges as a promising sweetener?

It is seen that in spite of several hundred times of sweetening capacity of artificial and natural sweeteners, each of them possesses one or more crucial limitations except stevia. Most of the sweeteners cause mild to severe side effects to human. A frequent metallic taste of such synthetic sweeteners does not provide the realistic taste of sugar. Moreover, most of them contain sulfur molecule in their structure causing unwanted side effects. For examples, consumption of aspartame must be avoided by people with the metabolic disease, phenylketonuria (Grenby, 1991). Aspartame causes headaches, brain tumors, brain lesions, and lymphoma (Roberts et al., 1997). Consumption of saccharin (Douglas, 1984) and cyclamate (Andreatta et al., 2008) are associated with risk of bladder cancer. Low heat stability and browning reaction also have restricted the use of some sweeteners. For this reason, stevia has been evaluated as an alternative sweetener to sucrose by several scientists. In the present work also, stevia based sweeteners have been chosen for further study. Before going further, a brief discussion on stevia and stevia based sweeteners are presented in the following section.

1.2.4 Stevia

Stevia rebaudiana (Bertoni) family is an herbaceous perennial plant indigenous to Paraguay and Brazil. About 150 stevia species are known, among them, *stevia rebaudiana* is the only one with significant sweetening properties. This plant is of worldwide importance because its leaves have been using as non-nutritive high potency sweetener, mainly in Japan, Korea, China and South America. It is also known as ‘Madhu Patra’ in India since long before. Stevia plant was discovered and described by Moises S. Bertoni, an Italian botanist. Before 1905, he had described it after the name of the chemist who first refined it, Dr. Rebaudi. Stevioside was first isolated by Bridel and Lavieille in 1931.

Stevia, a thin creeping tender perennial herb grows up to 100 cm in height. During cultivation in more fertile soils, the mature plant can go up to 1.8 m in height. Stems are long, flattened and twisted with small grey-green rounded leaves. Trichome structures on the leaf surface are of two distinct sizes, i.e., one is large (4-5.5 mm), and another one is small (2.5-5 mm). The flowers are small (7-15 mm), white and arranged in an irregular cyme. The seed is an achene with a feathery pappus. The species can also grow in grasslands, scrub forests, and sub-alpine areas.

Eight diterpene glycosides in stevia are responsible for its high sweetness. These are stevioside, rebaudioside A, rebaudioside B, rebaudioside C, rebaudioside D, rebaudioside E, steviolbioside and dulcoside A (Kinghorn et al., 2002). Among them, stevioside and rebaudioside A are the predominant. Stevioside and Reb-A are white, crystalline, odourless powders which are approximately 300 and 450 times sweeter than sucrose (0.4 %), respectively (Puri et al., 2011; Li et al., 2012; Liu et al., 2010; Chatsudthipong and Muanprasat, 2009). The major components of the stevia leaves are listed in Table 1.1, on a dry weight basis, with few other details of the glycosides. Both the sweeteners are non-fermentable, non-discoloring, thermally stable and lengthy shelf life.

Table1.1: Comparison of sweet glycosides present in the leaves of *stevia rebaudiana*.

Name	Abundance (% w/w)	Molecular weight	Sweetness (compared to 0.4 % solution of sucrose)	Melting point (°C)	Reference
Stevioside	5.0–10.0	804.87	250-300	196-198	Bridel and Lavieille, 1931; Soejarto et al., 1982
Rebaudioside A	2-8	967.01	350-450	242-244	
Rebaudioside B	<1.0	804.87	300-350	193-195	
Rebaudioside C	1.0-2.0	951.01	50-120	215-217	Sakamoto et al., 1977
Rebaudioside D	<1.0	1129.15	200-300	283-286	
Rebaudioside E	<1.0	967.01	250-300	205-207	
Steviolbioside	<1.0	642.73	100-125	188-192	Kohda et al., 1976
Dulcoside A	0.4-0.7	788.87	50-120	193-195	Kobayashi et al., 1977

The chemical structures of stevioside and Reb-A are shown in Figure 1.1. Chemically stevioside and Reb-A are (13-[2-Oß-D-glucopyranosyl-α-glucopyranosyl) oxy] kaur-16-en-19-oic-acid ß-D-glucopyranosyl ester) and 13-[(2-O-β-D-glucopyranosyl-3-O-β-D-glucopyranosyl-β-D-glucopyranosyl)oxy] kaur-16-en-18-oic acid, β-D- glucopyranosylester, respectively (Pol et al., 2007a).

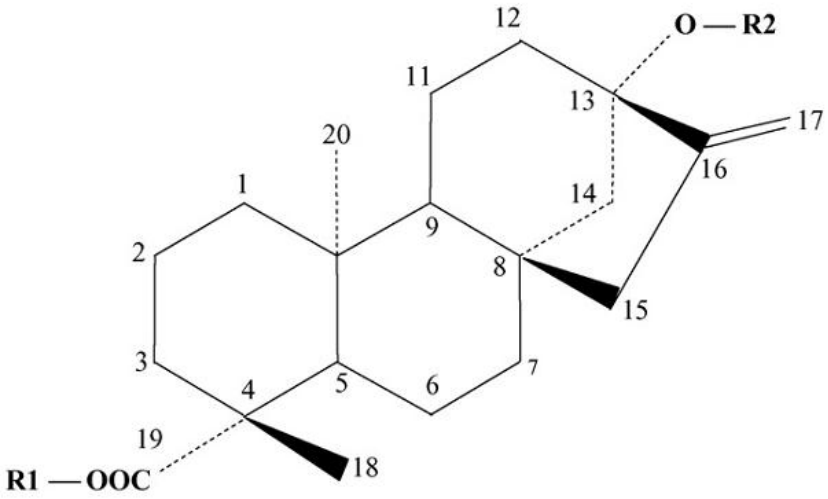

Sweetener	R1	R2
Stevioside	β-Glc	β-Glc-β-Glc(2-1)
Reb-A	β-Glc	β-Glc-β-Glc(2-1) β-Glc (3-1)

Figure 1.1: Structure of stevioside, and Reb-A (Glc- glucose, Rha- rhamnose, Xyl- xylose).

1.2.4.1 Medicinal properties of stevia

Apart from the sweetening property of the diterpene glycosides, stevioside and Reb-A pose many good impacts on the human body. It lowers the high blood sugar levels. There is a pronounced exhilarating effect in hypoglycemic, and a 35.2% fall in normal blood sugar level is noted in 6-8 h following the ingestion of a stevia leaf extract by diabetic patients. Stevia has been used by diabetic patients for centuries as a sweetener and also as a method of controlling blood sugar levels.

Due to high beneficial mineral content and anti-bacterial properties, stevia is a wonderful additive to toothpaste or diluted as a mouthwash. Stevia has been shown to lower the incidence of dental caries. It prevents the cavities in teeth.

Applied to the skin, stevia treats acne and other skin ailments. It also protects against premature aging. Stevia is also used to treat the skin inflictions. Apart from these, stevia is used as an antimicrobial and cardiotonic substance (www.steviocal.com/for-others.html, dt 25/7/2011). In addition, it is recently observed that stevioside has anti-amnesia properties (Sharma et al., 2010).

1.2.4.2 Safety aspects of stevioside and Reb-A

One of the main proofs of the safety of stevia is that there have never been any reports/complain of ill effects in over 1500 years of continuous use by Paraguayans (Kroger et al., 2006). As Dr. Daniel Mowrey reported (Tanaka, 1982), "More elaborate safety tests were performed by the Japanese during their evaluation of stevia as a possible sweetening agent. Few substances have ever yielded such consistently negative results in toxicity trial as has stevia. Almost every toxicity test imaginable has been performed on stevia extract (concentrate) or stevioside at one time or another. The results are always negative. No abnormalities in weight change, food intake, cell or membrane characteristics, enzyme and substrate utilization, or chromosome characteristics. No cancer, no birth defects, no acute and no chronic untoward effects. Nothing."

1.2.4.3 Current market status of stevia

Japan is the first country outside of South America to commercially cultivate stevia and marketed stevioside as a commercial sweetener (Ramesh et al., 2006). China has been using stevia since 1985. It is claimed that the production of stevia has reached to 11,789 ton

per annum in 2009 from around 5000 ton per annum in 2007 (Pasricha, 2009). Before 2008, stevioside was used only as a dietary supplement in the USA, but stevia-derived sweeteners had increased in popularity since December 2008, when the US Food and Drug Administration approved the stevia-derived sweetener Reb-A as generally recognized as safe (GRAS) for its use in foods and beverages. Stevioside has a 20% market share of low-calorie sweeteners in Japan (Kikuchi, 1985). Additionally, owing to advantages like completely natural and low-calorie, it is very likely that more countries will open up their markets for stevia sweetener in the future. However, India with its population of 1.25 billion and growing rates of obesity, offers "an untapped market" which creates a significant opportunity for stevia suppliers (Caroline, 2010).

In 2008, the world's high-intensity sweeteners market was estimated around $1.3 billion, with sucralose commanding a leading position of 36% share by value in food applications. Stevia-based high purity sweeteners are still in the developmental stage.

1.2.5 Estimation, extraction and purification techniques of stevioside and Reb-A from stevia leaves: Current research status

The separation and, purification of pure glycosides, stevioside, and Reb-A from stevia leaves involves three different unit operations. Extraction or solid-liquid extraction is the first step to extract the glycosides into the desired solvent. Then, the extract is concentrated using ion exchange, precipitation or coagulation, filtration, and at last, the whole concentrated liquor is subjected to drying or crystallization operation for the removal of solvent completely. Sometimes, the intermediate stages are skipped and, the extracted solution is directly led for drying. In the following paragraphs, various types of extraction and separation processes have been discussed.

1.2.5.1 Estimation of sweet tasting glycosides content

Several techniques have been employed to estimate the amount of sweet tasting glycosides in stevia leaves. High performance liquid chromatography (HPLC) is the most common analytical method employed for the estimation of glycosides (Nikolova-damyanova et al., 1994). Other methods include thin layer chromatography (Tanaka, 1982), droplet counter-current chromatography (Kinghorn et al., 1982), capillary electrophoresis (Mauri et al., 1996) and size exclusion chromatography (Ahmed and Dobberstein, 1982).

The amino column has been used in HPLC to determine the amount of stevioside and Reb-A in food and beverages (Chang and Cook, 1983). The process involved two steps: solvent extraction and HPLC analysis. The chromatographic process can be easily applied to estimate the quantity of stevioside and Reb-A in stevia leaves. HPTLC techniques can quantify three steviol glycosides simultaneously, i.e., stevioside, Reb-A, and steviolbioside. A mobile phase of solution ethyl acetate: ethanol: water (8:2:1.2, v/v/v) and pre-coated silica gel 60 F254 HPTLC plate are commonly used at 510 nm (Jaitak et al., 2009). Three steviol glycosides, stevioside, rebaudioside A and rebaudioside C, are successfully isolated and purified from the extract of leaves of stevia rebaudiana by high-speed counter-current chromatography (HSCCC) (Huang et al., 2010). Based on the principle of the partition coefficient values (k) for target compounds and the separation factor (α) between targets compounds, the two-phase solvent system containing n-hexane-n-butanol-water at an optimized volume ratio of 1.5:3.5:5 (v/v/v), is selected for the HSCCC separation. The lower phase is employed as the mobile phase.

1.2.5.2 Solid-liquid extraction processes of stevioside and Reb-A

Conventional approaches

Solid-liquid extraction is a separation process in which one or more components selectively come in the liquid phase from the solid. Solvent extraction involves following steps: stevia leaves are crushed and ground, treated with an organic extractant, filtered and concentrated into a thick syrup. (Persinos, 1973). Old conventional extraction procedure of stevioside from stevia leaves involve the alcoholic solution. The effect of temperature, extraction time, the mixed solvent ratio on the yield is studied (Zhang et al., 2000; Pol et at., 2007). Similar extraction processes are patented based on solvent (Haga et al., 1976), solvent plus decolorizing agent (Ogawa et al., 1980), ion-exchange (Unesh et al., 1977) and adsorption chromatography (Itagaki and Ito, 1979). In the latter stage, the recovery of stevioside from stevia leaves is promoted by eliminating the usage of hazardous chemicals or separation equipment. In this process, the raw material is first extracted with water and, a precipitation or coagulating agent or both, such as di- or tricarboxylic acid, calcium are added to remove metallic and other impurities. Then the aqueous extract is acid neutralized and extracted with a water-immiscible solvent. Purified stevioside crystals are recovered from the solvent extraction step (Phillips, 1989; Kumar, 1986; Dacome et al., 2005).

Pressurized fluid extraction

Pressurized water extraction at an elevated temperature is first reported by Hawthorne et al. in 1994, for the extraction of some polar and non-polar analytes from the soil. The term ‘pressurized hot water’ refers a phase of water between 100°C (boiling point of water) and 374°C (critical temperature of water) in which water acts as a highly polar substance. This pressurized water is a feasible green solvent which can reduce the usage of polar organic

solvents. It can dissolve a wide range of medium to low polarity solutes (Kim et al., 2009; Nieto et al., 2008; Jiang et al., 2009; Kalderis et al., 2008).

Pol et al. (2007b) used pressurized water and methanol for extraction of stevioside from stevia rebaudiana at 50 bar, a green alternative to methanol. Water showed a better extraction efficiency than methanol at <110°C. However, methanol outperformed water at higher extraction temperature. Both methanol and water displayed a similar thermal degradation of stevioside in the range from 70 to 160°C. They reported an optimal extraction of 5.2 and 4.7 % per g dry leaves for methanol and water, respectively, in 10 min of extraction at 110°C and 50 bar pressure. In another study, Teo et al. (2009) performed pressurized hot water extraction of stevia leaves. The better extraction is achieved at 100°C and 11-13 bar pressure. The solvent flow rate is 1.5 mL per min for 15 min.

Microwave-assisted extraction

Unlike conventional heating methods, the microwave directly excites the water molecules due to its high dielectric constant and, it causes faster heat generation. The application of microwave irradiation diminishes the drying time dramatically by the mechanism of volumetric heating (Prabhanjan et al., 1995).

Microwave-assisted extraction (MAE) is carried out at different power levels ranging from 20 to 160 W with the extraction time ranging between 30 s and 5 min with a temperature range of 10 to 90°C. MAE has an optimum yield at a power level of 80W for 1 min at 50°C (Jaitak et al., 2009). They performed stevioside and Reb-A extraction using methanol, ethanol or water, as well as in a combination with water. Methanol-water mixture (80:20 v/v) and ethanol showed the highest stevioside and Reb-A extraction of 7.2 and 1.7 (% w/w), respectively. Their experimental results evidence that water is a better solvent for Reb-A extraction in comparison to stevioside.

Ultrasound extraction

Liu et al. (2010) performed ultrasound-assisted extraction of total glycosides from stevia leaves by varying three independent parameters, i.e., extraction temperature (40-80°C), ultrasound power (20-100 W) and sonication time (10-60 min). The optimal extraction conditions are achieved at 68°C, sonic power of 60 W and an extraction time of 32 min. The corresponding stevioside and Reb-A yields are 7.4 and 4.9%, respectively.

Supercritical fluid extraction

As the steviol glycosides are less soluble in CO_2, they are dissolved in the mixture of CO_2 and a polar solvent in the supercritical process. Stevia leaves are extracted by supercritical fluid extraction using a two-step process: (i) pure CO_2 extraction at 200 bar and 30°C, and (ii) CO_2 with water extraction. The glycoside compositions in the extracts are analyzed by GC-FID, GC-MS, TLC and HPLC. Approximately, 72% of the CO_2-soluble compounds are removed. The process recovered approximately 50% of the stevioside and about 72% of the Reb-A (Yoda et al., 2003).

Few patents are filed on the supercritical fluid extraction of steviol glycosides based on co-solvents, such as methanol, ethanol, and acetone mixed with the primary solvent CO_2 (Tan et al., 1983, Yoo et al., 2001). Chemically, extracted stevioside and Reb-A cause a frequent 'bitter' aftertaste and, these methods are energy extensive (Ye et al., 2013). The taste quality of stevioside and Reb-A are better for supercritical fluid extraction with CO_2 and co-solvent as compared to other extraction processes (Pasquel et al., 2000). Pressure (150-350 bar), temperature (40-80°C) and concentration of ethanol-water mixture (70:30) as co-solvent (0-20%) by the CO_2 flow rate of 15 g min^{-1} for 60 min, are optimized using Box-Behnken statistical design. The most significant parameters are found to be co-solvent concentration and temperature for the stevioside extraction (Erkucuk et al., 2009).

In the following **Table 1.2,** different extraction processes of stevioside are summarized.

Table 1.2: Extraction processes from the leaves of *stevia rebaudiana*.

Method	Yield	Limitations	Reference
Organic solvent	2.36 mg/g	Loss of organic solvent	Pol et al., 2007
Pressurized fluid extraction			
Methanol	5.2%	Required complex steps	
Water	4.7%	Required high calories	
Microwave assisted extraction	7.2%	Energy expensive	Jaitak et al., 2009
Ultrasound	7.4%	Required complex steps	Liu et al.,2010
Supercritical fluid extraction		Higher cost	Choi et al., 2002
CO_2 : MeOH= 80:20 (v/v)	2.51 mg/g		Pol et al., 2007
CO_2 : MeOH: H_2O = 80:16:4 (v/v)	3.56 mg/g		

1.2.5.3 Downstream processing of stevioside and Reb-A

Downstream processing refers to the concentration and purification of stevioside and Reb-A after extraction leading to the final product. In general, the concentration may be achieved by ion exchange, adsorption, evaporation and membrane filtration processes. Giovanetto (1990) reported a process which involves pre-treatment of the extract with lime and the use of ion exchange column. Zeolites X and A are employed to selective adsorption in stevia extract. The effect of contact of CaX, BaX, CaA and BaA zeolites with aqueous stevia extract is evaluated. Moraes and Machado (2001) reported that the highest clarification of stevia extract was achieved using selective adsorption with zeolites CaX. The final product is obtained by drying the concentrated liquor.

Membrane separation is another energy efficient process to concentrate the extract. It is successfully applied in various industrial fields like biological suspensions (Chang et al., 2002; Nataraj et al., 2008) and fruit juice clarification (Cassano et al., 2003; Rai et al., 2007; Sarkar et al., 2008; Singh et al., 2013). Kutowy et al. (1998) first used membrane based clarification of sweetening components from stevia leaves using three step diafiltration

modes. Fuh and Chiang (1990) purified stevioside from aqueous extract using hybrid membrane processes followed by an ion exchange process. Ultrafiltration and diafiltration are employed to concentrate the extract using 25 and 100 kDa MWCO membranes. The permeate is further concentrated by reverse osmosis. Finally, the concentrate is purified using two mixed bed ion exchange columns. The processes achieved 90 % recovery of stevioside with purity of 46%. Zhang et al. (2000) performed three stages purification of stevioside from an aqueous extract of stevia. In the first stage, the extract is pretreated using the ceramic tubular membrane of pore size 0.35 μm at 104 kPa. Permeate is then passed through ultrafiltration membrane of 2.5 kDa at 440 kPa. In the last stage, nanofiltration is carried out to wash out lower molecular weight impurities. Around 80-100% recovery is obtained with varying pore sizes and operating conditions.

In the recent works, total steviol glycosides from stevia leaves are concentrated using micro and ultrafiltration (Vanneste et al., 2011, Rao et al., 2012). Roy and De (2014) synthesized cellulose acetate phthalate and polyacrylonitrile membranes for the extraction of steviol glycosides. They studied the optimum membrane cut off and permeate flux decline at various TMP drops and Reynolds numbers. Membrane fouling is a key determining criterion for selecting a membrane commercially and economically. There are fewer studies on the modeling and transport mechanism of ultrafiltration performance in the cross flow module towards the separation of stevioside from stevia extract (Mondal et al., 2012a; Mondal et al., 2012b; Mondal et al., 2013; Roy and De, 2014). The classical film theory is employed for modeling the steady state performance of ultrafiltration. The gel layer controlled model is found to be most predominant.

Fouling and concentration polarization are two common limitations which decline the permeate flux in membrane-based separations. Most of the cases, fouling are an irreversible phenomenon in which solute particles are adsorbed on or in the membrane pore walls resulted

as partial or complete pore blocking. The concentration polarization is formed by the reversible accumulation of solutes in a layer on the membrane surface. Membrane fouling is a determining factor which affects the economic and commercialization of a membrane system.

1.2.6 Drawbacks of stevioside and Reb-A extraction and purification

Although the various extraction and purification processes of stevioside and Reb-A have been discussed in the preceding sections, certain limitations have come into the picture which could restrict the practice of the existing methods. These are as follows.

(i) Dilute alkali solution is used for the regeneration of adsorption columns which may affect organoleptic properties and quality of the products.

(ii) Usage of organic solvents/chemicals in certain cases cannot be recycled. It arises pollution and disposal problems.

(iii) Removal of traces amount of organic solvent/chemical from final product is also troublesome.

(iv) In ion exchange process, the usage of certain chemicals may alter the taste and composition of the sweet glycosides.

(v) The emergence of ‘bitter’ aftertaste with the use of chemically extracted glycosides.

(vi) Supercritical fluid extraction, and pressurized solvent extraction involve high capital cost investment and complex steps.

(vii) High energy consumption at an elevated temperature during hot water extraction.

1.3 Aloe Vera

In ancient cultures of India, China, Egypt, Greece and Rome, aloe vera has been recorded for its medicinal properties. In the literature, aloe vera has been cited by various names, i.e., *Aloe barbadensis* Miller, *Aloe chinensis* Bak, *Aloe indica* Royale, *Aloe officinalis* Forsk, *Aloe vera* L. var. littoralis Konig ex Bak, *Aloe vera* L. var. chinensis Berger, etc. *Aloe barbadensis* Miller is regarded as the correct species name in most of the reference books and *Aloe vera* (L.) Burm f. as a synonym. Aloe vera (*Aloe barbadensis* Miller) is a perennial herb which belongs to the Liliacea family. The genus Aloe has over 400 various species; among them *Aloe barbadensis* Miller is considered as a most biologically active species. It is known as 'Ghratkumari' in India. The plant matures around in 4 years and, has a life span of about 12 years. It has a short stem with typically 15 to 30 fleshy leaves in each plant and weighing up to 1.5 kg when mature (Grindlay and Reynolds, 1986). The stem can grow up to 25 cm long in older plants. The species was identified by its physical anatomy, i.e., through its common physical characteristics (Surjushe et al., 2008). Aloe vera leaves are the main part of the plant. The inner portion of the aloe vera leaves has a semi-rigid matrix of many macromolecules. This is referred as aloe vera gel. It is colorless containing about 97-99 % water and, the rest is an absorbable solid mainly comprising of polysaccharide (pectins, cellulose, hemicellulose, glucomannan, acemannan and mannose derivatives), sugars, minerals, proteins, and lipids. Aloe vera gel is also a source of many vitamins including vitamins A, C and E. B_1 (thiamine) and B_2 (riboflavin) (Lawless and Allen 2000). Aloe vera gel comprises both mono and polysaccharides. The long chain polysaccharides contain glucose, and mannose, known as glucomannans [β (1, 4)-linked acetylated mannan]. Xylose, rhamnose, galactose and arabinose are also present in trace amounts. Acemannan is a main bio-active component of aloe vera gel which is composed of a long chain of acetylated mannose (Bozzi et al., 2007). In recent years, the antiviral, antitumor, antidiabetic and

anticancer properties of aloe vera gel have been revealed (Hamman 2008; Alemdar and Agaoglu 2009; Ramachandra and Rao 2008). Aloe vera gel has been introduced as an additive to food and vegetables for its therapeutic benefits (Gulia et al. 2010). Thus, it needs to be preserved for its future usage.

The gel should be separated out from the peel because of the presence of anthraquinones. It is a phenolic compound present in the sap or yellow exudates of leaf or aloe vera latex. This substance has a laxative and toxic effect on the body. Once this part of the plant is removed, the coveted inner gel of the aloe is ready to be processed (Turner et al., 2004).

For decades, the juice form of aloe vera gel has been thought as the only way for healing essence. Dehydrated aloe vera powder offers a greater concentration of broad spectrum of nutrients, rich in the healing constituents that have made aloe famous for centuries. For this reason, an understanding of different forms of aloe vera manufacturing practices is necessary.

1.3.1 Medicinal properties of aloe vera

Polysaccharides present in aloe vera leaves are unique for two reasons. First is the biological activity of the acetylated mannan, also known as an aloe polymannan, apart from the burning and healing essence. Polymannan is a special complex carbohydrate that is also known as polymannose. The most outstanding effect of polymannose in the human body is its ability to modulate the immune response and general immune function (Lobo et al., 2010).

The other reason is that polymannose is rare in nature. Every living creature depends on the presence of polymannose in the body in order to function at the cellular level. It is one of the few nutrients that the body is not capable of producing on its own. The polymannose molecule must be ingested on a regular basis to maintain optimal health. Above any other

botanical on the planet, the *Barbadensis* Miller species of Aloe contains the highest concentration of this essential master carbohydrate (Miranda et al., 2009). The other novel components of aloe vera are presented in Table 1.3 along with their health benefits (Ahlawat and Khatkar 2011).

Table 1.3: Novel components of aloe vera and their health benefits.

Components	Health benefits
Acemannan	Accelerate wound healing, modulate immune system, Antineoplastic, and antiviral effects
Alprogen	Anti-allergic
C-glycosyl chromone	Anti-inflammatory
Bradykinase	Anti-inflammatory
Magnesium lactate	Anti-allergic
Salicylic acid	Analgesic, Anti-inflammatory

1.3.2 Current market demand of aloe vera

The versatile use of aloe vera has made its journey worldwide from tropical Africa and, it is now cultivated in warm climatic areas of Asia, Europe, and America. Presently, the widespread popularity of aloe vera has been gained by the herbal movement initiated by naturopaths, yoga gurus, alternative medicine promoters and holistic healers. It is claimed that an initial investment of aloe vera raw material is estimated to be about $125 million dollars. The volume of the industry for finished products containing aloe vera is alleged to be around $110 billion dollars (Ahlawat and Khatkar 2011). In a market survey in 2008, America has spent almost $40 billion on functional foods, drinks, and supplements for the improvement of their appearance as well as to provide energy and added nutrition to handle health issues. Aloe vera products are the popular ones for these applications. The aloe vera industry is flourishing and, the gel is used in many products such as fresh gel, juice, and other formulations for health, medicinal and cosmetic purpose (Eshun and He 2004).

1.3.3 Drying processes: Current research status

Drying is the main operation used for increasing the partial concentration of solids in the aloe vera gel. It reduces bacterial activity; thereby increases the storage life and reduces the packaging cost, storage places, weight of the products and transportation cost (Okos et al. 1992). The rapidly growing aloe vera industry needs reliable drying methods or protocols to ensure the quality and quantity of bioactive chemicals present in the final dried products (Bozzi et al. 2007). Aloe vera gel is extracted from its leaves and, the suitable processing techniques are in need of the stabilization as well as for the preparation of the end products. In the following paragraphs, different drying methodologies have been outlined.

1.3.3.1 Hot air drying

Hot air drying (HAD) is the most commonly used method for the dehydration of foods and food components. Femenia et al. (2003) studied the physico-chemical properties of aloe vera gel using hot air treatment between 30 and 80°C. Total carbohydrate and functional properties are found to decrease significantly above 60°C. According to the study by Miranda et al. (2009), an acceptable commercial quality of dried aloe vera gel is obtained between 60 and 70°C. In another study, Gulia et al. (2010) worked on the physico-chemical and functional properties qualitative tests of aloe vera powder (e.g.: yield, ash content, pH (1 % solution), crude fat, crude protein, crude fibre, wettability, water absorption capacity) at 50, 60, 70 and 80°C. The results revealed that the yield is almost same at all the temperatures. pH of powder samples (1 % solution) is almost equal. The wettability of powder is the lowest at 70°C and, the water absorption capacity of powder is the highest at this temperature.

The suitable kinetic models of the dehydration process lead to an efficient way of controlling the quality of the final product, energy saving, and equipment stress. Several investigators have suggested different mathematical models for convective HAD of a thin

layer of food stuff (Vega et al., 2007; Vega-Galvez et al., 2009; Wang et al., 2007; Xanthopoulos et al., 2007). Direct hot air drying without pretreatment of the aloe gel is studied by Vega et al. (2007). They studied the temperature influence on the kinetic parameters of drying process using five empirical equations (Newton, Henderson-Pabis, Page, modified Page and Fick's diffusional model). The drying is carried out in a convective dryer at five different temperatures (50, 60, 70, 80 and 90°C) with an air flow rate of 2.0 m/s. The time required to achieve a moisture content lower than 2.0 g water/g d.b. at 50°C is 800 min, which is approximately double the time required to reach the same moisture content at a temperature of 70 °C (400 min) and triple at 90°C.

1.3.3.2 Freeze drying

Freeze drying (FD), or lyophilization, works under high vacuum to sublimate the frozen water from the substances/foods directly into water vapor. Because the material remains frozen, no heat damage occurs causing little or no loss in sensory qualities of the product. FD is the least disruptive method and, could retain the highest physico-chemical properties in the high-value products. FD is a tender drying process which is capable of retaining the structure, flavour, colour and aroma of heat sensible materials (Marques and Freire 2005; Kopjar et al. 2008). But an extended drying period due to lower heat and mass transfer in FD involves high expenses and energy consumption (Sadikoglu et al. 2006). FD of aloe vera has not been performed as a single drying procedure but as a partial drying step. Freeze dried aloe vera gel is used as a reference substance to compare with the products obtained from other drying processes.

1.3.3.3 High hydrostatic pressure

High hydrostatic pressure (HHP) processing of fruits and vegetables can provide an effective non-thermal alternative to conventional heat processing. Some of the advantages of high-pressure processing are process time reduction; minimum heat damage problems; retention of freshness, flavor, texture, and color, reduction in ice-crystal damage and, a low functionality change compared to thermal processing (Al-Khuseibi et al., 2005).

The effects of HHP treatment on functional and physico-chemical characteristics of aloe vera gel is performed at 300, 400 and 500 MPa by Vega-Galvez et al., (2011a). The total phenolic content and Vitamin C and E are found to decrease at 500MPa. The antioxidant activity and aloin content are increased at higher pressure. In another study, HHP and other pretreatments (blanching, microwave, and enzyme treatment) prior to the convective drying of aloe vera at 70°C are performed. HHP pretreatment (350 MPa for a period of 30 s) on drying kinetics, antioxidant activity, firmness, microstructure of aloe vera are compared with another pretreatment (Vega-Galvez et al., 2011b). The results show that microwaves followed by HHP pretreatment give the highest water diffusion coefficient. HHP gives the highest antioxidant activity where HHP increases the firmness of the product.

1.3.3.4 Osmotic dehydration

Non-thermal drying of aloe vera gel is performed using osmotic dehydration (OD) to remove a part of the water from the foods and vegetables (Torreggiani and Bertolo, 2004). The effective diffusivity in the liquid phase of osmotically dehydrated aloe and the kinetic constants of net mass transfer in the process are studied (Garcia-Segovia et al. 2010). The effective diffusivity varied from 0.19×10^{-8} to 1.98×10^{-8} m^2/s in the range of 25 to 40°C. The best condition is at 40°C with the highest diffusivity for the peeled samples.

1.3.4 Limitations of drying methods

It has become imperative that the aloe vera gel must be processed with the aim of retaining the essential bioactive components up to maximum possible limit or as much as contained in the fresh leaf. Unfortunately, because of selection of the improper processing techniques many aloe products contain very little or virtually no active ingredients. Uncontrolled heating/drying could modify the original structure, thereby leading to an irreversible modification of the properties of dried aloe vera gel. The conventional dehydration techniques, such as, drying using hot air, -solar, -vacuum exhibits the longer falling drying rate period which causes cringing of product quality such as color, flavor, aroma, texture and nutrient activity (Tsami et al., 1999). Further, these processes have the limitation of handling large quantities, low energy efficiencies, and consistent product quality (Ozbek and Dadali, 2007).

The individual dehydration techniques, such as hot air drying, often fails to retain the functional properties of the dried product (Femenia et al., 2003). This is one of the reasons that many aloe vera products come in the market as a partially concentrated form. Further, the presence of different preservatives in the thick aloe vera liquor alters its functional activities. Turner et al. (2004) performed a quality evaluation and comparison of thirty two commercially available aloe vera products and, they find a significant variation in high molecular weight content and biological activity compared to fresh aloe gel.

HHP requires high pressure which involves high capital cost investment. The osmotic dehydration process is less costly and, no drastic operational conditions are needed, but it could not remove all the moisture from the aloe vera gel.

1.4 Knowledge gap and objectives of the work

Based on the literature reviews in the fields of extraction and purification of steviol glycosides (stevioside and Reb-A) and dehydration of aloe vera gel, the knowledge gaps have been identified as:

1) Water is a promising green solvent for the extraction of Reb-A from stevia leaves. But, the challenges lie with the optimization of such processes which lacks in literature.

2) Total recovery cum purification of stevioside and Reb-A using membrane separation process is missing. The performance of membranes, their fouling behavior in cross flow modes are still to be studied.

3) Dehydration of aloe vera gel using conventional drying method hauls its quality due to prolonged drying time. Microwave-assisted drying of aloe vera gel could be a viable option due to its rapid volumetric heating rate. The study of microwave-assisted drying of aloe vera lacks in the literature. Further, the hybrid drying process (two or multiple stages drying process) must be innovated for the better retention of its quality.

4) Process optimization and modeling of microwave-assisted drying of aloe gel could be an innovative step towards the intensification of the drying efficiency, reduction in drying time, industrial scale up and product quality enhancement. Microwave-assisted drying of food stuff exhibits a drastic reduction in the falling rate period owing to a faster transport of moisture compared to hot air drying. So, a precise control and optimization are imperative to reduce the variation in the quality of the final products. The studies on optimization and modeling based prediction of microwave-assisted drying of aloe gel are missing in the literature.

5) Microwave drying processes drastically increase the rate of simultaneous heat and mass transfer and, the drying time is considerably lower as compared to that of hot air

drying with a minor variation in the quality of the products (Severini et al., 2005; Arslan and Ozcan, 2010). The study on the microwave-assisted drying kinetics of aloe vera gel is imperative. The modeling of microwave-assisted drying kinetics of aloe vera gel could help towards intensifying the drying efficiency, shortening drying time, industrial scale up and product quality improvement.

Therefore, the following objectives are accomplished in the current research.

- ✓ Extraction of Reb-A from stevia leaves using water as a green solvent.
- ✓ Optimization and modeling of the extraction process of Reb-A.
- ✓ Performance investigation of membrane-based purification of glycosides extract and the fouling behavior of the ultrafiltration membrane in cross flow module.
- ✓ Evaluation of hot air, microwave and hybrid drying processes for the dehydration of aloe vera gel towards the retention of its physicochemical properties
- ✓ Study on drying kinetics of microwave-assisted dehydration of aloe vera, process optimization, and kinetic modeling.

References

Ahlawat, K. S. and Khatkar, B. S., "Processing, food applications and safety of aloe vera products: a review", *J Food Sci Technol*, **48**, 525-533 (2011).

Ahmed, M. S. and Dobberstein, R. H., "Stevia rebaudiana II. High performance liquid chromatographic separation and quantitation of stevioside, rebaudioside A and rebaudioside. C", *J. Chromatogr.*, **236**, 523–526 (1982).

Alemdar, S. and Agaoglu, S., "Investigations of in-vitro antimicrobial activity of aloe vera juice", *J. Anim. Vet. Adv.*, **8**, 99-102 (2009).

Al-Khuseibi, M. K., Sablani, S. S. and Perera, C. O., "Comparison of water blanching and high hydrostatic pressure effects on drying kinetics and quality of potato", *Dry. Technol.*, **23**, 2449–2461 (2005).

Andreatta, M. M., Munoz, S. E., Lantieri, M. J., Eynard, A. R. and Navarro, A., "Artificial sweetener consumption and urinary tract tumors in Cordoba", *Prev. Med.*, **47**, 136-139 (2008).

Arslan, R. and Ozcan, M. M., "Study the effect of sun, oven and microwave drying on quality of onion slices", *Food Sci. Technol.*, **43**, 1121-1127 (2010).

Basu, S., Yoffe, P., Hills, N. and Lustig, R. H., "The Relationship of Sugar to Population-Level Diabetes Prevalence: An Econometric Analysis of Repeated Cross-Sectional Data", *Sugar and Diabetes.*, **8**, 1-8 (2013).

Bhandary, M. J., Chandrashekar, K. R. and Kaveriappa, K. M., "Medical ethnobotany of Siddis of Uttara Kannada district, Karnataka, India", *J. Ethnopharmacol*., **47**, 149–158 (1995).

Bozzi, A., Perrin, C., Austin, S. and Vera, A. F., "Quality and authenticity of commercial aloe vera gel powders", *Food Chem*., **106**, 22-30 (2007).

Bray, G. A., Nielsen, S. J. and Popkin, B. M., "Consumption of high-fructose corn syrup in beverages may play a role in the epidemic of obesity1,2", *Am. J. Clin. Nutr.*, **79**, 537-543 (2004).

Bridel, M. and Lavieille, R., "Le principle a Saveur Sucree du Kaa-he-e Stevia rebaudiana Bertoni", *Bull. Soc. Chem. Biol.*, **13**, 636–655 (1931).

Brown, C. M., Dulloo, A. G. and Montani, J. P., "Sugary drinks in the pathogenesis of obesity and cardiovascular diseases", *Int. J. Obes.*, **32**, S28-S34 (2008).

Caroline, M. A., "Sugar-sweetened soft drinks, obesity, and type 2 diabetes", *J. Am. Med. Assoc.*, **292**, 978-979 (2004).

Caroline, S. T., "GLG Life Tech seeks stevia market development in India", [AP-Food Technology.com], (2010).

Cassano, A., Drioli, E., Galaverna, G., Marchelli, R., Silvestro, G. D. and Cagnasso, P., "Clarification and concentration of citrus and carrot juices by integrated membrane processes", *J. Food Eng.*, **57**, 153–163 (2003).

Chang, S. S. and Cook, J. M., "Stability Studies of Stevioside and Rebaudioside A in Carbonated Beverages", *J. Agric. Food Chem.*, **31**, 409-412 (1983).

Chang, J., "Medicinal herbs: drugs or dietary supplements?", *Biochem. Pharmacol.*, **59**, 211–219 (2000).

Chang, I. S., Clech, P. L., Jefferson, B. and Judd, S., "Membrane fouling in membrane bioreactors for wastewater treatment", *J. Environ. Eng.*, **128**, 1018–1029 (2002).

Chatsudthipong, V. and Muanprasat, C., "Stevioside and related compounds: Therapeutic benefits beyond sweetness", *Pharmacol. Ther.*, **121,** 41-54 (2009).

Choi, Y. H., Kim, I., Yoon, K. D., Lee, S. J., Kim, C. Y., Yoo, K., Choi, Y. and Kim, J., "Supercritical fluid extraction and liquid chromatographic electrospray mass

spectrometric analysis of stevioside from Stevia rebaudiana leaves", *Chromatographia*, **55**, 617–620 (2002).

Dacome, A. S., Silva, C. C. and Costa, C. E. M., "Sweet diterpenic glycosides balance of a new cultivar of Stevia rebaudiana (Bert.) Bertoni: isolation and quantitative distribution by chromatographic, spectroscopic, and electrophoretic methods", *Process Biochem*, **40**, 3587-3594 (2005).

Douglas, L. A., "Toxicology of saccharin", *Fundamental and Applied Toxicology*, **4**, 674-685 (1984).

Erkucuk, A., Akgun, I. H. and Yesil-Celiktas, O., "Supercritical CO_2 extraction of glycosides from Stevia rebaudiana leaves: Identification and optimization", *J. Supercrit. Fluids.*, **51**, 29–35 (2009).

Eshun, K. and He, Q., "Aloe vera: a valuable ingredient for the food, pharmaceutical and cosmetic industries: a review", *Crit. Rev. Food. Sci. Nutr.* **44,** 91–96(2004).

Femenia, A., Garcia-Pascual, P., Simal, S. and Rossello, C., "Effects of heat treatment and dehydration on bioactive polysaccharide acemannan and cell wall polymers from Aloe barbadensis Miller", *Carbohydr. Polym.*, **51**, 397-405 (2003).

Fuh,W. S. and Chiang, B. H., "Purification of Stevioside by membrane and ion exchange processes", *J. Food Sci.*, **55**, 1454–1457 (1990).

Garcia-Segovia, P., Mognetti, C., Andres-Bello, A. and Martinez-Monzo, J., "Osmotic dehydration of aloe vera (Aloe barbadensis Miller)", *J. Food Eng.*, **97**, 154-160 (2010).

Giovanetto, R. H., "Method for the recovery of steviosides from plant raw material", *US Patent*, 4,892,938 (1990).

Grenby, T. H., "Intense sweeteners for the food industry: an overview", *Trends Food Sci. Tech.*, **2**, 2-6 (1991).

Grindlay, D. and Reynolds, T., "The aloe vera phenomenon: A review of the properties and modern uses of the leaf parenchyma gel", *J. Ethnopharmacol.*, **16**, 117-151 (1986).

Gulia, A., Sharma, H. K., Sarkar, B. C., Upadhyay, A. and Shitandi, A., "Changes in physico-chemical and functional properties during convective drying of aloe vera (Aloe barbadensis) leaves", *Food Bioprod. Process.*, **88**, 161-164 (2010).

Haga, T., Ise, R. and Kobayashi, T., "A method for purifying stevioside", *Jap. Patent*, 51-131900 (1976).

Hai, N. V., "The use of medicinal plants as immunostimulants in aquaculture: A review", *Aquaculture*, **446**, 88-96 (2015).

Hamman, J. H., "Composition and applications of Aloe vera leaf gel", *Molecules*, **13**, 1599-1616 (2008).

Harikrishnan, R., Balasundaram, C. and Heo, M. S., "Review: impact of plant products on innate and adaptive immune system of cultured finfish and shell fish", *Aquaculture*, **317**, 1-15 (2011).

Hawthorne, S. B., Yang, Y. and Miller, D. J., *Anal. Chem.*, **66**, 2912 (1994).

Huang, X., Fang-Fu, J. and Di Duo-Long., "Preparative isolation and purification of steviol glycosides from Stevia rebaudiana Bertoni using high-speed counter-current chromatography", *Sep. Purif. Technol.*, **71**, 220–224 (2010).

Itagaki, K. and Ito, T., "Purification of stevioside", *Jap. Patent*, 54, 041898 (1979).

Jain, S. P. and Puri, H. S., "Ethnomedicinal plants of Jaunsar-Bawar Hills, Uttar Pradesh, India", *J. Ethnophamacol.*, **12**, 213-222 (1984).

Jaitak, V., Singh, B. B. and Kaul, V. K., "An Efficient Microwave-assisted Extraction Process of Stevioside and Rebaudioside-A from Stevia rebaudiana (Bertoni)", *Phytochem. Anal.*, **20**, 240-245 (2009).

Jiang, Z. J., Liu, F., Goh, J. J. L., Yu, L. J., Li, S. F. Y., Ong, E. S. and Ong, C. N., "g, Determination of senkirkine and senecionine in Tussilago farfara using microwave-assisted extraction and pressurized hot water extraction with liquid chromatography tandem mass spectrometry", *Talanta*, **79**, 539-546 (2009).

Johnson, R. J., Segal, M. S., Sautin, Y., Nakagawa, T., Feig, D. I., Kang, D-H., Gersch, M. S., Benner, S. and Sanchez-Lozada, L. G., "Potential role of sugar (fructose) in the epidemic of hypertension, obesity and the metabolic syndrome, diabetes, kidney disease, and cardiovascular disease1,2,3", *Am. J. Clin. Nutr*., **86**, 899-906 (2007).

Joshi, S. R. and Parikh, R. M., "India - diabetes capital of the world: now heading towards hypertension", *J. Assoc. Physicians. India*, **55**, 323–324(2007).

Kalderis, D., Hawthorne, S. B., Clifford, A. A. and Gidarakos, E., "Interaction of soil, water and TNT during degradation of TNT on contaminated soil using subcritical water.", *J. Hazard. Mater.*, **159**, 329-334 (2008).

Kikuchi, K., "Steviosides derivative as a new sweetener", *Food Sci.*, **85**, 52 (1985).

Kim, W-J., Kim, J., Veriansyah, B., Kim, J-D., Lee, Y-W., Oh, S-G. and Tjandrawinata, R. R., "Extraction of bioactive components from Centella asiatica using subcritical water", *J. Supercrit. Fluids*, **48**, 211-216 (2009).

Kinghorn, A. D. and Kim., "Stevia: The genus Stevia", Taylor & Francis., (2002).

Kinghorn, A. D., Nanayakkara, N. P. D., Soejarto, D. D., Medon, P. J. and Kamath, S., "Potential sweetening agents of plant origin. I. Purification of Stevia rebaudiana sweet constituents by droplet counter-current chromatography", *J. Chromatogr*., **237**, 478–83 (1982).

Kobayashi, M., Harikawa, S., Degrandi, I. H., Ueno, J. and Mitsuhashi, H., "Dulcosides A and B, new diterpene glycosides from Stevia rebaudiana", *Phytochem*., **16**, 1405–1408 (1977).

Kohda, H., Kasai, R., Yamasaki, K., Murakami, K. and Tanaka, O., "New sweet diterpene glycoside from Stevia rebaudiana", *Phytochem.*, **15**, 981–983 (1976).

Kopjar, M., Pilizota, V., Hribar, J., Simcic, M., Zlatic, E. and Nedic Tiban, N., "Influence of trehalose addition and storage conditions on the quality of strawberry cream filling", *J. Food Sci.*, **87**, 341–350 (2008).

Kroger, M., Meister, K. and Kava, R., "Low-calorie Sweeteners and Other Sugar Substitutes: A Review of the Safety Issues", *Comp. Rev. Food Sci. Food Saf.*, **5**, 35-47 (2006).

Kumar, A., Goel, M. K., Jain, R. B., Khanna, P. and Chaudhary, V., "India towards diabetes control: Key issues", *Australas Med. J.*, **6**5, 24–31 (2013).

Kumar, S., "Methods for recovery of stevioside", *US Patent*, 4,599,403 (1986).

Kutowy, O., Zhang, S. Q. and Kumar, A., "Extraction of sweet compounds from Stevia rebaudiana Bertoni", *US patent*, 5,972,120 (1998).

Larry, W. and Greenly, D. C., "A doctor's guide to sweeteners", *J. Chiropr. Med.*, 2, 80-86 (2003).

Lawless J, Allen J (2000) Aloe vera- Natural wonder care. Harper Collins Publishers, Hammersmith, pp 5–12.

Li, J., Chen, Z. and Di, D., "Preparative separation and purification of Rebaudioside A fromStevia rebaudiana Bertoni crude extracts by mixed bed of macroporous adsorption resins", *Food Chem.*, **132**, 268-276 (2012).

Liu, J., Li, J. and Tang, J., "Ultrasonically assisted extraction of total carbohydrates from Stevia rebaudiana Bertoniand identification of extracts", *Food Bioprod. Process.*, **88,** 215-221 (2010).

Lobo, R., Prabhu, K. S., Shirwaikar, A., Ballal, M., Balachandran, C. and Shirwaikar, A., "A HPTLC densitometric method for the determination of aloeverose in Aloe vera gel", *Fitoterapia*, **81**, 231–233 (2010).

Marques, L. G. and Freire, J. T., "Analysis of freeze-drying of tropical fruits", *Dry. Technol.*, **23**, 2169-2184 (2005).

Maundu, P., Berger, D. J., Ole., Saitabau, C., Nasieku, J., Kipelian, M., Mathenge, S. G., Morimoto, Y. and Hoft, R., "Ethnobotany of the Loita Maasai: Towards Community Management of the Forest of the Lost Child —Experiences from the Loita Ethnobotany Project", People and Plants working paper 8. UNESCO, Paris (2001).

Mauri, P., Catalano, G., Gardana, C. and Pietta, P., "Analysis of Stevia glycosides by capillary electrophoresis", *Electrophoresis*, **17**, 367-371 (1996).

Miranda, M., Héctor, M., Katia, R. and Vega-Galvez, A., "Influence of temperature on the drying kinetics, physicochemical properties, and antioxidant capacity of Aloe Vera (Aloe Barbadensis Miller) gel", *J. Food Eng*., **91**, 297–304 (2009).

Mondal, S., Chhaya. and De, S., "Prediction of ultrafiltration performance during clarification of stevia extract", *J. Membr. Sci*., **396**, 138-148 (2012a).

Mondal, S., Chhaya. and De, S., "Modeling of cross flow ultrafiltration of stevia extract in a rectangular cell", *J. Food Eng*., **112**, 326-337 (2012b).

Mondal, S., Rai, C. and De, S., "Identification of fouling mechanism during ultrafiltration of stevia extract", *Food Bioprocess Technol*., **6**, 931-940 (2013).

Moraes, E. P. and Machado, N. R. C. F., "Clarification of Stevia rebaudiana (Bert.) Bertoni extract by adsorption in modified zeolites", *Maringa*, **23**, 1375-1380 (2001).

Nataraj, S., Schomacker, R., Kraume, M., Mishra, I. M. and Drews, A., "Analyses of polysaccharide fouling mechanisms during cross-flow membrane filtration", *J. Membr. Sci*., **308**, 152–161 (2008).

Nieto, A., Borrull, F., Marce, R. M. and Pocurull, E., *Curr. Anal. Chem*., **4**, 157 (2008).

Nikolova-damyanova, B., Bankova, V. and Popov, S., "Separation and quantitation of stevioside and rebaudioside A in plant extracts by normal-phase high performance liquid chromatography: a comparison", *Phytochem. Anal*., **5**, 81–85 (1994).

Ogawa, T., Nozaki, M. and Matsui, M., "Total synthesis of stevioside", *Tetrahedron*, **36**, 2641–2648 (1980).

Okos, M. R., Narsimhan, G., Singh, R. K. and Weitnauer, A. C., "Food dehydration" In: Hand book of food engineering, (D.R. Heldman, D.B. Lund and C. Sabliov, eds.), CRC Press., (1982).

Ouyang, X., Cirillo, P., Sautin, Y., McCall, S., Bruchette, J. L., Diehl, A. M., Johnson, R. J. and Abdelmalek, M. F., "Fructose consumption as a risk factor for non-alcoholic fatty liver disease", *J. Hepatol*., **48**, 993-999 (2008).

Ozbek, B. and Dadali, G., "Thin-layer drying characteristics and modelling of mint leaves undergoing microwave treatment", *J. Food Eng*., **83**, 541-549 (2007).

Pasquel, A., Meireles, M. A. A., Marques, M. O. M. and Petenate, A. J., "Extraction of stevia glycoside with CO_2+Water, CO_2+Ethanol and CO_2+Water+Ethanol", *Braz. J. Chem. Eng*., **17**, 271–282 (2000).

Pasricha, S., "Stevia beverages and replacing aspartame. Frost & Sullivan", (2009).

Persinos, G. J., "Method of producing stevioside", *US Patent*, 3723410 (1973).

Phillips, K. C., "Stevia: Steps in developing a new sweeteners", In: Grenby TH, editor.Developments in sweeteners, Vol.3. London: Elsevier Applied Science., 1–43 (1989).

Pol, J., Hohnova, B. and Hyotylainen, T., "Characterisation of Stevia Rebaudiana by comprehensive two-dimensional liquid chromatography time-of-flight mass spectrometry", J. Chromatogr. A, **1150**, 85–92 (2007a).

Pol, J., Ostra, E. V., Karasek, P., Roth, M., Benesova, K., Kotlarikova, P. and Caslavsky, J., "Comparison of two different solvents employed for pressurised fluid extraction of stevioside from Stevia rebaudiana: methanol versus water", *Anal. Bioanal. Chem*., **388**, 1847–1857 (2007b).

Prabhanjan, D. G., Ramaswamy, H. S. and Raghavan, G. S. V., "Microwave-assisted convective air drying of thin layer carrots", *J. Food Eng*., **25**, 283-293 (1995).

Puri, M., Sharma, D. and Tiwari, A. K., "Downstream processing of stevioside and its potential applications", *Biotechnol. Adv*., **29**, 781–791 (2011).

Rai, P., Majumdar, G. C., DasGupta, S. and De, S., "Effect of various pretreatment methods on permeate flux and quality during ultrafiltration of mosambi juice", *J. Food Eng*., **78**, 561–568 (2007).

Rajan, S., Sethuraman, M. and Mukherjee, P. K., "Ethnobiology of the Nilgiri hills, India", *Phytother. Res*., **16**, 98–116 (2002).

Ramachandra, C. T. and Rao, P. S., "Processing of Aloe vera leaf gel: A review", *Am. J. Agric. Biol. Sci.*, **3**, 502-510 (2008).

Ramesh, K., Singh, V. and Megeji, N. W., "Cultivation of Stevia Stevia rebaudiana (Bert.) Bertoni: a comprehensive review", *Adv. Agron*., **89**, 137–177 (2006).

Rao, A. B., Reddy, G. R., Ernala, P., Sridhar, S. and Ravikumar, Y. V. L., "An improvised process of isolation, purification of Steviosides from Stevia rebaudiana Bertoni leaves and its biological activity", *Int. J. Food Sci. Technol*., **47**, 2554–2560 (2012).

Roberts, H. J., "Aspartame and brain cancer", *Lancet*, **349**, 362 (1997).

Roy, A. and De, S., "Resistance-in-series model for flux decline and optimal conditions of Stevia extract during ultrafiltration using novel CAP-PAN blend membranes", *Food Bioprod. Process*., **94**, 489-499 (2015).

Roy, A. and De, S., "Extraction of steviol glycosides using novel cellulose acetate phthalate (CAP)–Polyacrylonitrile blend membranes", *J. Food Eng*., **126**, 7-16 (2014).

Sadikoglu, H., Ozdemir, M. and Seker, M., "Freeze drying of pharmaceutical products: Research and development needs", *Dry. Technol*., **24**, 849-861 (2006).

Sakamoto, I., Yamasaki, K. and Tanaka, O., "Application of 13 C NMR spectroscopy of chemistry of natural glucoside rebaudioside C a new sweet diterpene glucoside of Stevia rebaudiana", *Chem. Pharm. Bull*., **25**, 844–846 (1977).

Sarkar, B., DasGupta, S. and De, S., "Cross-flow electro-ultrafiltration of mosambi (Citrus sinensis(L.) Osbeck) juice", *J. Food Eng*., **89**, 241–245 (2008).

Severini, C., Baiano, A., Pilli, T. D., Carbone, B. F. and Derossi, A., "Combined treatments of blanching and dehydration: study on potato cubes", *J. Food Eng*., **68**, 289-296 (2005).

Sharma, D., Puri, M., Tiwari, A., Singh, N. and Jaggi, A., "Anti-amnesic effect of Stevioside in scopolamine treated rats", *Ind. J. Pharmacol*., **42**, 164–167 (2010).

Singh, V., Jain, P. K. and Das, C., "Performance of spiral wound ultrafiltration membrane module for with and without permeate recycle: Experimental and theoretical consideration", *Desalination*., **322**, 94–103 (2013).

Singh, V., Purkait, M. K. and Das, C., "Cross flow microfiltration of industrial oily wastewater: experimental and theoretical consideration", *Sep. Sci. Technol*., **46**, 1213-1223 (2011).

Soejarto, D. D., Kinghorn, A. D. and Farnsworth, N. R., "Potential sweetening agents of plant origin. III organoleptic evaluation of stevia leaf herbarium samples for sweetness", *J. Nat. Prod*., **45**, 590–599 (1982).

Surjushe, A., Vasani, R. and Saple, D. G., "Aloe vera: a short review", *Indian J. Dermatol*., **53**, 163-166 (2008).

Tan, S., Shibuta, Y. and Tanaka, O., "Isolation of sweetener from Stevia rebaudiana", Jpn Kokai, Patent no. 63:177,764 (1983).

Tanaka, O., "Steviol-glycosides: new natural sweeteners", *Trends Anal. Chem.*, **1**, 246–248 (1982).

Teo, C. C., Tan, S. N., Yong, J. W. H., Hew, C. S. and Ong, E. S., "Validation of green-solvent extraction combined with chromatographic chemical fingerprint to evaluate quality of Stevia rebaudiana Bertoni", *J Sep Sci*., **32**, 612–622 (2009).

Torreggiani, D. and Bertolo, G., "Present and future in process control and optimization of osmotic dehydration", In: Taylor, Steve L. (Ed.), Advanced in Food and Nutrition Research, vol. 48. Academic Press, Inc., USA, pp. 174–225 (2004).

Touger-Decker, R. and van Loveren, C., "Sugars and dental caries1,2,3,4", *Am. J. Clin. Nutr*., **78**, 881S-892S (2003).

Tsami, E., Krokida, M. K. and Drouzas, A. E., "Effect of method drying on sorption characteristics of model fruit powders", *J. Food Eng*., **38**, 381-392 (1999).

Turner, C. E., David, A. W., Paul, A. S. and Doug, J. T., "Evaluation and comparison of commercially available Aloe vera L. products using size exclusion chromatography with refractive index and multi-angle laser light scattering detection", Int. Immunopharmacol., **4**, 1727–1737 (2004).

Unesh, H., Ise, R. and Kobayashi, T., "Purification of a stevia sweetening agent", *Japanese Patent*, 54,030199 (1977).

Vanneste, J., Sotto, A., Courtin, C. M., Craeyveld, V. V., Bernaerts, K., Impe, J. V., Vandeur, J. S., Taes, B. V. B., "Application of tailor-made membranes in a multi-stage process for the purification of sweeteners from Stevia rebaudiana", *J. Food Eng*., **103**, 285–293 (2011).

Vega, A., Uribe, E., Roberto, L. and Margarita, M., "Hot-air drying characteristics of Aloe vera (Aloe barbadensis Miller) and influence of temperature on kinetic parameters", *Food Sci. Technol*., **40**, 1698-1707 (2007).

Vega-Galvez, A., Notte-Cuello, E., Lemus-Mondaca, R., Zura, L. and Miranda, M., "Mathematical modelling of mass transfer during rehydration process of Aloe vera (Aloe barbadensis Miller)", *Food Bioprod. process*., **87**, 254-260 (2009).

Vega-Galvez, A., Miranda, M., Aranda, M., Henriquez, K., Vergara, J., Tabilo-Munizaga, G. and Perez-Won, M., "Effect of high hydrostatic pressure on functional properties and quality characteristics of Aloe vera gel (Aloe barbadensis Miller)", *Food Chem.*, **129**, 1060-1065 (2011a).

Vega-galvez, A., Uribe, E., Perez, M., Tabilo-Munizaga, G., Vergara, J., Garcia-Segovia, P., Lara, E. and Scala, K. D., "Effect of high hydrostatic pressure pretreatment on drying kinetics, antioxidant activity, firmness and microstructure of aloe vera (Aloe barbadensis Miller) gel", *Food Sci. Technol*., **44**, 384-391 (2011b).

Wang, R., Zhang, M., Mujumdar, A. S. and Sun, J. C. "Microwave freeze-drying characteristics and sensory quality of instant vegetable soup", *Dry. Technol*., **27**, 962–968 (2009).

Wang, Z., Sun, J., Chen, F., Liao, X. and Hu, X., "Mathematical modelling on thin layer microwave drying of apple pomace with and without hot air pre-drying", *J. Food Eng*., **80**, 536-544 (2007).

Wild, S., Roglic, G., Green, A., Sicree, R. and King, H., "Global prevalence of diabetes-estimates for the year 2000 and projections for 2030", *Diabetes Care*, **27**, 1047-1053 (2004).

World Health Organisation, 2002. WHO Traditional Medicine Strategy 2002-2005.

Xanthopoulos, G., Oikonomou, N. and Lambrinos, G., "Applicability of a single-layer drying model to predict the drying rate of whole figs", *J. Food Eng.*, **81**, 553-559 (2007).

Yabesh, J. E. M., Prabhu, S. and Vijayakumar, S., "An ethnobotanical study of medicinal plants used by traditional healers in Silent valley of Kerala, India", *J. Ethnopharmacol.*, **154**, 774–789 (2014).

Ye, F., Yang, R., Hua, X., Shen, Q., Zhao, W. and Zhang, W., "Modification of stevioside using transglucosylation activity of Bacillus amyloliquefaciens a-amylase to reduce its bitter aftertaste", *Food Sci Technol.*, **51**, 524-530 (2013).

Yoda, S. K., Marques, M. O. M., Petenate, A. J. and Meireles, M. A. A., "Supercritical fluid extraction from Stevia rebaudiana Bertoni using CO_2 and CO_2+water: extraction kinetics an identification of extracted components", *J. Food Eng.*, **57**, 125–134 (2003).

Yoo, K. P., Choi, Y. H. and Kim, J., "SFE of Natural pharmaceuticals and nutraceuticals with emphasis on commercialization," In: Tenth International Symposium & Exhibit on Supercritical Fluid Chromatography, Extraction, and Processing, Myrtle Beach, USA (2001).

Zhang, S. Q., Kumar, A. and Kutowy, O., "Membrane based separation scheme for processing sweeteners from Stevia leaves", *Food Res. Int.*, **33**, 617–620 (2000).

भारतीय प्रौद्योगिकी संस्थान गुवाहाटी
Indian Institute of Technology Guwahati

CHAPTER 2

Materials and Methods

In this chapter, the experimental procedures and protocols of analytical methods, namely, high performance liquid chromatography (HPLC), laser particle size analysis, color and clarity test, UV-VIS spectroscopy, Fourier transformed infrared (FT-IR) spectroscopy, carbohydrate and protein estimation and physico-chemical properties test have been discussed. It comprises the extraction processes of stevioside and Reb-A from the stevia leaves, ultrafiltration of extract and dehydration methodologies of aloe vera. Specifications of all the chemicals and reagents are also documented.

CHAPTER 2

Materials and Methods

2.1 Chemicals and reagents

Pure stevioside (>98% assay) and Reb-A (>96% assay) were procured from M/s Sigma- Aldrich (USA). Dried and ground stevia leaves were obtained from M/s RAS Agro Associates, Maharashtra, India. Aloe vera was planted in the vicinity of the Chemical Engineering Department at IIT Guwahati, India. HPLC grade acetonitrile was purchased from M/s Merck India Ltd., Mumbai, India. Polyethersulfone (PES) membranes of 10, 20, 30 and 50 kDa were supplied by M/s Permionics Membrane Pvt. Ltd., Vadodara, Gujarat, India. Other chemicals and reagents were procured mostly from Merck, Mumbai (India), Loba-Chemie, Mumbai (India) and Himedia (India) are listed in Table 2.1.

Table 2.1: List of common chemicals/reagents used for analytical tests.

Reagents/chemicals	Purity (%)	Grade	CAS	Make
Stevioside	≥98	HPLC	57817-89-7	Sigma-Aldrich (USA)
Reb-A	≥96	HPLC	58543-16-1	
Acetone ($CH_3CO\ CH_3$)	99	AR	67-64-1	Merck, Mumbai (India)
Acetonitrile (CH_3CN)		HPCL		
Buffer solution pH 4.0 (phthalate)	99	AR	91-05-11	
Buffer solution pH 7.0 (phthalate)	99	AR	99-62-00	
Dipotassium hydrogen phosphate (K_2HPO_4)	99	AR	10361-37-2	
Di-sodium hydrogen orthophosphate (Na_2HPO_4)	99	AR	7758-79-4	
Methanol (CH_4OH)	99	AR	67-56-1	
Nitric acid (HNO_3)	70	AR	7697-37-2	
Phenol (C_6H_5OH)	99	AR	108-95-2	
Potassium bromide (KBr)	99.5	GR	03-02-7758	
Sulphuric acid (H_2SO_4)	98	AR	7664-93-9	
Ethanol (C_2H_5OH)	99.9	AR	GB678-90	Changshu Yangyuan Chemicals (China)

De-ionized water (Model: Elix 3, Millipore, USA) was used for the preparation of all the reagents, standard solution, and extraction media. All the plastic wares used were made of polypropylene procured from M/s Tarson Products Pvt. Ltd., Kolkata (India). Glassware with a low coefficient of thermal expansion was obtained from Borosil, Mumbai (India).

2.2 Analytical methods

2.2.1 Particle size distribution

The dried and ground stevia leaves are composed of a different fraction of particle size. It was screened through 120 mesh and, the oversize particles and impurities were discarded. A precision Laser Particle Size Analyzer (LPSA) (M/s Malvern Instruments UK, Model: Master Seizer 2000) was employed to determine the size distribution of the undersized leaves particles.

The method of particle size distribution was based on the size of a particle using the angle and intensity of scattered light when particles are irradiated with a laser beam. For particles larger than a certain size, the majority of light distribution pattern is vastly by diffraction. These larger particles diffract light at narrow angles with high intensity and, the 'certain size' is determined as a multiple of the wavelength of light used for the measurement. Higher particle size scatters light through diffraction and not by refraction. The smaller particles reflect light at wider angles but with low intensity (Bohren and Huffman, 2007). The use of a refractive index directly affects the accuracy of this size range. The optical properties of the dispersant can be found out from published data, and many modern instruments have inbuilt databases that include common dispersants. The particle size is determined as a volume equivalent sphere diameter.

2.2.2 Functional group identification

The presence of different functional groups in various samples was confirmed by obtaining the FT-IR spectra using KBr pellet method. FT-IR spectrophotometer (M/s Shimadzu, Japan; Model: IR affinity 1) was employed for this purpose. Analytical grade KBr was dried overnight at 105°C in a hot air oven (Model: ISO 9001-2008; Make: Navyug, India). The sample to KBr in a ratio of 1:99 (w/w) was mixed and, ground in a clean mortar and pestle for the homogenization. It was then transferred to pellet casting die. The sample was pressurized under 5 to 7 tons to create a thin circular disk. The background correction was done at first with pure KBr pellet by scanning in the range from 450 to 4500 cm^{-1} wavenumber with a resolution of 5 cm^{-1}. The mixed sample was scanned in the same range. The number of scans was 45 for each specimen for the noise reduction.

2.2.3 UV-Vis spectroscopy to determine the absorbance of stevia extracts and permeates

UV-Vis spectrophotometer (Thermo Scientific, India; Model: UV-2300) with an optical path length of 1 cm was used to acquire absorbance/transmittance spectra of the samples. The diluted solution of stevioside and Reb-A were used to find out their concentrations using the chromatographic technique by scanning in the suitable wavelength range for absorption maxima. Color and clarity of stevia extracts and permeates, and total carbohydrate were determined by spectrophotometrically.

The principle of UV-Vis spectroscopy is based on Beer-Lambert law. A source of monochromatic light with continuous UV spectrum (200-380 nm wavelength) and visible light (380-780 nm wavelength) split into two equal intensity beams by a half-mirrored device. One part of the beam passes through the sample container while other passes through a

reference substance. The spectrometer records the wavelengths of all the components passing through the sample containers. The net intensity of each wavelength is measured by electronic detectors and, produces a graph, called a spectrum.

2.2.4 HPLC for measurement of stevioside and Reb-A concentration in stevia extracts and permeates

High Performance Liquid Chromatography (M/s Simadzu, Japan; Model: LC-20AD) was employed to determine the concentration of stevioside and Reb-A in extracts and permeates. The sample was injected into an amine column (4.6 mm I.D., 250 mm length, and 5 µm particle size). The mobile phase was acetonitrile and water mixture in the ratio of 80:20 ratio (v/v) for the chromatographic separation at the flow rate of 1 mL/min in UV detection mode at 210 nm wavelength. The retention times for stevioside and rebaudioside A were around 12 and 20 min, respectively (Figure A2).

The calibration curve was prepared by plotting known stevioside and Reb-A concentrations in the horizontal axis and corresponding area in the vertical axis. A straight line (R^2 = 0.997), passing through origin was obtained for Reb-A (Figure A3).

Stevioside and Reb-A content in stevia leaves were determined using the protocol published by 68th JECFA (2007). In this method of assay, standard solutions of stevioside and Reb-A were prepared separately. The mobile phase was acetonitrile and water mixture at 80:20 ratio (v/v) for the chromatographic separation at the flow rate of 1 mL/min in UV detection mode at 210 nm wavelength. pH of the mobile phase was maintained at 3.0 using phosphoric acid (5.9 N). Standard solution of stevioside was prepared by mixing with the mobile phase composition at 1:2 (w/v) ratio. The leaves extract was prepared by adding 100 mg dried stevia leaves into 100 mL mobile phase. The percentage of each steviol glycosides is estimated using the following formula (Eq. 2.1).

$$\text{Steviol glycoside (\%)} = \frac{W_s}{W} \times \frac{f_x A_x}{A_s} \times 100 \quad (2.1)$$

Where, W_s is the amount (mg) of stevioside in the standard solution; W is the amount (mg) of leaves in the sample solution; A_s is the peak area for stevioside from the standard solution; A_x is the peak area of steviol glycoside for the sample solution, and f_x is the ratio of the formula weight of steviol glycoside to the formula weight of stevioside.

2.2.5 Color, clarity and total solid tests

The color of clarified stevia extracts was measured in terms of optical absorbance (A) at 420 nm wavelength by UV–Vis spectrophotometer. Clarity of the extracts was measured as percentage transmittance (% T), where % $T = 100 \times 10^{-A}$. A is the optical absorbance at 660 nm (Singh et al., 2013).

Total solids (TS) were measured gravimetrically (Singh et al., 2013). The samples were heated at 105 ± 2°C in a hot air oven until constant weight was reached for two successive time intervals. TS of samples were reported in mg L^{-1}.

2.2.6 Carbohydrate content estimation

Carbohydrate content in dried aloe vera gel was estimated by the method of phenol-sulphuric acid. 5% (w/v) aqueous phenolic solution, concentrated sulphuric acid and aloe vera gel were added at 1:5:1 ratio (v/v/v). Then, the solution was heated at 80°C to form a yellowish color complex. A color complex is formed by the reaction between phenol and glucose in acidic solution. The absorbance was measured at 490 nm in UV-Vis spectrophotometer against the blank solution (Pawar and D'Mello, 2011). Carbohydrate concentration was calculated from the calibration curve. A fingerprint of carbohydrate content was obtained by HPLC using an amine column. Acetonitrile and water (80:20 v/v) at

flow rate of 1 mL/min was used as the mobile phase. Glucose was used as a reference compound for the chromatographic peak identification (http://web.vscht.cz/~kohoutkj/ENG/LAPP_ANGL_LC2_2012.pdf, Dt. 24.06. 2016).

2.2.7 Protein content estimation

Protein content was measured using the standard Bradford method (AOAC 1990). The process involves the formation of a complex between Brilliant Blue G dye and proteins. The protein-dye complex caused a shift in the maximum absorbance of wavelength from 465 to 595 nm. Like, carbohydrate, a chromatographic evidence of protein content was also obtained using a C18 column and, same mobile phase and flow rate. Here, Bovine serum albumin (BSA) was used for the chromatographic identification (http://nptel.ac.in/courses/102103047/26xesxewx, Dt. 24.06.2016).

2.2.8 Ash content/Inorganic residues

The amount of ash content/inorganic residues in fresh and dried aloe vera gel was measured gravimetrically. According to the AOAC method, samples were heated overnight at 550°C (AOAC 1990).

2.2.9 Functional properties

The swelling test measures the bed volume of water retained by dried aloe vera gel at equilibrium with excess solvent. 20 mg dried sample was soaked in 8 mL DI water. The suspension was stirred occasionally and kept for 16 h to attain the equilibrium. After equilibrium, the change in volume was recorded and expressed as mL/g d.m. (Femenia et al. 2003).

Water retention capacity (WRC) is a measure of water retained by the fibrous material, expressed in terms of mass. 25 mg of dried sample was soaked in 5 mL DI water for 24 h and, it was then centrifuged at 3940*g* for 30 min. The supernatant was filtered. The residual solids in the supernatant along with the pellet was weighted and dried at 102°C for overnight. The pellet was cooled and further weighted. WRC was calculated as water retained by per g of dry material (g/g d.m.) (Femenia et al. 2003).

Fat adsorption capacity (FAC) was determined by measuring the amount of oil (sunflower) adsorbed by dried samples (10–30 mg) when soaked in oil (2–6 mL) for overnight at room temperature. The suspension was centrifuged at 3940*g* for 30 min and, excess oil was decanted. FAC was expressed as g oil/g d.m. (Femenia et al. 2003).

The details of various instruments used to conduct this work are summarized in Table 2.2.

Table 2.2: Instrumental details for analysis of experimental work.

Instrument	Model and make	Purpose	Detection/performance range
Analytical balance	Make: Sartorius Model: BSA 224S-CW India	To measure various reagents and samples weight	0 to 220 g, Resolution: 0.1 mg
Centrifuge	Model: HA01-10092 Make: Remi India	To centrifuge aloe vera gel	Maximum speed: 8000 rpm
FT-IR spectrometer	Make: Shimadzu Model: IR affinity 1 Japan	Functional group characterization	Frequency: 350 to 7500 cm^{-1}
HPLC	Make: Simadzu Model: LC-20AD Japan	To determine the concentration of stevioside and Reb-A in extracts and permeates	0.01 to 1µg/mL
Hot air oven	Make: Universal hot air oven Navyug Model: NU-101 India	To dry some reagents and hot air drying of aloe vera gel	Temperature: 30 to 250°C

Hot plate	Make: Tarsons Model: Spinot India	To heat up and magnetic stirring of samples	
Laser particle size analyzer	Make: Malvern Instruments Model: Master Seizer 2000 UK	To determine the particle size distribution of grounded stevia leaves	0.02 to 2000 µm
Lyophilizer	Make: Martin Christ Model- ALPHA 2-4 LDplus,Serial-A6A65 Germany	To lyophilize the aloe vera gel	Condenser capacity: 4 kg Condenser temperature: -85 °C
Magnetic stirrer	Make: Tarson Model: Spinot 6020 India	For magnetic stirring of samples	Stirrer speed: 100 to 1000 rpm
Micropipette Capacity	Make: Tarson Model: T100 & T1000 India	To liquid sample pipetting out in µL range for analytical works	T100:10 to 100 µL T1000:100 to 1000 µL
Microwave oven	Make: LG Electronics Model: MH-2046HB India	For microwave assisted drying of aloe vera	Frequency: 2450 MHz (fixed) Microwave: 800 W (fixed)
Millipore water purification unit solutions	Make: Millipore Model: Elix 3 USA	To prepare the analytical samples	TOC: <30 µg/L Pyrogens (endotoxins):<0.001 EU/mL Water resistivity (@ 25 °C): >5 MΩ cm
Mixer and blender	Make: Philips Model: HLI 606 India	To blending the aloe vera gel	500 W
Orbital shaker	Make: Lab Tech Model: LSI-3016R Korea	To agitate the aloe vera and stevia samples and, reagents	Maximum speed: 350 rpm Temperature: ± 0.5°C
pH meter	Make: Eutech Instruments Model: pH 510 Singapore	To measure pH of stevia and aloe vera samples	pH: 0 to 14 Resolution: 0.01 pH
UV-Vis spectrophotometer	Make: Thermofisher Scientific Model: Spectrascan UV-2300 India	To determine the solute concentration by measuring absorbance	Wavelength: 190-1100 nm Resolution: 0.05 nm

2.3 Experimental procedures

2.3.1 Extraction of Reb-A

The grounded stevia leaves were dried at 105°C for 2 h in a hot air oven. A fixed amount of dried stevia leaves was added to 100 mL DI water at a fixed temperature for each run. The particle size distribution of grounded stevia leaves is shown in Figure A1. Borosilicate glass beakers of 250 mLwere used as extraction vessel. Unless otherwise stated, 1 g of stevia leaves per 100 mL of DI water was used to express the percentage leaves to water ratio (% w/v). The desired temperature was maintained by adjusting heat input in a magnetic stirrer hot plate with an in-build heat controller knob. The stirring speed was kept at 700 rpm using a magnetic stirrer bar of 40 mm length and 8 mm O.D. (M/s. Tarsons India). The extract was cooled down to room temperature (27 ± 2°C) in around 30 min. The clear supernatant was then collected by filtration using Whatman filter papers (Grade 1). It was preserved at 4°C prior to HPLC analysis.

The extraction time (t), leaves to water ratio ($\mathscr{R}$) and extraction temperature (T) were independently varied over certain values as shown in Table 2.3.

Table 2.3: Experimental values of process parameters chosen for the experiment of Reb-A extraction.

Parameters	Values
Extraction time, t (min)	15, 30, 45, 60 and 75
Leaves to water ratio, $\mathscr{R}$ (%)	2, 3 and 5
Extraction temperature, T (°C)	50, 60, 70 and 80

2.3.2 Ultrafiltration of stevia extract

2.3.2.1 Experimental setup for ultrafiltration

An unstirred batch and a cross-flow ultrafiltration processes were used separately for clarification of Reb-A from stevia extract.

Unstirred batch setup

The batch cell setup with a capacity of 400 mL, made of stainless steel, was consisted of two matching flanges with an internal groove and a cylindrical vessel of inner diameter of 78 mm. Circular flat sheet membrane was placed over an aluminum grid base on the lower flange to provide mechanical support. The two flanges and the cylinder were tightened, and leak proofed using two rubber gaskets. The effective membrane area was 35.27 cm^2. The feed was poured through the feed inlet and, permeate was collected from the bottom of the lower flange. Air pressure was maintained from a compressor (Matrix, AC 20–50) with an adjustable pressure control valve. The schematic diagram of the batch cell is shown in Figure 2.1.

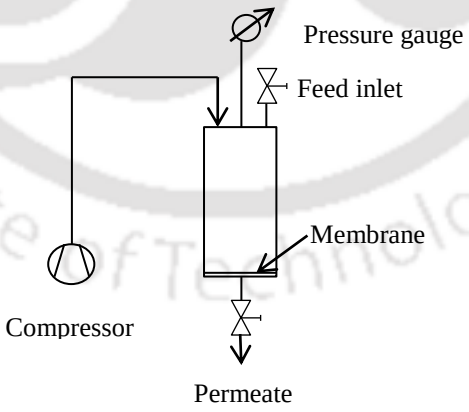

Figure 2.1: Schematic diagram of unstirred batch cell.

Cross-flow ultrafiltration setup

A rectangular cross-flow ultrafiltration cell, made of stainless steel, was used for clarification of stevia extract. The cell was formed using two horizontally matching flanges. The lower flange was internally grooved and, channels were fabricated for permeate flow. The upper flange was seated over the lower flange (Figures 2.2(a) and (b)). The channels in the bottom flange with the internal grid structure are shown in Figure 2.2(c). Rectangular flat sheet membrane was placed over a porous stainless steel plate in the bottom plate to provide mechanical support. The top view of lower plate is shown in Figure 2.2(d). Two flanges were tightened by nuts and bolts to create a leak proof channel. The effective length and width of the membrane available for filtration were 18.5 cm and 6.4 cm, respectively. The height of the flow channel was determined as 2 mm of gasket thickness after tightening the two flanges.

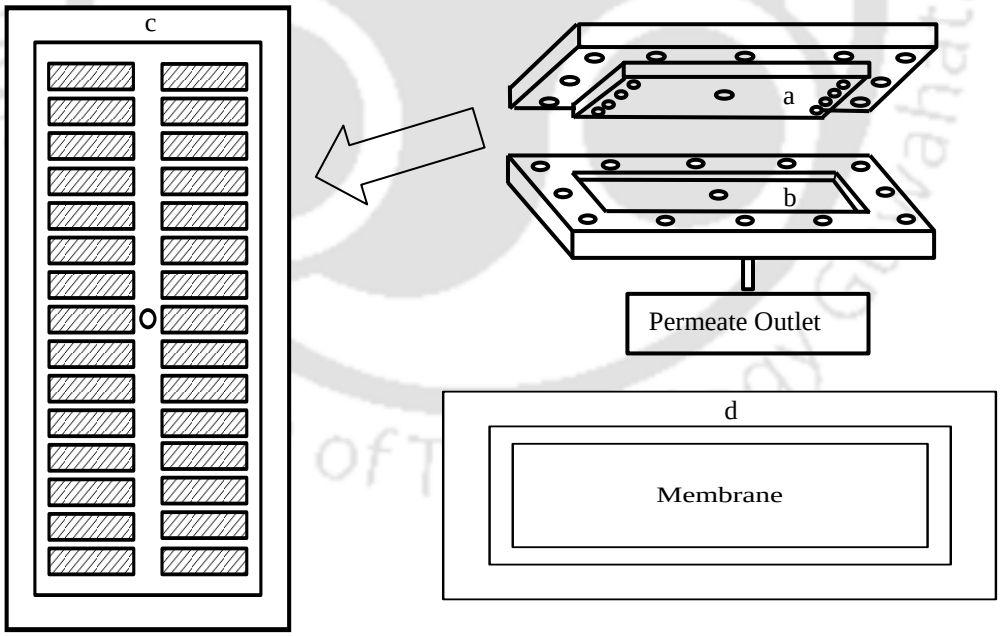

Figure 2.2: Schematic diagram of the cross-flow membrane module. (a) upper flange, (b) lower flange, (c) bottom flange with the internal grid structure and, (d) top view of lower plate with membrane.

The schematic diagram of the experimental setup is shown in Figure 2.3. The stevia extract was poured in a stainless steel feed tank of 6 L capacity. A high pressure reciprocating pump (M/s Aircomp Enterprise, India, Model: T-2, Serial No. 7) was used to circulate the stevia extract into the cross-flow membrane cell. The retentate stream was recycled to the feed tank routed through a rotameter (M/s Five Star Enterprise, India). The permeate stream was also recycled to maintain a constant concentration of feed tank. A bypass line from the pump delivery to the feed tank was also provided. The two valves in the bypass and retentate lines were used to control the pressure and the flow rate independently.

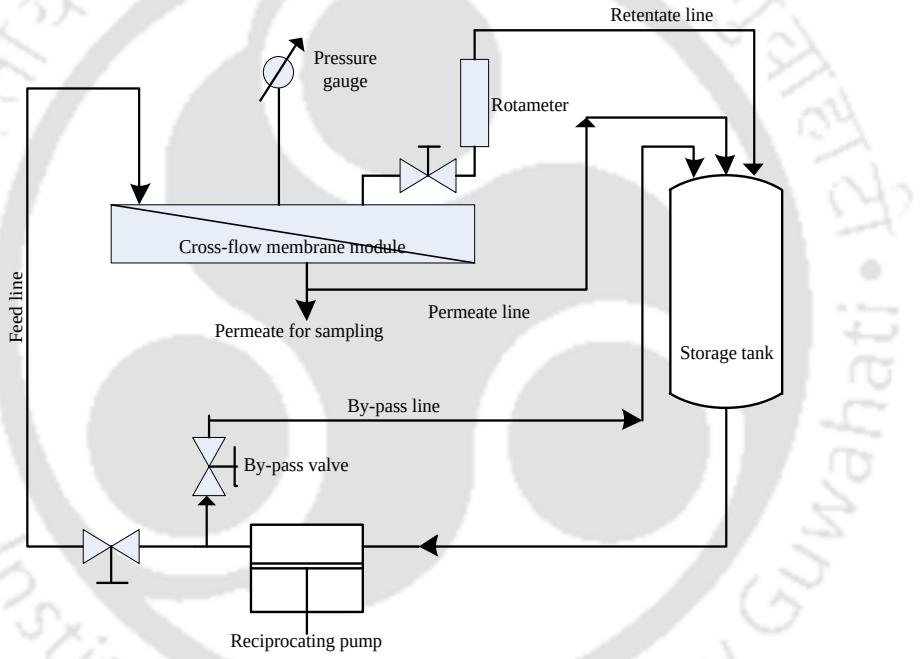

Figure 2.3: Process flow diagram of cross-flow membrane setup.

2.3.2.2 Ultrafiltration in unstirred batch cell

The unstirred batch cell was used for the assessments of % recovery and flux decline behavior. Four different polyethylene sulfone (PES) membranes of MWCO 10, 20, 30 and 50 kDa were compacted separately for an hour at 552 kPa trans-membrane pressure (TMP) drop using distilled water. The steady state water flux was measured at three different TMP drops

of 310, 414 and 517 kPa. 300 mL stevia extract was poured into the cell for filtration. This is one of the reasons for batch system study needing lesser amount of feed extract. The temperature was maintained at 27 ± 2°C. The volume of permeate was collected in a measuring cylinder with the progress of operating time until a steady state flux was reached. The cumulative volume of permeate was collected. The batch cell was dismantled and, membrane was cleaned mechanically by gently rubbing with a brush and, then it was kept in 2% sodium dodecyl sulfate (SDS) solution for overnight before each run. The membrane was again rinsed with distilled water to remove any traces of surfactant. The water permeability was measured before further experiment. The study of permeates quality and fouling behavior at various operating conditions were performed in a cross-flow cell.

2.3.2.3 Cross-flow ultrafiltration

Fresh membranes as used in batch ultrafiltration were also compacted under identical conditions for the cross-flow process. The best performed UF membrane, selected from unstirred batch cell experiments, was used in cross-flow ultrafiltration. 3 L extract was taken in the feed tank and, was circulated through the cross-flow membrane module. Permeate was collected at different time intervals and analyzed for color, clarity, total solids, purity of Reb-A and selectivity. After each experiment, the membrane was washed with distilled water, in situ, at low pressure (69 kPa) for 30 min. The cleaning of membranes and verification of water permeability were carried out as outlined before. All the experiments were performed at 27 ± 2°C.

2.3.3 Dehydration methodologies for aloe vera gel

Fresh leaves corresponding to three and half years old plants were cut from the roster and, washed with distilled water to remove mud and dirt. The serrated edges of the leaves

were removed and suspended vertically to drain all the exudates. The epidermis was then removed from the inner parenchyma filet and sliced into slabs of 10±1 mm thickness. The rectangular pieces of aloe vera gel are shown in Figure 2.4. The experiments were performed in triplicate on three separate days within 1 h after preparing the samples.

Figure 2.4: Rectangular pieces of aloe vera gel.

2.3.3.1 Freeze drying

Aloe vera filets of weight 5±0.2 g were frozen at -20°C in a deep-freezer and, it was then placed on the sample tray in the drying chamber of freeze drier. Freeze drying was carried out in two stages. The first stage was at -50°C and 0.040 mbar pressure and, the second stage was performed at -75°C and 0.010 mbar pressure as per recommendation by the manufacturer. The freeze dried sample was packed in flexible polyethylene pouches and kept at 4°C until further analyses.

2.3.3.2 Hot air drying

Hot air drying (HAD) of aloe vera gel was performed over a wide temperature range, i.e., between 50 and 90°C in a pilot scale hot air oven. The heat was supplied from three sides of the oven to attain a quick and uniform heating. A blower fan at constant air velocity of 1.5 m/s was used to withdraw the moist air from the oven. HAD had been continued until the

equilibrium moisture content was reached. The corresponding moisture at the end of drying was 0.079±0.002 g water/ g dry matter (d.m.). The relative humidity was around 10% during hot air drying process.

2.3.3.3 Microwave-assisted drying

Microwave-assisted drying (MWAD) was performed in a microwave dryer of LG India Ltd. with a facility of a blower fan to pull out moisture from the inside to the surrounding air. The input power and emission time were controlled through a digital terminal. In MWAD, around 6 g of aloe gel slices of thickness 10±1 mm (total weight around 24 g) was taken, into a petri dish and placed inside the microwave dryer. Drying was performed at three different powers, i.e., at 160, 320 and 480 W. MWAD was continued to moisture ratio of 0.05 for microbial stability of the product (Ghanem et al. 2012). The temperature raised during MWAD of aloe vera gel was studied separately. In this experiment, fresh aloe vera filet was blended in a mixer due to the semi-rigid matrix structure. Then, around 5±0.2 g of blended gel, in a small glass beaker, was placed in the microwave oven and dehydrated for 2, 3 and 5 min at different microwave powers, namely 160, 320 and 480 W, respectively. The gel temperature was recorded immediately by placing a thermometer. It was observed that the gel temperature was around 95±2°C irrespective of operating powers and drying time. The process was repeated three times for every sample. Further, the temperature raised within the gel is same as microwave causes volumetric drying and no thermal gradient is developed. So, the temperature during microwave drying remains around 95±2°C.

2.3.3.4 Hybrid drying techniques

Four different hybrid drying processes, namely, ‘centrifugation followed by freeze drying’ (CFFD), ‘microwave followed by freeze drying’ (MWFFD), ‘centrifugation followed

by hot air drying' (CFHAD) and 'microwave followed by hot air drying' (MWFHAD) were performed. Centrifugation is a mechanical dewatering process which can be a feasible pretreatment for solids having high water content. High rotational speed breaks down the lattice structure of solids and separates the residual solids from the water in quick succession. This pretreatment process is economically worthwhile due to its rapid separation of solids from water. During centrifugation process, fresh aloe vera filet was sliced into small pieces and blended in a mixer. Then, the semi-solid blended mixture was centrifuged at 3940*g* for 30 min. After centrifugation, the thick pellet was collected and, the supernatant was further separated by vacuum filter (Whatman filter papers, Grade 1). The residues after vacuum filtration and pellet were kept at 4°C for further use. The centrifugation process was carried out at room temperature (27±2°C). The solid collected was freeze dried in the case of CFFD and, it was hot air dried at 50°C up to an equilibrium moisture content for CFHAD.

In the case of MWFFD and MWFHAD, aloe vera gel was dried using microwave at 160 W up to moisture ratio of 0.4 which corresponded to 60 % water reduction from fresh aloe gel. It was then freeze-dried and hot air dried at 50°C up to equilibrium moisture content for MWFFD and MWFHAD, respectively. Hot air drying followed by freeze drying was not performed since both the drying processes were time-consuming.

References

AOAC, Official Method of Analysis of the Association of Analytical Chemists, 15th ed. Washington, DC. Association of Official Analytical Chemists (1990).

Bohren, C. F. and Huffman, D. R. "Absorption and Scattering of Light by Small Particles", Wiley-VCH Verlag GmbH, Weinheim, Germany (2007).

Femenia A, Garcia-Pascual P, Simal S, Rossello C (2003) Effects of heat treatment and dehydration on bioactive polysaccharide acemannan and cell wall polymers from Aloe barbadensis Miller. Carbohydr Polym 51:397-405.

Ghanem, N., Mihoubi, D., Kechaou, N. and Mihoubi, N.B., "Microwave dehydration of three citrus peel cultivars: Effect on water and oil retention capacities, color, shrinkage and total phenols content", Ind. Crop. Prod. 40, 167-177 (2012).

JECFA, "Steviol glycosides. Combined Compendium of Food Additive Specifications", 68th Meeting of the Joint FAO/WHO Expert Committee on Food Additives. FAO/JECFA Monograph, vol. 4. Food and Agriculture Organization of the United Nations (FAO), Rome, Italy, pp. 61–64 (2007).

Pawar, H. A. and D'Mello, P. M., "Spectrophotometric Estimation of Total Polysaccharides in Cassia Tora Gum", *J. Appl. Pharma. Sci.*, **01**, 93-95 (2011).

Singh, V., Jain, P. K. and Das, C., "Performance of spiral wound ultrafiltration membrane module for with and without permeate recycle: experimental and theoretical consideration", *Desalination*, **322,** 94–103 (2013).

भारतीय प्रौद्योगिकी संस्थान गुवाहाटी
Indian Institute of Technology Guwahati

CHAPTER 3

Rebaudioside-A Extraction, Purification, and Modeling

In this chapter, the extraction of Reb-A using water, a green solvent, was investigated. The central composite design (CCD) was employed to optimize the extraction process and, the artificial neural network (ANN) based modeling was used to predict the extraction yield at various operating conditions.

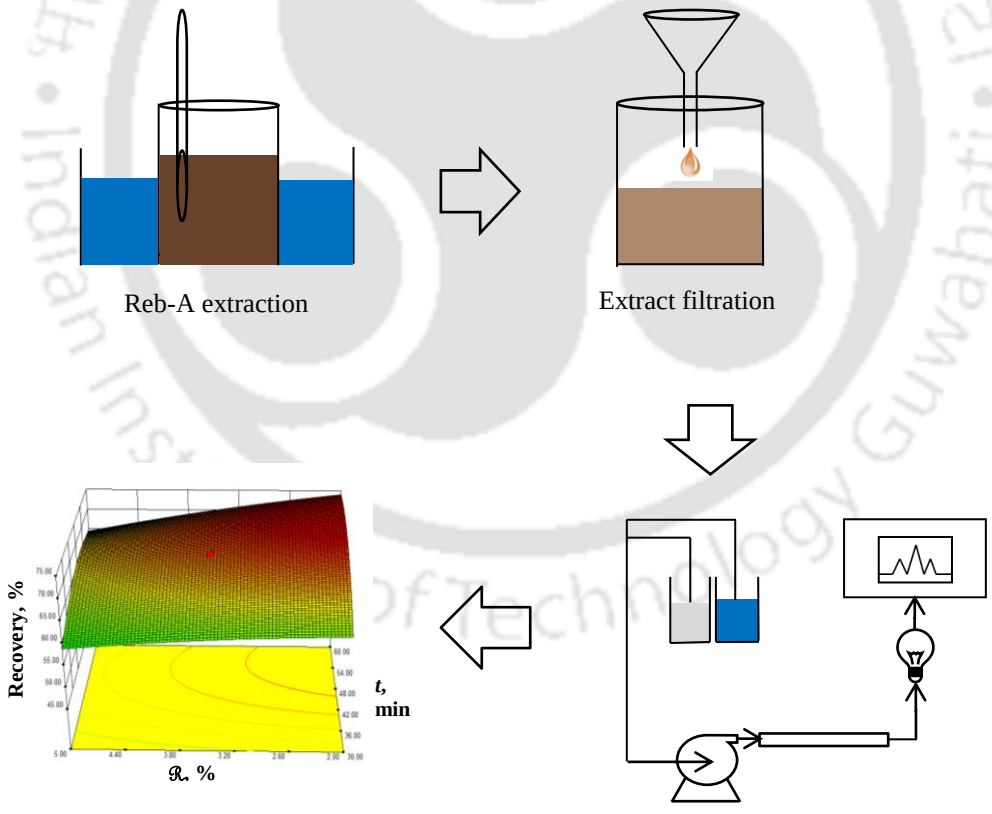

Table of content image

Further, the clarification of stevia extract using ultrafiltration was studied and, the Field's fouling models were tested for their fitness to the flux decline behavior in cross flow.

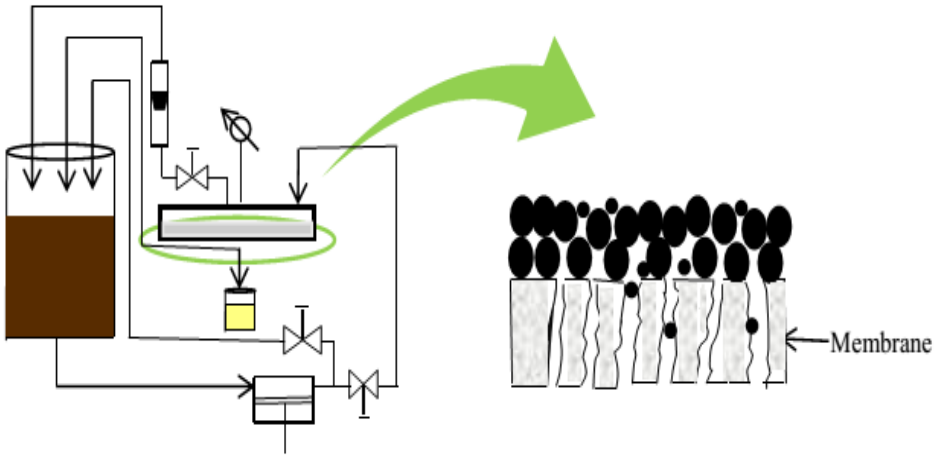

Schematic presentations of stevia extract filtration process and pore blocking

CHAPTER 3

Rebaudioside-A Extraction, Purification, and Modeling

3.1 Extraction of Rebaudioside-A from stevia leaves, modeling and optimization

It is evident from the literature that water is a promising green solvent for the extraction of Reb-A from stevia leaves. The challenges lie with the optimization of such process (Puri et al., 2011) for Reb-A extraction and recovery using water. This part of the work broadly comprises of two parts. Firstly, the effects of leaves concentration at various temperatures even up to 80°C on the dynamics of Reb-A extraction were investigated. Secondly, the optimization of Reb-A extraction was carried out using response surface methodology. Furthermore, the artificial neural network based prediction was performed from a set of 20 experimental runs at various operating conditions.

3.1.1 Response surface methodology

A statistical based optimization technique of process variables has become widespread nowadays for its acceptable outcomes, a concise design of experiments and, minimization of effort, time and resources (Anderson and Whitcomb, 2005).

The prediction of physiochemical processes, such as, drying kinetics and extraction of foods and natural products using empirical and semi-empirical model equations involves large number of theoretical assumptions, initial and boundary conditions, and experimental errors (Aghbashlo et al., 2011). None of the model equations are applicable over a range of

food and natural products, processing techniques and conditions as the processes highly depend on physiochemical properties such as internal tissue structure, water content, and rheological properties. As a result, these models often lead towards erroneous prediction of process variables. Highly complex and nonlinear behavior are involved in the processes of extraction and drying. Response surface methodology (RSM) is a well-equipped tool for process modeling and optimization based on approximation of the objective function by a low-order polynomial on a small subregion of the domain. The main features of RSM include the minimization of hands-on experiments, interactive assessment among process variables and generation of optimum response within the experimental data. It preciously produces the optimized values of process variables through statistical analysis and considering the combined effects of process variables.

Optimization of process parameters hugely improves the performance of the method, product yield, and system operating cost. In the recent years, RSM has been successfully employed for the optimization of various processes like drying, extraction and purification (Diptee et al., 1989; Galvez et al., 1995). In RSM, the interactive dependency of independent variables of the process was taken into consideration.

The central composite design (CCD) is a powerful tool in RSM which generates the best fit empirical equation describing all the independent variables and response and, optimize the process. Based on the number of independent variables, CCD suggests a fixed number of experiments to be performed. CCD analyses the significance of the model and the individual term of the model equation using statistical analysis (ANOVA). In the present study, extraction time (t), leaves to water ratio ($\mathcal{R}$), and temperature (T), were the three independent variables.

"Design-Expert" Version 7 (STAT-EASE Inc., USA) was used for the central composite design (CCD) and graphical analysis. The interactive dependency of independent

variables taken into consideration includes extraction time (t), leaves to water ratio ($\mathcal{R}$) and temperature (T). The circumscribe central composite design was employed for the optimization of process variables, where % recovery of Reb-A was defined as the dependent variable.

3.1.2 Artificial neural network

Artificial neural network (ANN), a computational and mathematical model is developed based on the concept of biological neural networking. ANN is employed to correlate the non-linear relationship between the input and output parameters. ANN is successfully employed to predict various process outcomes such as drying characteristics of agricultural crops (Bala et al., 2005; Menlik et al., 2009; Poonnoy et al., 2007). ANN outperforms RSM to take care of large amounts of noisy data from dynamic and nonlinear systems, especially when the underlying physical phenomena are not well defined (Aghbashlo et al., 2011).

The main structure of ANN is consisted of an input layer (independent variables), hidden layers and output layers (dependent variables). All the variables are termed as neurons. The input layer neurons receive information from data sources. These information pass through the hidden layer to the output layer. The incoming data from the input layer to hidden layer are weighted individually and, modifies using a transform function (Ozdemir et al., 2011). In the hidden layer, all the data are processed and, produces output by summing the weighted values from the input layer.

MATLAB R2009a (The Mathworks, Inc., Ver. 7.8.0.347) neural network toolbox was used in this work. Three independent variables, i.e., t, R and T were in the input layer. The output layer was % recovery of Reb-A. The neural network was trained using a single hidden layer with 3-x-1 topology where x was the number of neurons in the hidden layer. To

determine the optimum number of neurons in the hidden layer, x was varied from 1 to 15. The experimental data in Table 3.1 were used to train the neural network. Total 20 data points were distributed into three sets: training (14 points), validation (3 points) and test set (3 points). All the nine combinations of transfer functions (Tansig, Logsig and Purelin) from input to hidden layer and from hidden to output layer were performed. The best training performance of the neural network was based on the minimization of root mean square error (*RMSE*) and, the highest regression coefficient (R^2).

Table 3.1: Three factors CCD of Reb-A extraction process.

Experiment No.	t min	$\mathcal{R}$ %	T ^{0}C
1	60	5	50
2	30	5	90
3	60	5	90
4	30	2	90
5	45	3.5	70
6	30	5	50
7	60	2	90
8	45	3.5	70
9	30	2	50
10	60	2	50
11	70.23	3.5	70
12	45	3.5	70
13	45	0.98	70
14	45	3.5	70
15	45	3.5	103.64
16	45	3.5	36.36
17	45	3.5	70
18	19.77	3.5	70
19	45	6.02	70
20	45	3.5	70

3.1.3 Results and discussions

3.1.3.1 Leaves to water ratio and temperature on the dynamic of Reb-A extraction

The recovery was defined by the ratio of Reb-A extracted to total Reb-A in the leaves as shown in Eq. 3.1. The amount of Reb-A in stevia leaves was extracted using a mixture of acetonitrile and H_2O (80:20 v/v) with a very low concentration of leaves (i.e., just 0.1 g per 100 mL solvent) to ensure the complete extraction of the steviol glycol according to the JECFA protocol (2007).

$$\text{Recovery (\%)} = \frac{\text{Total extracted Reb-A}}{\text{Total Reb-A in stevia leaves}} \times 100 \qquad (3.1)$$

Figure 3.1 shows the effect of extraction time on the Reb-A recovery. There were two different domains of Reb-A extraction. The rate of extraction varied linearly up to 45 min irrespective of the leaves concentration (marked in Figure 3.1). At the beginning of extraction, the Reb-A concentration remained less in water. With the progress of extraction process, the recovery was found to increase almost linearly up to 45 min. It increased gradually with leaves to water ratio of 2% even after 60 min of contact time. Whereas, at higher leaves to water ratio (3 and 5%), the extraction yield did not increase beyond 45 min of contact time. Around 1639, 2369 and 3779 mg/L Reb-A was determined in solution at 45 min with leaves to water ratio of 2, 3 and 5%, respectively. It implies that in the second stage of Reb-A extraction, higher Reb-A concentration with the rise of leaves to water ratio probably lowered the overall concentration gradient for Reb-A extraction. Thus, the cumulative accumulation of Reb-A hindered the overall extraction process. In this region, the concentration gradient of Reb-A between leaves and water became lower which resulted from a persistent or a slight drop in Reb-A recovery. It caused a lower extraction efficiency of Reb-A per unit leaves in solvent at a higher dose of leaves. The maximum recovery was noted at 45 min for 3 and 5% leaves to water ratio. The recovery of Reb-A was of 67.1, 68.7

and 77% in 60 min with leaves to water ratio of 2, 3 and 5%, respectively. The corresponding stevioside recovery was around 69.6, 71.8 and 75.3 % respectively.

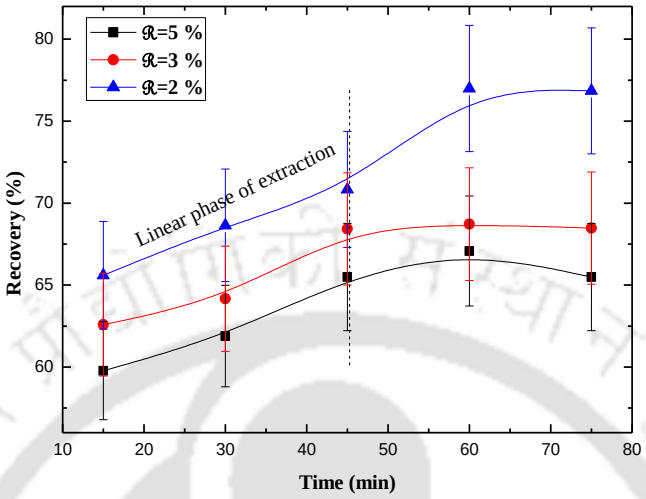

Figure 3.1: Variation of Reb-A recovery with the progress of contact time at different leaves to water ratio (extraction temperature 60°C, agitation speed 700 rpm and solvent 100 mL). A leaf to water ratio ($\mathcal{R}$) was defined as g of stevia leaves added per 100 mL of DI water (%, w/v).

The temperature played an important role in Reb-A extraction. The variation of Reb-A recovery at four different extraction temperatures, i.e., 50, 60, 70 and 80°C at various leaves to water ratio is shown in Figure 3.2. It is evident that there was a sharp improvement in recovery between 50 and 60°C at all leaves to water ratio. For an example, the recovery of Reb-A increased to 67.7 from 58.3% when the temperature was raised to 60 from 50°C for the leaves to water ratio of 3%. Reb-A recovery was insignificant beyond the extraction temperature of 60°C with leaves to water ratio of 2%. Whereas, about 8.5% more extraction was noted with the increase to 60 from 50°C with leaves to water ratio of 3%. On the other hand, it was about 4.2% less with leaves to water ratio of 5%. Higher temperature caused a deeper penetration of solvent into the cell wall which led to a quicker bulk diffusion of Reb-A. It was also visibly observed that higher temperature gave more swelled leaves. Higher

temperature decreased solvent viscosity that could have resulted in a better extraction efficiency (Guo-Qing et al. 2005). Further, the increase in extraction temperature (≥70°C) probably caused Reb-A decomposition. The rate of improvement in Reb-A extraction and its decomposition compensated with increasing temperature with leaves to water ratio of 2%. The rate of decomposition was some what less than enhanced Reb-A recovery with increasing temperature with leaves to water ratio of 3%. The decomposition rate superseded the temperature effect on Reb-A extraction with leaves to water ratio of 5%. It implies that Reb-A decomposition was more at the same temperature with increasing of its concentration. The degradation study showed that the degradation of Reb-A increased with the rise of its concentration for all the leaves to water ratio. The degradation was the highest at 80°C. It confirmed that higher degradation occurred at the same temperature with increasing Reb-A concentration.

The dependency of Reb-A recovery on temperature can also be illuminated in terms of the partition coefficient. It is defined as the ratio of concentration of Reb A (mg/L) in water to the amount in leaves (mg/g) at equilibrium. The variation of partition coefficient at different temperatures is shown in Figure 3.3. The partition coefficient of Reb-A increased from 105.2 to 147.5 g/L when the temperature was increased from 30 to 70°C. At higher temperature, the solubility of stevioside in water was reduced as it has a polar character (Pol et al., 2007). Similar observation was noted for Reb-A. It is in line with the decrease in partition coefficient above 70°C.

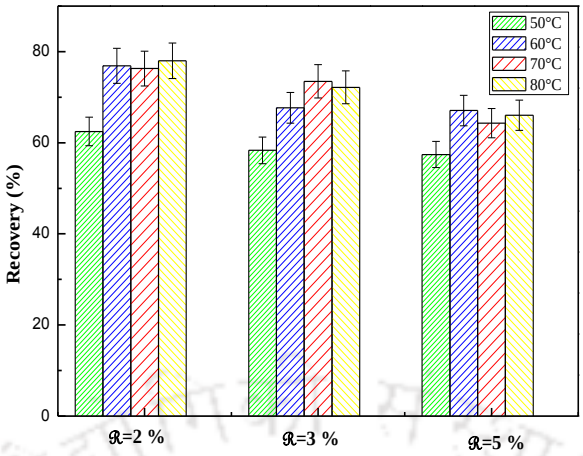

Figure 3.2: Variation of Reb-A recovery with extraction temperatures at different leaves to water ratio (contact time 60 min, agitation speed 700 rpm and solvent 100 mL). A leaf to water ratio ($\mathcal{R}$) was defined as g of stevia leaves added per 100 mL of DI water (%, w/v).

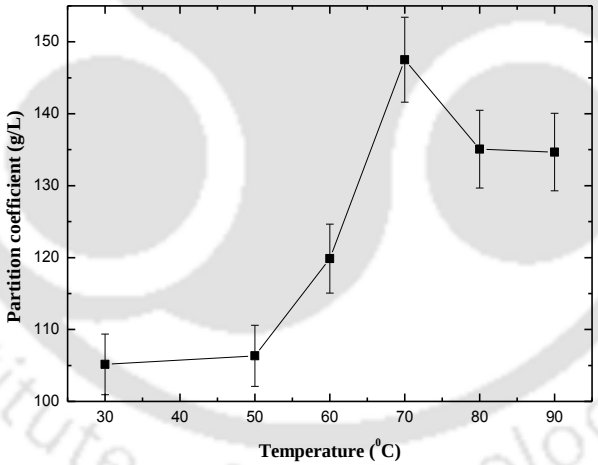

Figure 3.3: Variation of partition coefficient with extraction temperatures (For $\mathcal{R}$=3 % and t=60 min).

In order to find the interdependency of extraction parameters and to optimize the process variables, a statistical based design is highly desired. RSM optimization was successfully employed to find the interaction among the independent process parameters (Maran et al., 2013; Rai et al., 2012).

3.1.3.2 RSM optimization of Reb-A extraction and statistical analysis

Table 3.2 shows the ranges of each extraction factor, and their corresponding axial values as designed by CCD. The circumscribe central composite (CCC) design was chosen for the optimization since it provides a better curvature of the three-dimensional curves and a good accession of the optimized values. The lower and upper limits were selected such that the axial points lie within the scope of experimental possibilities. Table 3.1 shows the twenty numbers of experiments performed according to CCD for the optimization. Out of twenty experimental combinations, eight and six experiments were performed according to the factorial and axial points of CCD. The rests were as per the center point. The repeated center point experiments provide a good error estimation (Anderson and Whitcomb, 2005).

Table 3.2: Ranges and levels of input factors in CCD.[a]

Input factors	Factorial and central values					
	Unit	-1	0	+1	-α	+α
t	min	30	45	60	19.77	70.23
$\mathcal{R}$	%	2	3.5	5	0.98	6.02
T	°C	50	70	90	36.36	103.64

[a]Here, '-1', '0' and '+1' represent the lower, central and upper values of the corresponding factors, respectively. '-α' and '+α' refer to the axial values.

CCD fits the experimental results to various types of model equations which would show a better dependency based on the statistical analysis. For the present study, a quadratic model showed the best fit with respect to all combinations of t, $\mathcal{R}$ and T, as in Table 3.1. The best fit empirical quadratic model equation is in Eq. 3.2. The recovery of Reb-A was the output response of the CCD model equation.

$$\text{Recovery, \%} = -111.01+2.70t + 4.34\mathcal{R} + 2.92T-0.07\mathcal{R}t - 0.01Tt - 0.02\ \mathcal{R}\ T-0.02t^2+0.29\ \mathcal{R}^2 - 0.02T^2 \quad (3.2)$$

The statistical data for the analysis of variance (ANOVA) is summarized in Table 3.3. High F-value with a low p-value (< 0.001) implies that the recovery of Reb-A could be better expressed by a quadratic model equation. Regression coefficient (R^2) implies how well the

data points are fitted to a statistical model. It ranged from 0 to 1. The value of coefficient of determination was 0.973. It signifies that 97.3% variation of Reb-A recovery can be explained by the variation of t, $\mathcal{R}$ and *T*. The predicted determination coefficient (0.802) showed a reasonable agreement to the adjusted determination coefficient (0.950). Low coefficient of variance (3.12%) implies that the experiments were performed precisely.

Table 3.3: Statistical parameters of CCD predicted model equation using ANOVA.

Source	**Sum of square**	**Mean square**	**F-value**	**p-value Prob >F**
Model	1414.3	157.1	41.5	<0.0001
t	261.7	261.7	69.1	<0.0001
$\mathcal{R}$	131.4	131.4	34.7	0.0002
T	215.9	215.9	57.0	<0.0001
$\mathcal{R}t$	17.8	17.8	4.7	0.0555
Tt	69.4	69.4	18.3	0.0016
$\mathcal{R}T$	3.0	3.0	0.79	0.394
t^2	198.7	198.7	52.5	< 0.0001
$\mathcal{R}^2$	5.96	5.96	1.6	0.2381
T^2	575.5	575.5	152.0	< 0.0001
Residual	37.86	3.78		
Lack of fit	37.8	7.57		0.1936
Model statistics				
Std. Dev.	1.94	R-Squared		0.973
Mean	62.21	Adj. R-Squared		0.950
C.V.%	3.12	Predicted R-Squared		0.802

The extraction efficiency was predominantly influenced by the extraction time (*t*), leaf to water ratio ($\mathcal{R}$) and temperature (*T*). It is corroborated by the high F-value and low probability value (<0.0001) (Table 3.3). The corresponding F-values were 69.1, 34.7 and 57.0, respectively. The high p-value (0.1936) of 'lack of fit' suggested that the 'lack of fit' is non-significant. It implies that the synthesized quadratic model is valid for the optimization study.

Influence of extraction time and leaves to water ratio on Reb-A recovery

The combined effects of extraction time and leaves to water ratio on the recovery of Reb-A are shown in Figure 3.4. The leaves to water ratio had a strong effect on the recovery

of Reb-A. It is observed from Figure 3.4 that the recovery of Reb-A increased with decreasing the leaves to water ratio. The recovery was increased with the increase in extraction time keeping the temperature constant at the center point. At a lower leaves to water ratio, a lesser amount of stevia leaves was present in water and, a higher amount of Reb-A was extracted. When the leaves to water ratio was high, i.e., more stevia leaves was present in same volume of water, the extraction efficiency became low. The higher cummulative yield of Reb-A in water at higher leaves to water ratio hindered the extraction yield. A better extraction efficiency with increasing the extraction time was also noted. The observed and predicted values using CCD were very close. At the center point, i.e., for 3.5 % leaves to water ratio and extraction time of 45 min at 70°C temperature, the observed and predicted values of Reb-A recovery were 69.57 and 69.46 %, respectively.

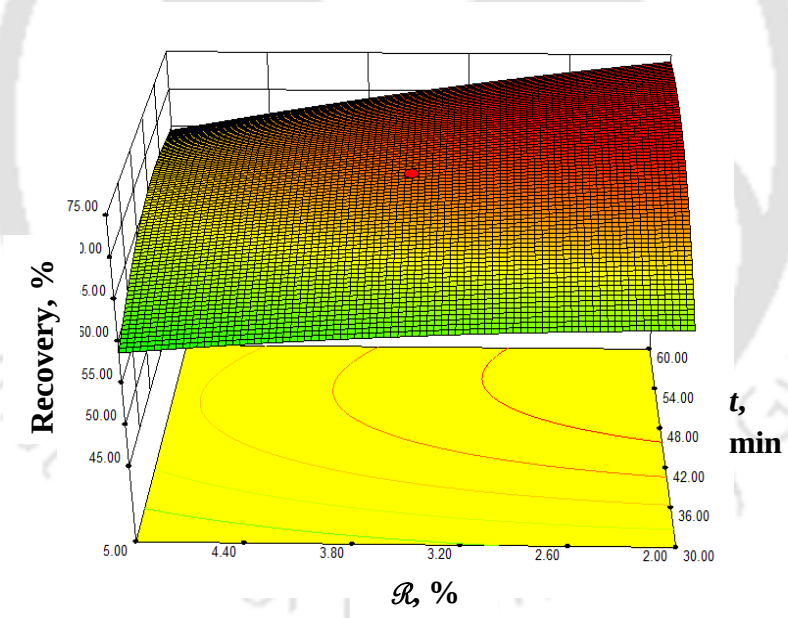

Figure 3.4: CCD prediction for the recovery of Reb-A with the variation of extraction time and leaves to water ratio (experimental condition: extraction temperature 70°C, agitation speed 700 rpm and solvent 100 mL). A leaf to water ratio ($\mathcal{R}$) was defined as g of stevia leaves added per 100 mL of DI water (%, w/v).

At 70°C for 2 % leaves to water ratio, the predicted value of Reb-A recovery was increased from 62.35 to 74.07 % for increasing the extraction time from 30 to 60 min (Figure 3.4). But decreasing the leaves to water ratio from 5 to 2 % at 70°C for 60 min, the predicted value of Reb-A recovery was increased from 64.88 to 74.07 %.

Role of extraction time and temperature on Reb-A recovery

The variations of Reb-A recovery with respect to the extraction time and temperature are shown in Figure 3.5. The results were for 3.5 % leaves to water ratio. The recovery was increased with the extraction time. The temperature had a notable effect on the recovery. It increased with the increase in extraction temperature up to a certain point and, then slightly dropped. Chang and Cook (1983), showed around 40 % Reb-A degradation in 4 h of storage in phosphoric and citric acidified beverage at 100°C. However, there was no notable degradation at the neutral pH up to 12 h heating at this temperature. pH of Reb-A extract was found to be 5.6 at 70°C, $\mathscr{R}$ =3.5 % and t=51 min. The decrease in Reb-A recovery above 70°C may be because of Reb-A decomposition. In the case of stevioside, Kroyer (1999) reported about 5% decomposition in the aqueous medium at 80°C under both acidic and basic medium.

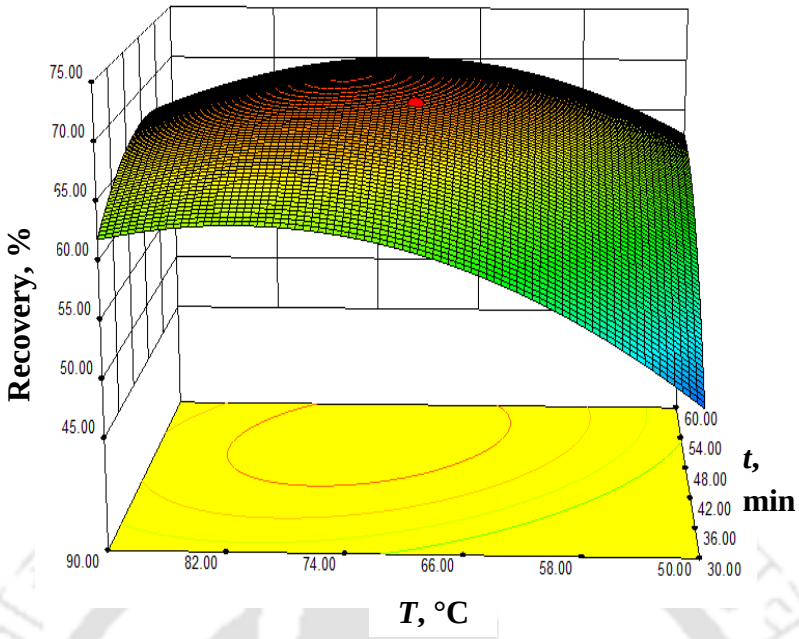

Figure 3.5: CCD prediction for the recovery of Reb-A with the variation of extraction time and temperature (experimental condition: leaves to water ratio at 3.5 %, agitation speed 700 rpm and solvent 100 mL).

Different extraction temperature and leaves to water ratio on Reb-A recovery

The effects of extraction temperature and leaves to water ratio are depicted in Figure 3.6, keeping the extraction time at 45 min.The recovery increased with decreasing the leaves to water ratio. A possible explanation is provided previously. With increasing temperature, Reb-A recovery was also increased. At a higher temperature, the enhanced movement of water molecules caused deeper penetration into the cell wall of stevia leaves. It was caused a better extraction efficiency. The solubility of Reb-A also increased at a higher temperature. For an example, the experimental values of Reb-A recovery was increased from 63.3 to 71.5 % by lowering the leaves to water ratio from 5 to 2 % at 70°C for 45 min of extraction. The corresponding predicted values by CCD were 65.7 and 71.9 %, respectively.

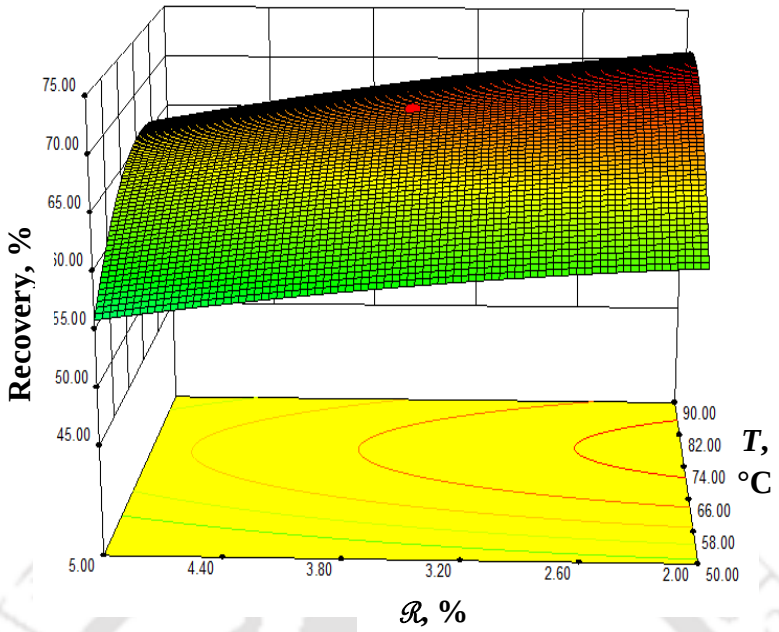

Figure 3.6: CCD prediction for the recovery of Reb-A with the variation of temperature and leaves to water ratio (experimental condition: extraction time 45 min, agitation speed 700 rpm and solvent 100 mL). A leaf to water ratio ($\mathcal{R}$) was defined as g of stevia leaves added per 100 mL of DI water (%, w/v).

3.1.3.3 Prediction of Reb-A extraction using ANN modeling

For the maximization of recovery, the lower and upper limit of response were set as 47.4 and 81.6 %. The numerical optimization of CCD generated 20 solutions with different desirability. CCD suggested maximum 73.1 % recovery of Reb-A. It is observed that the extraction time was 50.9 min, the stevia leaves to water ratio was 2.36 % and, the extraction temperature was 70.8 °C to achieve the maximum recovery.

The goodness-of-fit between the observed and the predicted recovery of Reb-A given by the CCD is shown in Figure 3.7. The data points are well distributed near the diagonal line in the parity plot with a correlation coefficient of 0.91. The equation of best fitted straight line is also shown in Eq. 3.3.

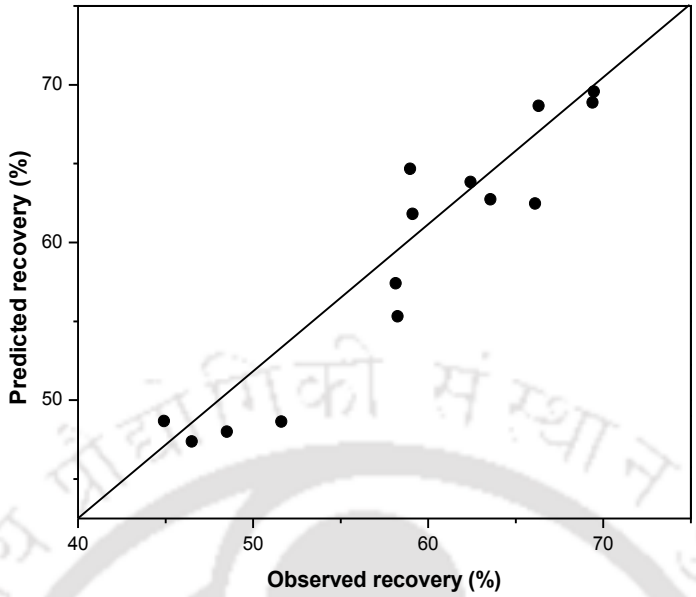

Figure 3.7: Comparison of the observed data with those predicted by the CCD.

Predicted recovery (%) = 1.024×*observed recovery (%)* - 0.808 (3.3)

A three layer feed forward neural network was developed to correlate the input and output data. In this network, the input layer was consisted of three neurons, i.e., three independent parameters, *t*, $\mathcal{R}$ and *T* and, the output layer were comprised of a single neuron, % recovery. The Tansig and Logsig transfer functions from hidden layer to output layer were failed to train the network. The Purelin function from hidden layer to output layer only could successfully train the neural network. The best selected topologies with varying transfer functions are shown in Table 3.4. The best training performance was found with 3-8-1 topology and, the Logsig and Purelin transfer functions in hidden and output layers were employed. A brief flow chart of the feedforward backpropagation neural network is given in Figure 3.8. This optimized topology had the highest regression coefficient (R^2=0.993) and the lowest root mean square error (*RMSE* = 0.010) during the training process. After testing process, the regression coefficient (R^2) between experimental and predicted results by neural

network was obtained as 0.965. A comparison among experimental and ANN model is presented in Figure 3.9. The model fitted well to the experimental results. The close prediction of Reb-A recovery by ANN accomplished them as the significant tools for extraction of value added products.

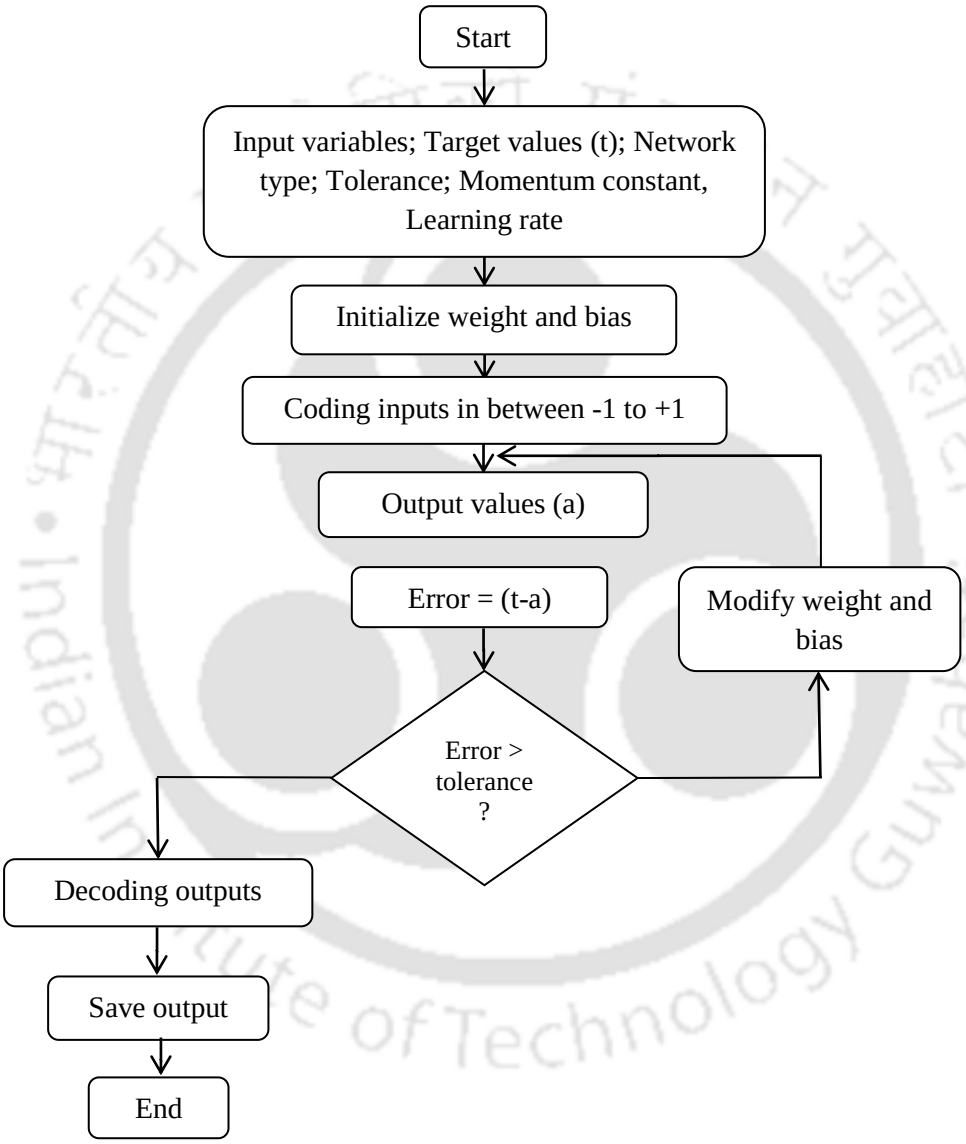

Figure 3.8: Artificial neural network (ANN) flow chart.

Table 3.4: Best fitted topologies with various transfer functions and corresponding values of R^2, *RMSE* and *AAD*.

Transfer function	Topology	R^2	*RMSE*	*AAD*
Logsig-Purelin	3-8-1	0.993	0.010	0.0001
Tansig-Purelin	3-9-1	0.974	1.5453	0.0166
Purelin-Purelin	3-1-1	0.960	1.9149	0.0256

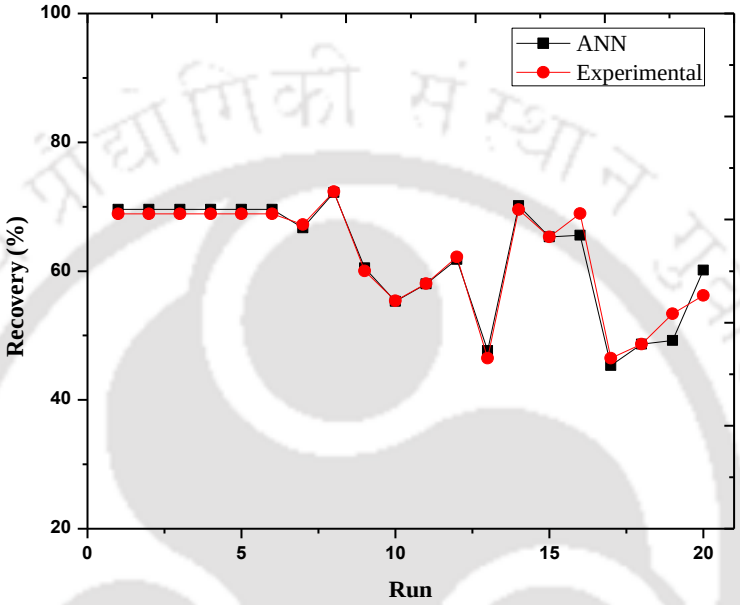

Figure 3.9: ANN prediction versus the experimental recovery of Reb-A. Each run number represents the extraction conditions as designed by CCD shown in Table 3.1.

3.2 Rebaudioside-A Separation: Membrane selection, permeate quality, and fouling behavior

In this section, the membrane-based clarification of stevia extract towards the recovery of Reb-A is documented. The work provides the details on the selection of ultrafiltration membrane, flux behavior both in batch and continuous operations, effects of operating conditions on the clarified extract quality, comparative separation of Reb-A and stevioside in permeates, and fouling nature of the selected membrane. All these aspects are extremely significant for an efficient industrial scale-up. The present study is, therefore, taken up to fill this gap.

3.2.1 Fouling mechanism

The fouling of membrane is caused by a build-up of a layer of retained particles on the membrane surface and/or partial or complete blocking of pores. Field (1995) proposed four different membrane fouling models to anticipate the way of membrane fouling in cross flow. These are complete pore blocking (CPB) (Eq. 3.4), standard pore blocking (SPB) (Eq. 3.5), intermediate pore blocking (IPB) (Eq. 3.6) and cake filtration (CF) (Eq. 3.7) models.

$$J = J_{lim} + (J_0 - J_{lim})exp(-k_2 t) \quad (3.4)$$

$$J^{-0.5} = J_0^{-0.5} + (k_s/2)\, A^{0.5}\, t \quad (3.5)$$

$$\sigma t = \frac{1}{J_{\lim}[\ln(\frac{J(J_0 - J_{\lim})}{J_0(J - J_{\lim})}]} \quad (3.6)$$

$$Gt = \frac{1}{J_{\lim}^{\,2}[\ln(\frac{J(J_0 - J_{\lim})}{J_0(J - J_{\lim})}) - J_{\lim}(\frac{1}{J} - \frac{1}{J_0})]} \quad (3.7)$$

where, J is permeate flux ($m^3\ m^{-2}\ s^{-1}$), J_0 is initial permeate flux ($m^3\ m^{-2}\ s^{-1}$), J_{lim} is the limit value of the permeate flux attained in steady-state conditions ($m^3\ m^{-2}\ s^{-1}$), k_2 is complete pore

blocking model constant (s^{-1}), k_s is standard pore blocking model constant ($m^{-0.5}\ s^{-0.5}$), σ is intermediate pore blocking model constant (m^{-1}), G is cake filtration model constant ($s\ m^{-2}$), A is the membrane area (m^2) and, t is time (s) of filtration.

The fouling mechanisms are schematized in Figure 3.10. CPB, SPB, and IPB lead towards a significant irreversible membrane fouling. The selection of fouling mechanism is based on the fitness of the model having the maximum value of the regression coefficient (R^2). Depending on the morphology and feed properties, the membrane does not necessarily follow any one of the mechanisms during entire flux decline profile. For this reason, either a single or a combination of two models was studied to fit the ultrafiltration data in between initial and steady state flux.

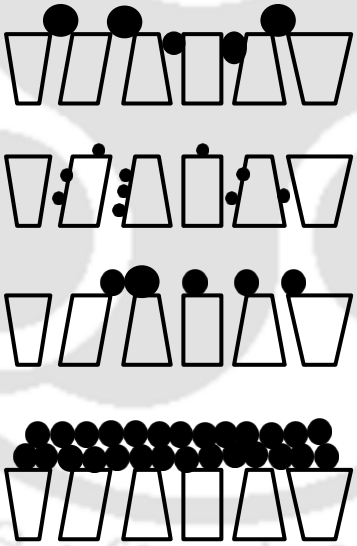

Figure 3.10: Diagrammatic representation of membrane fouling mechanisms. (a) CPB, (b) SPB, (c) IPB and, (d) CF.

3.2.2 Results and discussions

3.2.2.1 Selection of ultrafiltration membrane in unstirred batch cell

The selection of membrane was based on the permeate flux values and quality in terms of Reb-A content using 10, 20, 30 and 50 kDa MWCO in an unstirred batch cell. The steady state permeates flux values for various membranes at three TMP drops are shown in Figure 3.11 (a). The permeates were collected upto 100, 103 and 101 min at 310, 414 and 514 kPa TMP drop for 10 kDa MWCO membrane, respectively. The corresponding time permeate collection were 85, 92 and 63 min, 72, 75 and 60 min and, 65, 52 and 48 min for 20, 30 and, 50 kDa MWCO membrane, respectively. It varied from 0.74×10^{-6} to 1.08×10^{-6} m^3 m^{-2} s^{-1} for 10 kDa, 0.71×10^{-6} to 0.96×10^{-6} m^3 m^{-2} s^{-1} for 20 kDa, 0.84×10^{-6} to 1.27×10^{-6} m^3 m^{-2} s^{-1} for 30 kDa and 0.21×10^{-6} to 0.84×10^{-6} m^3 m^{-2} s^{-1} for 50 kDa. The fouling phenomena and subsequent flux decline were the highest in 50 kDa membrane. It was comparable for 10 and 20 kDa. The flux decline mechanism can be interpreted in terms of pore blocking and concentration polarization. High molecular weight (HMW) compounds present in stevia extract could lead to a dynamic cake layer over the membrane surface rather than pore blocking for 10 and 20 kDa membranes. On the other hand, 50 kDa MWCO membrane exhibited severe pore blocking and concentration polarization. Thus, higher MWCO membrane did not necessarily produce a higher flux. The same behavior is also observed by Chamchong and Noomhorm (1991), and Fukumoto et al. (1998). The highest steady state flux was observed for 30 kDa as both pore blocking and cake layer formation were relatively lower.

In this regard, the purity (Eq. 3.8), yield (Eq. 3.9) and selectivity (Eq. 3.10) of steviol glycol (here, either stevioside or Reb-A) were defined as follows (Chhaya et al., 2012). These were measured at each operating conditions after collecting the cumulative volume of permeate up to 1 h.

$$\text{Purity} = \frac{\text{Steviol glycol (SG) concentration in permeate}}{\text{Permeate TS content}} \quad (3.8)$$

$$\text{Yield of SG (\%)} = \frac{\text{SG in permeate}}{\text{SG in feed}} \times 100 \quad (3.9)$$

$$\text{Selectivity} = \frac{\text{SG concentration in permeate}}{\text{Concentration of lower molecular weight (LMW) in permeate}} \quad (3.10)$$

The purity is defined as the ratio of concentration of the steviol glycoside (SG) (here, either stevioside or Reb-A) to the concentration of total solid (TS) content in permeate. In this regard, TS in feed can be considered as the summation of HMW, the SG, and lower molecular weight (LMW) solids. LMW solids can be regarded as the solids having a lower molecular weight than that particular SG. It was assumed that all LMW solids were freely passed through the membrane along with the SG and, it was hardly retained by the membrane. All the solids having molecular weight higher than the SG, i.e., HMW solids were retained by the membrane. With this assumption, a gross mass balance can be established as, $TS_{feed} = LMW_{feed} + HMW_{feed} + SG_{feed}$ and $LMW_{feed} = TS_{permeate} - SG_{permeate}$ (Chhaya et al., 2012a; 2012b). Since, LMW_{feed} is freely permeable, it is equal to $LMW_{permeate}$, therefore HMW in feed can be estimated as $HMW_{feed} = (TS_{feed} - TS_{permeate}) - (SG_{feed} - SG_{permeate})$.

In this regard, TS in feed can be considered as the summation of HMW, SG, and lower molecular weight (LMW) solids. LMW solids can be regarded as the solids having a lower molecular weight than SG. It was assumed that all LMW solids were freely passed through the membrane along with SG and, it was hardly retained by the membrane. All the solids having molecular weight higher than SG, *i.e.*, HMW solids were retained by the membrane.

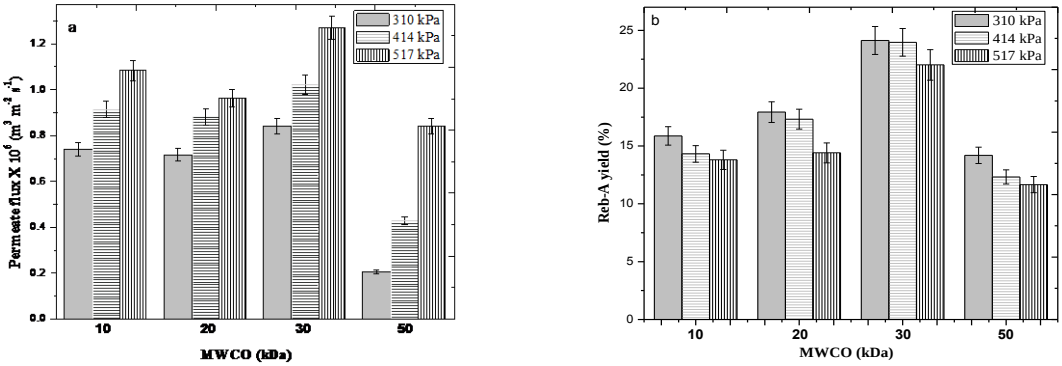

Figure 3.11: (a) Steady state permeates fluxes and, (b) Reb-A yield of different MWCO membranes at different TMP drops in batch filtration.

The variation of Reb-A yield with MWCO is presented in Figure 3.11 (b). The yield of Reb-A was the lowest for 50 kDa membrane. As the pore diameter was larger in 50 kDa membrane, most of the pores were blocked and, concentration polarization was also severely formed. For this reason, the rejection of Reb-A was higher for 50 kDa membrane. As the pore size becomes higher, the membrane is more prone to fouling since more solutes enter the pores and block them (Mondal et al., 2013; Rai et al., 2006). For 10 and 20 kDa membranes, Reb-A rejection was almost similar. 13.8 and 14.4 % yield of Reb-A were observed for 10 and 20 MWCO membranes at 517 kPa. For stevioside, the yield was around 21.4 and 23.3 % at the same condition. 10 and 20 kDa membranes showed a similar performance for the recovery of Reb-A in accordance with the dynamic behavior of cake formation outlined before. The deposition and growth of cake layer over the membrane are reported in the case of ultrafiltration of mosambi juice (Rai et al., 2004) and protein fouling in micro and ultrafiltration (Marshall et al., 1993). Rai et al. (2010) claimed a predominant cake layer formation in microfiltration of watermelon. The highest recovery of Reb-A was observed for 30 kDa membrane. Around 24 and 28% recovery of Reb-A and stevioside were achieved for 30 kDa membrane at 414 kPa, respectively. The pore blocking and cake formation over the membrane was minimal for 30 kDa membrane giving the higher recovery of Reb-A among

all different MWCO membranes. The reason for a higher yield of Reb-A for 30 kDa membrane is in line with the higher permeate flux (Figure 3.11 (a)). Hence, 30 kDa MWCO membrane was selected for the clarification of stevia extract for the higher yield of Reb-A and steady state flux. For the recovery of stevioside from stevia extract, 30 kDa MWCO membrane also showed a better performance (Mondal et al., 2013).

3.2.2.2 Performance of cross-flow ultrafiltration for Reb-A recovery

The clarification of stevia extract was performed in the cross-flow process using 30 kDa MWCO membrane which was selected based on the performance of the unstirred batch ultrafiltration experiments. The permeate flux decline profiles with the time of filtration at two different feed flow rates and three TMP drops are shown in Figures 3.12 (a) and 3.12 (b). The flux decline was not sharp and, the steady state reached shortly. The steady state fluxes increased with TMP drops at fixed Reynolds number (*Re*). *Re* number for the rectangular duct was calculated according to Eq. 3.11, where, D_H is the hydraulic diameter; V is volumetric flow rate; ρ is density and, μ is viscosity. For the rectangular duct of width 'w' and height 'h', the hydraulic diameter is defined as in Eq. 3.12.

$$Re = D_H V\rho/\mu \tag{3.11}$$

$$D_H = \frac{4\times Area}{Perimeter} = \frac{2\times h\times w}{(h+w)} \tag{3.12}$$

Theoretically, the permeate flux increases with TMP drops till a steady flux reaches. The steady state fluxes varied from 0.70×10^{-6} - 5.27×10^{-6} to 2.28×10^{-6} - 5.86×10^{-6} $m^3\ m^{-2}\ s^{-1}$ (TMP drops 138-414 kPa) at *Re* numbers of 833 and 1667, respectively (Figures 3.12(a) and (b)). It was also higher with increasing *Re* numbers in the laminar regime at a particular TMP drop. The results are in agreement with ultrafiltration of oil-in-water using polysulfone membrane (Singh et al., 2011). Higher shear rate facilitates removal of particles deposited on the membrane surface at higher cross-flow velocities. In the cross-flow process, the feed

passes the membrane in the tangential direction of the permeate flow which controls the growth of cake layer on the membrane surface. The tangential flow of the feed stream causes a disturbance in the flow channel which promotes a backward diffusion of solutes from the cake layer to the bulk. After a short period of operation, the backward diffusion and convective fluxes of solutes due to pressure gradient towards the membrane become equal and, the equilibrium is reached. For this reason, the flux decline profile was not sharp and, the steady state reached quickly.

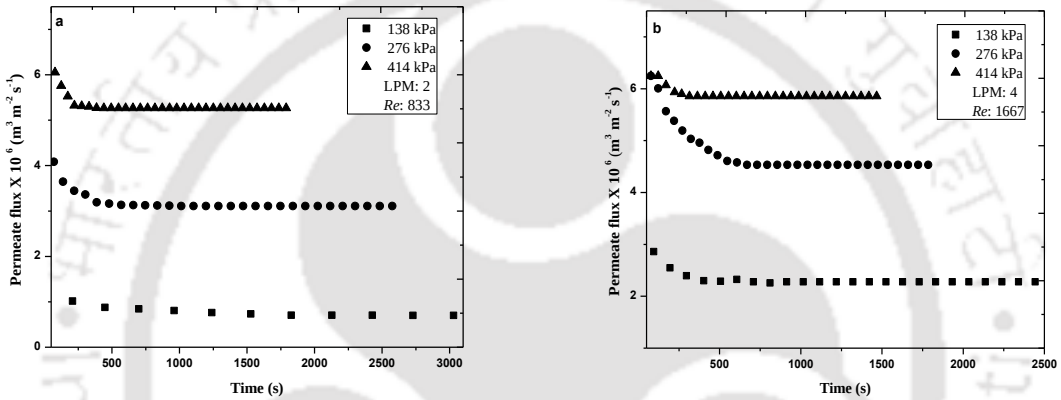

Figure 3.12: Transient flux decline at *Re* numbers (a) 833 and, (b) 1667.

The variations of steady state permeate flux at different TMP drops with feed flow velocities is shown in Figure 3.13. The steady state flux increased almost linearly with TMP drops and feed velocity. Hence to get higher permeate flux, the operating pressure and flow rate must be higher. But, the selection of operating conditions also depends on the permeate quality. Table 3.5 summarizes the permeate quality at steady state in cross-flow ultrafiltration of stevia extract. A general trend was observed from the Table 3.5. At a fixed *Re* number, the permeate color decreased with higher TMP drops and, the clarity increased. The higher molecular pigment particles faced a higher resistance by the cake layer over the membrane surface at higher TMP drops which was resulted in the color reduction. The permeate clarity

increased from 65.6 to 74.5 % at *Re* number of 833 and from 69.3 to 71.8 % at *Re* number of 1667.

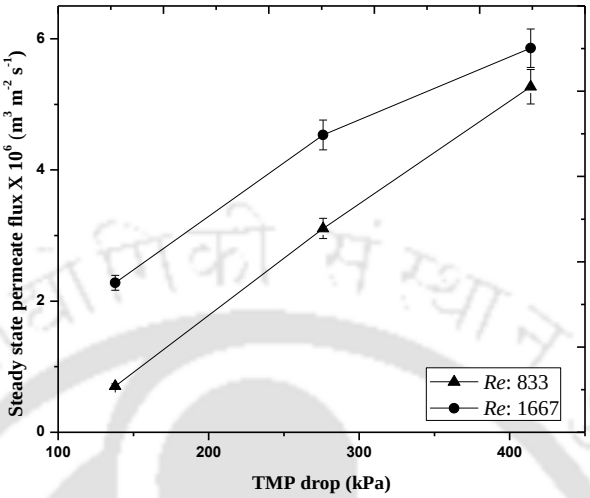

Figure 3.13: Variation of steady state permeate flux with TMP drops at two different *Re* numbers.

Table 3.5: Permeate quality under different operating conditions in cross-flow ultrafiltration using 30 kDa membrane.

Re	**TMP drops (kPa)**	**Color (A)**	**Clarity (% T)**	**Yield**		**Selectivity**		**Purity**	
				Reb-A	Stevioside	Reb-A	Stevioside	Reb-A	Stevioside
833	138	0.83	65.6	27.28	29.20	0.23	0.62	0.19	0.38
	276	0.75	68.1	31.07	34.44	0.27	0.83	0.21	0.45
	414	0.60	74.5	30.46	33.60	0.27	0.79	0.21	0.44
1667	138	0.64	69.3	35.50	36.84	0.34	1.00	0.25	0.50
	276	0.62	69.8	40.27	39.23	0.40	1.14	0.29	0.53
	414	0.61	71.8	43.43	44.22	0.45	1.51	0.31	0.60
Extract	-	1.75	1.17	-	-	-	-	-	-

Around 4.2 % Reb-A and 7.8 % stevioside were found in the leaves. The purity varied from 0 to 100 % and, a higher value of it implies that a lesser amount of undesirable materials passes through the membrane in comparison to the target compound, i.e., Reb-A for this study. The purity of Reb-A and stevioside were around 17.6 and 33.6 % after extraction. The

purity of Reb-A in permeate was found to vary between 19 and 31 %. The corresponding selectivity ranged from 0.23 to 0.45. The purity and selectivity increased with TMP drops and *Re* numbers. Membrane rejection of Reb-A was found to decrease with *Re* numbers. Reb-A rejection decreased up to 56 % at TMP drop of 414 kPa and *Re* number of 1667. It emphasized that even the molecular weight of Reb-A was much less than the MWCO of the membrane and, all the Reb-A did not necessarily pass through the membrane. The retention of Reb-A was due to the combined effects of pore blocking and cake layer formation over the membrane surface by HMW particles which indeed determined the recovery of Reb-A (Mondal et al., 2013). Similar observation was also found for stevioside also. The purity and selectivity of stevioside were in the ranges of 38-60 % and 0.62-1.51, respectively (Table 3.5). The purity and selectivity were much higher by considering both the sweeteners together in permeate. The purity of these two sweeteners all together increased from 57 % at 138 kPa TMP drop and *Re* number of 833 to 91 % at 414 kPa TMP drop and *Re* number of 1667. By considering the occurrence of only stevioside and Reb-A in permeates, the selectivity of Reb-A and stevioside were in the range of 0.47-0.54 and 1.86-2.04, respectively. The suitable operating condition was selected based on the maximum purity and selectivity with a reasonable permeate flux. Vanneste et al. (2011) separated total sweetening glycosides using 27 % PES membrane from stevia extract. They achieved around 30 % yield with 37 % purity of total sweetener from the initial purity of 11 %. In another study, 44.5 % stevioside is recovered with 60 % purity (Chhaya et al., 2012). Roy and De (2014) also perform steviol glycosides separation using CAP-PAN membrane with 68 % recovery and 34 % purity. Therefore, 414 kPa and *Re* number of 1667 were selected as a suitable operating condition for cross-flow ultrafiltration for Reb-A recovery with a steady state permeate flux of 5.86×10^{-6} m^3 m^{-2} s^{-1}, the selectivity of 0.45 and purity of 31 % (around 90 % purity considering both Reb-A and stevioside).

3.2.2.3 Fitness of Field's models

Field's fouling models had been fitted to the flux decline data in cross flow operation for 30 kDa membrane at *Re* number of 833 and 1667 and at TMP drops of 138, 276 and 414 kPa. The linearized form of these models was used to check the goodness of fitting. The best fitted fouling model was selected on the basis of the highest value of regression coefficients (R^2). The regression coefficients were varied from 0.806 to 0.940, 0.546 to 0.941, and 0.408 to 0.714 for CPB, SPB and IPB models, respectively whereas it was in the range of 0.955 to 0.983 for CF model. Among the four fouling models, the CF model provided the best fit to the flux decline data in cross flow operation for 30 kDa membrane at *Re* number of 833 and 1667 (Figure 3.14). The corresponding values of R^2 are listed in Table 3.6.

Table 3.7 summarizes the CF model constant and resistance at different operating conditions. The cake filtration phenomena was also supported by the experiments since the membrane almost resumed the water permeability to its initial value after cleaning with SDS solution and distilled water (Figure 3.15).

Table 3.6: Comparison of R^2 for various combination of fouling models for 30 kDa membrane.

Re	**Pressure (kPa)**	***R*²**			
		CPB	**SPB**	**IPB**	**CF**
833	138	0.878	0.941	0.714	0.974
	276	0.930	0.611	0.409	0.983
	414	0.940	0.748	0.604	0.968
1667	138	0.893	0.634	0.450	0.956
	276	0.763	0.929	0.408	0.955
	414	0.806	0.546	0.563	0.980

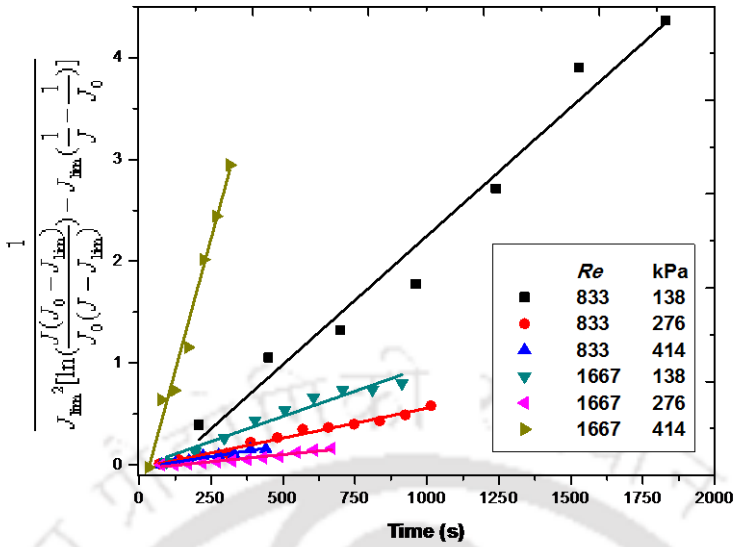

Figure 3.14: Linearized fitness plots for Field's cake filtration models for 30 kDa membrane at *Re* = 833 and 1667.

Table 3.7: Summary of the model parameters from the cake filtration model for 30 kDa membrane.

Re	**Pressure (kPa)**	$G\times10^{2}$ **(s m^{-2})**	$R_T\times10^{-13}$ **(m^{-1})**
833	138	0.25	6.54
	276	0.06	7.18
	414	0.04	7.79
1663	138	0.10	5.73
	276	0.03	5.76
	414	1.04	6.82

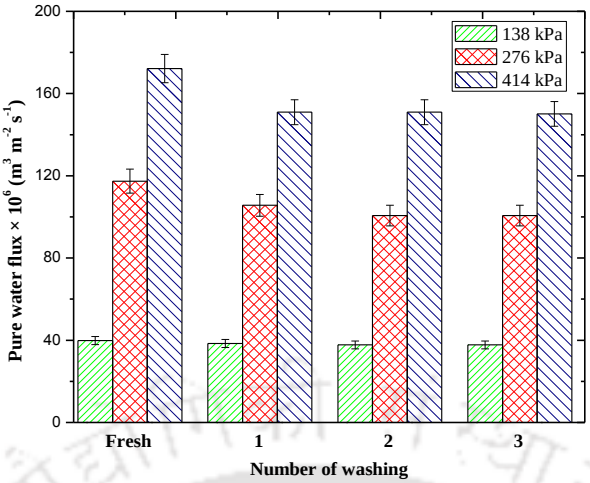

Figure 3.15: Comparison of pure water flux between fresh and cleaned 30 kDa membrane (cleaning with 2 % SDS and distilled water) at three operating TMP drops and *Re*=833.

3.3 Summary

Hot water was found to be a promising solvent for the extraction of Reb-A from stevia leaves and, the maximum Reb-A recovery can be achieved within an hour of contact. The efficiency of Reb-A recovery was more at lower leaves to water ratio. The increase in temperature favored Reb-A recovery up to 60°C. However, a further rise in extraction temperature decreased the recovery. It was supported by the partition coefficient determined at different temperatures. It was found that CCD is an effective tool for the optimization of Reb-A extraction. CCD generated quadratic model well fitted to the experimental data. It gave the maximum recovery of 73.12% at the optimal condition as: extraction time 51 min, leaves to water ratio 2.36% and extraction temperature 71°C. The recovery of Reb-A was also successfully predicted using a three layers ANN with the feed forward back propagation algorithm with a close agreement to the experimental outcomes.

In this study, the ultrafiltration of aqueous stevia extract was performed both in batch and cross-flow operations towards the separation of Reb-A. The influences of pore blocking and concentration polarization had a lesser effect on 30 kDa MWCO membrane leading higher flux and permeate quality. 30 kDa MWCO membrane showed about 14.6 to 83.7 and 25.7 to 51.5 % higher permeate flux and yield of Reb-A compared to 10, 20 and 50 kDa MWCO membranes in batch filtration. In a cross-flow operation, the highest purity and selectivity of Reb-A obtained at *Re* number of 1667 were 32.3 and 40 % more than the same at *Re* number of 833 at TMP drop of 414 kPa. A TMP drop of 414 kPa and *Re* number of 1667 exhibited the highest purity of 31 % and flux value of 5.86×10^{-6} m^3 m^{-2} s^{-1}. The variation of permeate flux with filtration time was best fitted using the Field's fouling model and, CF model well described the fouling mechanism under the whole operating conditions for 30 kDa membrane.

References

Aghbashlo, M., Kianmehr, M. H., Nazghelichi, T. and Rafiee, S., "Optimization of an artificial neural network topology for predicting drying kinetics of carrot cubes using combined response surface and genetic algorithm", Drying Technol., **29**, 770-779 (2011).

Anderson, M. J. and Whitcomb, P. J., *RSM simplified: optimizing processes using response surface methods for design of experiments*, CRC Press, Taylor & Francis (2005).

Bala, B. K., Ashraf, M. A., Uddin, M. A. and Janjai, S., "Experimental and neural network prediction of the performance of a solar tunnel drier for drying jackfruit bulbs and leather", *J. Food Process Eng*., **28**, 552–566 (2005).

Chamchong, M. and Noomhorm, A., "Effect of pH and enzymatic treatment on microfiltration and ultrafiltration of tangerine juice", *J. food process Eng.*, **14**, 21–34 (1991).

Chang, S. S. and Cook, J. M., "Stability Studies of Stevioside and Rebaudioside A in Carbonated Beverages", *J. Agric. Food Chem*., **31**, 409-412 (1983).

Chhaya, Mondal, S., Majumdar, G. C. and De, S., "Clarifications of stevia extract using cross-flow ultrafiltration and concentration by nanofiltration", *Sep. Purif. Technol.*, **89**, 125–134 (2012).

Chhaya, Sharma, C., Mondal, S., Majumdar, G. C. and De, S., "Clarification of Stevia extract by ultrafiltration: Selection criteria of the membrane and effects of operating conditions", *Food Bioprod. Process*., **90**, 525-532 (2012).

Diptee, R., Smith, J. P., Alli, I. and Khanizadeh, S., "Application of response surface methodology in protein extraction studies from brewer's spent grain". *J. Food Process. Preserv.*, **13**, 457-474 (1989).

Field, R. W., Wu, D., Howell, J. A. and Gupta, B. B., "Critical flux concept for microfiltration fouling", *J. Membr. Sci.*, **100,** 250–272 (1995).

Fukumoto, L. R., Delaquis, P. and Girard, B., "Microfiltration and ultrafiltration ceramic membranes for apple juice clarification", *J. Food Sci*., **63**, 845–850 (1998).

Galvez, F. C. F., Resurreccion, A. V. A. and Ware, G. O., "Formulation and process optimization of mungbean noodles", *J. Food Process. Preserv*., **19**, 191-205 (1995).

Guo-Qing, H., Hao-Ping, X., Qi-He, C., Ruan, H., Zhao-Yue, W. and Traore, L., "Optimization of conditions for supercritical fluid extraction of flavonoids from hops (Humulus lupulus L.)", *J. Zhejiang University SCI B.*, 6, 999-1004 (2005).

JECFA, "Steviol glycosides. Combined Compendium of Food Additive Specifications", 68th Meeting of the Joint FAO/WHO Expert Committee on Food Additives. FAO/JECFA Monograph, vol. 4. Food and Agriculture Organization of the United Nations (FAO), Rome, Italy, pp. 61–64 (2007).

Kroyer, G. TH., "The Low Calorie Sweetener Stevioside: Stability and Interaction with Food Ingredients", *Food Sci. Technol*., **32**, 509-512 (1999).

Maran, J. P., Manikandan, S. and Mekala, V., "Modeling and optimization of betalain extraction from Opuntia ficus-indica using Box–Behnken design with desirability function", *Ind. Crop. Prod.*, **49**, 304 – 311 (2013).

Marshall, A. D., Munro, P. A. and Tragardh, G., "The effect of protein fouling in microfiltration and ultrafiltration on permeate flux, protein retention and selectivity: a literature review", *Desalination*, **91**, 65-108 (1993).

Menlik, T., Kirmaci, V. and Usta, H., "Modelling of freeze drying behaviors of strawberries by using artificial neural network", *J. Therm. Sci. Technol*., **29**, 11–21 (2009).

Mondal, S., Rai, C. and De, S., "Identification of fouling mechanism during ultrafiltration of stevia extract", *Food Bioprocess Technol*., **6**, 931-940 (2013).

Omid, M., Baharlooei, A. and Ahmadi, H., "Modeling drying kinetics of pistachio nuts with multi-layer feed-forward neural network", Drying Technol., **27**, 1069-1077 (2009).

Ozdemir, U., Ozbay, B., Veli, S. and Zor, S., "Modeling adsorption of sodium dodecyl benzene sulfonate (SDBA) onto polyaniline (PANI) by using multi linear regression and artificial neural networks", *Chem. Eng. J.*, **178**, 183–190 (2011).

Pol, J., Ostra, E. V., Karasek, P., Roth, M., Benesova, K., Kotlarikova, P. and Caslavsky, J., "Comparison of two different solvents employed for pressurised fluid extraction of stevioside from Stevia rebaudiana: methanol versus water", *Anal Bioanal Chem*., **388**, 1847–1857 (2007).

Poonnoy, P., Tansakul, A. and Chinnan, M. S., "Estimation of moisture ratio of a mushroom undergoing microwave-vacuum drying using artificial neural network and regression models", *Chem. Prod. Process Model*., **2**, 1934–2659 (2007).

Puri, M., Sharma, D. and Tiwari, A. K., "Downstream processing of stevioside and its potential applications", *Biotechnol. Adv*., 29, 781–791 (2011).

Rai, C., Majumdar, G. C. and De, S., "Optimization of process parameters for water extraction of stevioside using response surface methodology", *Separ. Sci. Technol.*, **47**, 1014 – 1022 (2012).

Rai, C., Rai, P., Majumdar, G. C., De, S. and DasGupta, S., "Mechanism of permeate flux decline during microfiltration of watermelon (*Citrullus lanatus*) juice", *Food Bioprocess. Technol.*, **3**, 545-553 (2010).

Rai, P., Majumdar, G. C., DasGupta, S. and De, S., "Effect of various pretreatment methods on permeate flux and quality during ultrafiltration of mosambi juice", *J. Food Eng.*, **78**, 561–568 (2007).

Rai, P., Majumdar, G. C., Sharma, G., DasGupta, S. and De, S., "Effect of various cutoff membranes on permeate flux and quality during filtration of mosambi (Citrus sinensis (L.) Osbeck) juice", *Food Bioprod. Process*., **84**, 213-219 (2006).

Roy, A. and De, S., "Extraction of steviol glycosides using novel cellulose acetate phthalate (CAP)–Polyacrylonitrile blend membranes", *J. Food Eng*., **126**, 7-16 (2014).

Singh, V., Purkait, M. K. and Das, C., "Cross-flow microfiltration of industrial oily wastewater: experimental and theoretical consideration", *Sep. Sci. Technol.*, **46**, 1213-1223 (2011).

Vanneste, J., Sotto, A., Courtin, C. M., Craeyveld, V. V., Bernaerts, K., Impe, J. V., Vandeur, J., Taes, S. and Van der Bruggen, B., "Application of tailor-made membranes in a multi-stage process for the purification of sweeteners from Stevia rebaudiana", *J. Food Eng*., **103**, 285–293(2011).

CHAPTER 4

Dehydration of Aloe Vera Gel in Freeze Drying, Hot Air, Microwave, and Hybrid Processes

In this chapter, the performance of hot air, microwave-assisted and hybrid-drying processes, namely, 'centrifugation followed by freeze drying (CFFD)', 'microwave followed by freeze drying (MWFFD)', 'centrifugation followed by hot air drying (CFHAD)' and 'microwave followed by hot air drying (MWFHAD)' towards the retention of physico-chemical and functional properties of dried aloe vera gel was elucidated. For this purpose, carbohydrate, protein and ash contain, swelling, water retention capacity, and fat adsorption capacity were analyzed in dry aloe gel.

In the next part, microwave-assisted drying (MWAD) process was optimized using central composite design (CCD). An Artificial neural network (ANN) model was generated for mapping between the process variables and desired response. The drying kinetics of aloe vera gel using microwave radiation at various input powers was investigated. The kinetic models, namely, Newton, Page, Modified Page, Henderson and Pabis, Logarithmic, Wang and Singh, Two term, and Midilli were tested to predict the variation of moisture content with irradiation time. The effectiveness of the models was verified in terms of the correlation coefficient (R^2), root mean square error (RMSE) and chi-square (χ^2).

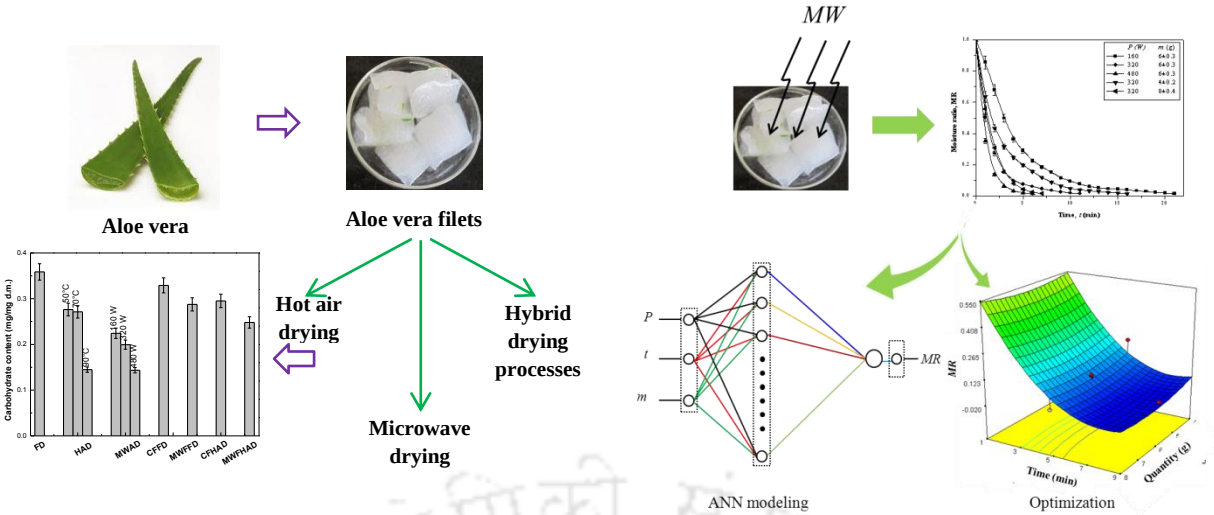

Schematic presentation of drying operations and its performance in quality retention

CHAPTER 4

Dehydration of Aloe Vera Gel in Freeze Drying, Hot Air, Microwave, and Hybrid Processes

4.1 Background of selection of drying protocols

Drying is the main operation used for increasing the partial concentration of solids present in aloe vera gel. It reduces bacterial activity; thereby increases the storage life and, reduces the packaging cost, storage places, weight of the products and transportation cost (Okos et al., 1992). Drying techniques and conditions have a noteworthy effect on the quality of the dry aloe vera gel. Improper or uncontrolled heating/drying could modify the original structure, leading to irreversible modification of the properties of the dry product (Garcia-Segovia et al., 2010). Hot air drying is the most conventional technique for the drying of aloe vera gel. But, an extended drying period due to lower heat and mass transfer, affects on its final product quality. Thermal drying also may promote the breaking of cell wall polysaccharide network (Cohen and Yang, 1995). On the other hand, the application of microwave irradiation diminishes the drying time dramatically by the mechanism of volumetric heating (Severini et al., 2005; Wang et al., 2009). Unlike conventional heating, the microwave directly excites the water molecules due to its high dielectric constant, and, it causes a faster evaporation of water (Prabhanjan et al., 1995). Further, the energy absorption in microwave drying is proportional to the residual moisture content of solids. Hence, the solids with high water content are very responsive to the microwave.

For high water content solids, the mechanical dewatering processes are becoming widespread nowadays. High hydrostatic pressure and centrifugation are widely used in food industries. Quick removal of bulk of water from the solids using mechanical process reduces the drying time which is manifested in retention of its physico-chemical properties. Vega-Galvez et al. (2011a, 2011b) studied the effect of high hydrostatic pressure treatment on functional properties and quality characteristics of aloe vera gel. Similar studies have been performed by Yucel et al. (2010) for carrot, apple and green bean for enhancing the drying rate. Osmotic dehydration of aloe vera gel using concentrated sugar solution is performed where the exchange of water soluble component with sugar solution takes place (Garcia-Segovia et al., 2010). In all these cases, some of the water-soluble components of the solid are lost with the water but, the emphasis is given on the retention of quality of the dried products over the minute loss of the solids.

The integrated drying techniques comprising of two or more drying processes (termed as hybrid processes) must be innovated towards a better retention of its physico-chemical properties. Performing of the drying operations in two successive stages improves the quality of the dried gel since the products degraded at ending the prolonged conventional drying process. A rapid removal of bulk water in the first stage and, the dehydration of low moisture, viscous solid in the second stage preserve the bioactivity of the product. Therefore in this section, the two-stage hybrid drying processes for the dehydration of aloe vera gel was studied. The performance of the hybrid and microwave assisted drying processes was evaluated in terms of functional properties and quality characteristics including carbohydrate and protein contents. The statistical analysis was performed by ANOVA to estimate the average statistically significant differences for a confidence level 95% (p value<0.05).

In this regard, the performance of other drying processes was compared with freeze dried aloe vera gel. In the freeze drying (FD) process, after sublimation, the aloe gel matrix

gets transformed into a honey-comb like structure and, the cell wall matrix of the solid is least affected. For this reason, the freeze-dried gel was rehydrated rapidly and more completely (Holloway and Greig, 1984). It also showed a higher water retention capacity and swelling values. Freeze drying is the least disruptive method and, could retain the highest physico-chemical properties in the high-value products.

4.2 Theoretical considerations

4.2.1 Experimental design using RSM

The face-centered central composite design (FCCD) in RSM was employed to build a response surface for describing the MWAD of aloe gel. The interactive dependency of independent variables, namely, microwave power (*P*), drying time (*t*) and gel quantity (*m*) on response parameter, moisture ratio (*MR)*, was taken into consideration. Table 4.1 shows the ranges and levels of each independent variable in MWAD as designed by FCCD. Here, '-1', '0' and '+1' represent the lower, central and upper values of the corresponding factors, respectively. The range of drying parameters in CCD was selected based on the preliminary studies in such a way so that the variation of moisture ratio becomes significant during MWAD of aloe vera gel. According to FCCD, 20 experimental runs were performed with six repetitions at the center point (Table 4.2). "Design-Expert" Version 7.0.0 (STAT-EASE Inc., USA) was employed for FCCD and graphical analysis of the experimental results.

Table 4.1: The ranges of input parameters in MWAD of aloe vera gel.

Input factors	Factorial and central values			
	Unit	-1	0	+1
P	W	160	320	480
m	g	4	6	8
t	min	1	5	9

Moisture content was expressed on the dry basis and, *MR* was defined below as in Eq. 4.1.

$$MR = (X_{wt} - X_{we})/(X_{w0} - X_{we}) \quad (4.1)$$

where, X_{w0} = initial moisture content (g water/g dry matter (d.m.)), X_{wt} = moisture content at time '*t*' (g water/g d.m.), and X_{we} = equilibrium moisture content (g water/g d.m.). X_{wt} is calculated by the difference between the amount of moisture present initially and at time '*t*' per unit dry matter. The estimation of equilibrium moisture content was performed in a hot air oven until the equilibrium was reached. Under microwave drying, X_{we} was expected to vary slightly due to the structural alteration of product, variation in temperature and, relative humidity, but its effect on moisture ratio was negligible.

Table 4.2: Three factors FCCD in MWAD of aloe vera gel.

Experiment no.	*P* (W)	*m* (g)	*t* (min)
1	320	6	1
2	320	6	5
3	480	6	5
4	320	4	5
5	160	8	1
6	320	8	5
7	480	8	9
8	160	8	9
9	320	6	5
10	160	4	1
11	320	6	5
12	480	4	9
13	160	6	5
14	320	6	5
15	480	8	1
16	320	6	5
17	320	6	5
18	320	6	9
19	160	4	9
20	480	4	1

4.2.2 ANN model architect

ANN consists of a set of processing elements, known as neurons. Here, three independent variables, *i.e.*, *P*, *m*, and *t* consist of three input layer neurons and *MR* as output layer neuron. The hidden layer acts as a gathering of feature detectors. The weighted sum of all input layer neurons is summed up in each neuron of the hidden layer and, goes through an activation or transfer function to generate an output signal. One or more hidden layers with a variable number of neurons may form the neural network model, but more hidden layers may cause data over the fitting problem. Hence, the model becomes nonadaptive to input data (Torrecilla et al., 2004). So, a single hidden layer was employed in the present study. Figure 4.1 shows the architecture of a 'feed forward' artificial neural network model using a single hidden layer with 3-*x*-1 topology where *x* was the number of hidden layer's neurons. '*x*' varied from 1 to 10 for a better prediction of *MR*. In fact, in feed-forward architecture, information moves only in forward direction, *i.e.*, from input to hidden to output layer (Razavi et al., 2004). The hyperbolic tangent sigmoid transfer function (Tansig) from input to hidden layer and Purelin transfer function from hidden to output layer were employed to generate a reasonably accurate estimation for a single hidden layer feed-forward network (Marini, 2009; Nourbakhsh et al., 2014). A three layered feed-forward backpropagation neural network was used for the modeling of MWAD of aloe gel. Total 20 data points (Table 4.2) were randomly distributed into three parts, i.e., training (70 % data), validation (15 % data) and testing (15 % data). ANN model was developed using MATLAB R2009a (The Mathworks, Inc., Ver. 7.8.0.347) toolbox. The best training performance of the network was selected based on the highest regression coefficient (R^2) (Eq. 4.2), lowest mean square error (*MSE*) (Eq. 4.3) and absolute average deviation (*AAD*) (Eq. 4.4) (Sinha et al., 2013).

$$R^2 = \frac{(\sum_{i=1}^{n}(MR_{\exp,i} - \overline{MR_{\exp,i}})(MR_{pre,i} - \overline{MR_{pre,i}}))^2}{\sum_{i=1}^{n}(MR_{\exp,i} - \overline{MR_{\exp,i}})^2 (MR_{pre,i} - \overline{MR_{pre,i}})^2} \quad (4.2)$$

$$MSE = \frac{1}{n}\sum_{i=1}^{n}(MR_{pre,i} - MR_{\exp,i})^2 \quad (4.3)$$

$$AAD = \frac{1}{n}\sum_{i=1}^{n}\left|(MR_{pre,i} - MR_{\exp,i})\right| \quad (4.4)$$

where, n is the number of data points; MR_{exp} and MR_{pre} are the predictive and experimental values, respectively. '$\overline{MR}$' is the mean of the related values.

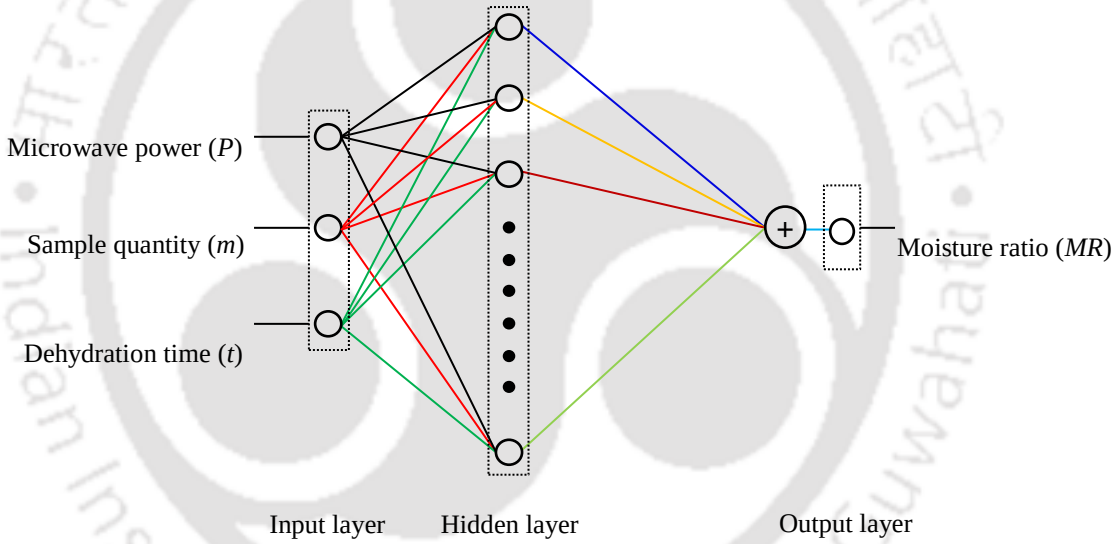

Figure 4.1: Architecture of feed forward ANN model (3-*x*-1topology) architecture.

4.2.3 Foundation and selection of drying models

4.2.3.1 Moisture diffusion coefficient

Let us consider that the unidirectional diffusional flux at $x=x$ be J_x and at $x=(x+\Delta x)$ be J_{x+dx}. Let the local concentration at 'x' at time 't' be $c(x, t)$ (Figure 4.2).

Therefore, from the concept of mass balance in the region Δx,

$$(J_x - J_{x+\Delta x})\Delta t = \Delta c \Delta x$$

$$\frac{\Delta c}{\Delta t} = \frac{J_x - J_{x+\Delta x}}{\Delta x}$$

If $\Delta x \rightarrow 0$, then,

$$\frac{\delta c}{\delta t} = -\frac{\delta J}{\delta x}$$

Putting $J = -D_{eff}\frac{\delta c}{\delta x}$ (from Fick's first law of diffusion),

$$\frac{\delta c}{\delta t} = -\frac{\delta}{\delta x}(-D_{eff}\frac{\delta c}{\delta x})$$

$$\frac{\delta c}{\delta t} = D_{eff}\frac{\partial^2 c}{\partial x^2} \qquad (4.5)$$

Eq. (4.5) is known as Fick's second law of diffusion.

In general, it is expressed as:

$$\frac{\delta c}{\delta t} = D_{eff}.\nabla^2 c \qquad (4.6)$$

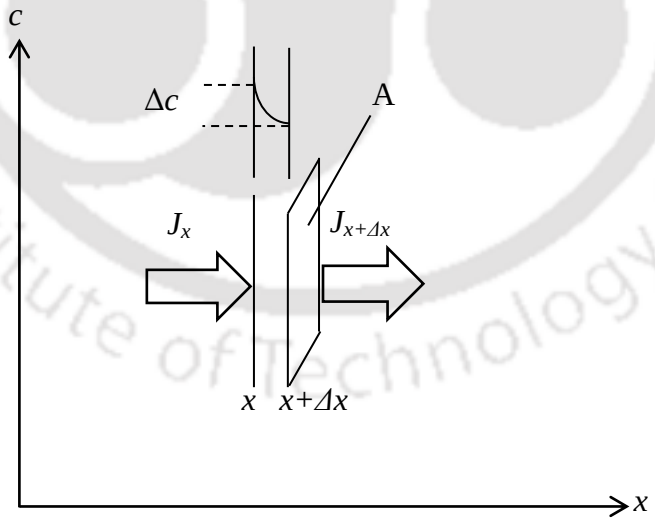

Figure 4.2: Variation of diffusional flux with time and position.

The Fick's second law of diffusion is typically employed to determine the diffusion coefficient of moisture during dehydration of fruits and vegetables where the constant drying rate periods are not usually present (Crank, 1975; Kaya et al., 2007). In which, the moisture ratio (*MR*) as a dependent parameter is related to the initial, final, and equilibrium moisture content of the specimen. The analytical solution of Eq. (4.5) depends on the initial and boundary conditions for various shapes of geometry (Crank, 1975). The typical initial and boundary conditions for flat materials of half thickness *L* are as follows:

at $t=0$ $c(x, 0)=c_0$

at $t>0$ $\frac{\delta c}{\delta t}(0, t)=0$ and $c(L, t)=c_e$

With the assumption of uniform internal moisture distribution, constant diffusion coefficient, no shrinkage, and negligible external resistance for a semi-infinite slab, the solution of Eq. (4.5) follows as (Garcia-Pascual et al., 2006; Vega-Galvez et al., 2009):

$$MR=\frac{8}{\pi^2}\sum_{n=0}^{\infty}\frac{1}{(2n+1)^2}\exp\left[\frac{-(2n+1)^2 D_{eff}\pi^2 t}{4L^2}\right] \tag{4.7}$$

where, *L* is half thickness of the slab (5±0.5 mm) and, *MR* is defined as in Eq. 4.1. The temperature and relative humidity of air were uncontrollable under microwave drying, but its effect is negligible on the equilibrium moisture content (Prabhanjan et al., 1995). Hence, the error involved in computing *MR* in Eq. 4.1 is negligible by considering X_{we} as equal to zero (Akgun and Doymaz, 2005; Zarein et al., 2015).

Representing Eq. 4.7 up to the first term, it takes the form of Eq. 4.8.

$$MR=\frac{8}{\pi^2}\exp\left[\frac{-D_{eff}\pi^2 t}{4L^2}\right] \tag{4.8}$$

4.2.3.2 Determination of activation energy

The dependency of D_{eff} on microwave power and activation energy (E_a) could be found using the modified form of the Arrhenius equation. The drying temperature of the materials was not measured and, whereas, the ratio of microwave power to sample quantity (P/m) was substituted in place of temperature as shown in Eq. 4.9 (Dadali et al., 2007; Ozbek and Dadali, 2007).

$$D_{eff} = D_0 \exp\left[\frac{-E_a m}{P}\right] \tag{4.9}$$

where, E_a is the activation energy of moisture diffusion (W g^{-1}), D_0 is the pre-exponential factor (m^2 s^{-1}), m is the quantity of raw sample (g) and, P is the microwave input power (W).

4.2.3.3 Estimation of drying efficiency

The microwave drying efficiency (η_d) is defined as the ratio of average energy consumed for evaporation to microwave energy supplied (Soysal et al., 2006). It is expressed as in Eq. 4.10.

$$\eta_d = \frac{m_w \lambda_w}{P \Delta t} \times 100, \% \tag{4.10}$$

where, m_w is the amount of water (kg) evaporated, λ_w is the latent heat of vaporization (2257 kJ kg^{-1}) and, Δt is the time interval (s).

4.2.3.4 Models for prediction of drying kinetics

The empirical and semi-empirical drying models (Table 4.3) developed based on the diffusion theory are typically employed to describe the falling rate period during dehydration process of vegetables and crops (Phoungchandang and Woods, 2000; Xanthopoulos et al., 2007). Newton, Henderson and Pebis, Wang and Singh, Logarithmic and Two term models consider that the resistance to moisture diffusion occurs only at the interface of food-stuff and

surrounding. The Henderson and Pabis model can be regarded as the special form of infinite series solution of Eq. (4.8) considering only the first term, whereas, the 'two term' model consists of the first two terms of the series. Page model is widely applied for the drying of thin layer foodstuffs under the falling rate period. Page, Modified Page, and Midilli are purely empirical models developed by introducing an exponent '*n*' to the time *t* in the normal drying equation.

Table 4.3: Thin layer drying kinetic models.

Model	**Model expression** $MR=$	**Reference**
Newton	$\exp(-kt)$	Brooker et al., 1992
Page	$\exp(-kt^n)$	Diamante and Munro, 1993
Modified Page	$\exp[-(kt)^n]$	Whith et al., 1978
Henderson and Pabis	$a\exp(-kt)$	Zhang and Litchfield, 1991
Logarithmic	$a\exp(-kt)+c$	Yaldiz and Ertekin, 2002
Wang and Singh	$1+at+bt^2$	Wang and Singh, 1978
Two term	$a\exp(-k_0t)+b\exp(-k_1t)$	Henderson, 1974
Midilli et al	$a\exp(-kt^n)+bt$	Midilli et al., 2002

4.2.3.5 Statistical analysis

MATLAB R2009a (The Mathworks, Inc., Ver. 7.8.0.347) was used for the numerical calculations. The quality of model fitting was assessed using the linear regression coefficient (R^2) (Eq. 4.2), root mean square error (*RMSE*) (Eq. 4.11), and Chi-square (χ^2) (Eq. 4.12) which are given as follows (Ozdemir and Devres, 1999; Vega et al., 2007; Radhika et al., 2011):

$$RMSE=\left[\frac{1}{N}\sum_{i=1}^{N}(MR_{pre,i}-MR_{exp,i})^2\right]^{1/2} \tag{4.11}$$

$$\chi^2=\frac{\sum_{i=1}^{N}(MR_{pre,i}-MR_{exp,i})^2}{N-z} \tag{4.12}$$

where, n is the number of data points, MR_{exp} and MR_{pre} are the experimental and predictive values of MR, respectively. '$\overline{MR}$' is the mean of related values, N is the number of observations and, z is the number of constants in the equation.

4.3 Results and discussions

4.3.1 Drying processes and quality of dried gel

4.3.1.1 Retention of carbohydrate

The initial moisture content of fresh aloe vera gel was found to be 97.5-98.5% of the total weight. The amounts of carbohydrate and protein content were 0.359 and 0.213 mg/mg d.m., respectively. The variations of the carbohydrate content of dried aloe vera gel in the hot air drying (HAD), MWAD, CFFD, MWFFD, CFHAD and MWFHAD are shown in Figure 4.3. The highest carbohydrate content was 0.359 mg/mg d.m. for the freeze-dried sample. In this process, the fresh aloe vera filet was directly lyophilized and, it preserved all constituents as well as cell wall matrix structure of aloe vera. The removal of ice crystals retained the matrix of honeycomb-type structure which tends to rehydrate rapidly and more completely. For this reason, FD sample exhibited the highest value of carbohydrate and protein content, and functional properties.

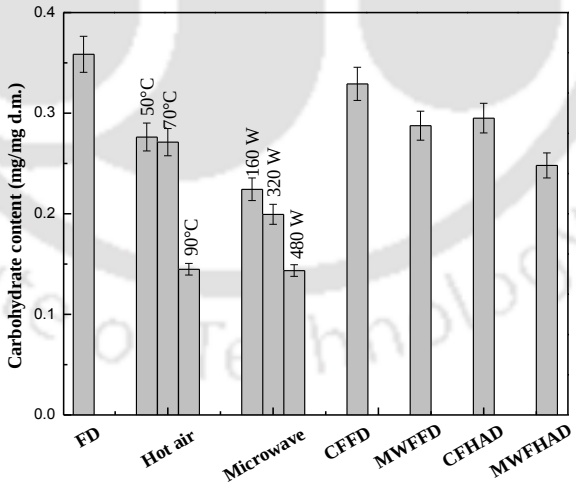

Figure 4.3: Performance of FD, HAD, MWAD, CFFD, MWFFD, CFHAD and MWFHAD on the carbohydrate content of aloe vera gel (Conditions: Centrifugation at 3940g for 30 min; MWAD at 160 W up to moisture ratio of 0.4 and HAD at 50°C for hybrid drying).

Carbohydrate content was sensitive to the drying temperature beyond 70°C. The amounts of carbohydrate were 0.276 and 0.271 mg/mg d.m. at 50 and 70°C. It dropped by about 59.6% at 90°C. MWAD at three different powers led to a significant change in the carbohydrate content (p<0.05). The operating power in microwave-assisted drying also influenced the carbohydrate content notably. It decreased by 37.4 and 44.4% at 160 and 320 W. MWAD at the input power of 480 W exhibited similar results as that of at 90°C in HAD. Furthermore, HPLC of the specimens obtained from FD and MWAD at 480 W provide a fingerprint for the possible chemical alterations in the total carbohydrate content (Figure A4a) which is in accordance with the results in Figure 4.3.

At higher temperature, polysaccharide and polypeptide interact to form complex molecules. The formation of such molecules is favored by the increase in temperature. The hydrophobic interaction also facilitates the formation of complexes between polymers which cause conformational and structural modifications. This, in turn, lowered the carbohydrate and protein content in HAD, and MWAD at higher temperatures and powers (Magnin and Dumitriu, 2010).

CFFD could retain the maximum amount of carbohydrate followed by CFHAD. There was only 8.2 and 17.7% decrease in the carbohydrate content in CFFD and CFHAD, respectively. The reduction of carbohydrate in the CFFD process was due to the fact that some amount of water soluble solids were lost with the supernatant during centrifugation (5±1%). About 92% water was removed by centrifugation and, it helped for the quick drying of gel in the subsequent FD. A faster initial dehydration by MWAD up to moisture ratio of 0.4 followed by FD in MWFFD could retain 80.2% carbohydrate.

Femenia et al. (2003) studied the effect of temperature on the carbohydrate content of aloe vera gel in HAD. They reported around 13.6, 22.7 and 28.2% decrease in carbohydrate

content at 50, 70 and 80°C, respectively. In the present study, it was around 22.9, 24.37% at 50 and 70°C, respectively.

4.3.1.2 Retentivity of protein content

Figure 4.4 shows the retention of protein content in different drying techniques. It exhibited a similar trend of strong dependency on drying temperatures (>70°C) and microwave power (>160 W), as observed for the carbohydrate content as well. HAD at 90°C led to a significant change in the protein content (p<0.05). There were about 17.7, 21.8, and 75.1% loss in protein content at 50, 70 and 90°C in HAD. MWAD decreased the total protein contents (p<0.05) significantly. It was 54.8, 72.3 and 75.8% at 160, 320 and 480 W in MWAD, respectively. However, denaturation of protein was more significant than carbohydrate under the identical drying conditions. The same is also evidenced from the chromatographic analyses (Figure A4b). Generally, carbohydrates are less susceptible to denaturation as compared to proteins and lipids towards heat treatment (Fennema, 1985). Heating causes structural and functional changes in protein molecules. Hydrogen bonds are broken and, the protein molecules lose their quaternary, tertiary and secondary characteristic structures because of the heat treatment. Thermal denaturation also leads to protein coagulation. The spatial arrangement of molecules is collapsed to amorphous granules with no biological function when proteins are thermally treated (Thomsen and Pearce, 2011). It can be seen from Figure 4.4 that there was only 9.1, 23.7, 14.5 and 27.4% protein decomposition in CFFD, MWFFD, CFHAD, and MWFHAD, respectively. The non-thermal operation for removal of bulk water content could prevent protein denaturation.

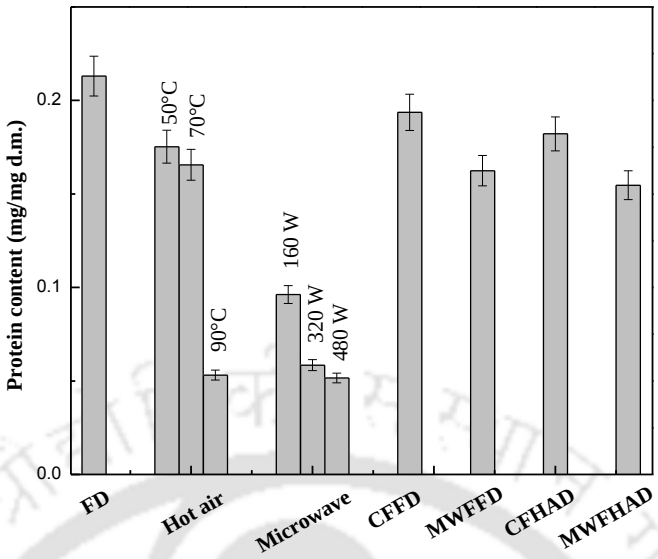

Figure 4.4: Performance of FD, HAD, MWAD, CFFD, MWFFD, CFHAD and MWFHAD on the protein content of aloe vera gel (Conditions: Centrifugation at 3940g for 30 min; MWAD at 160 W up to moisture ratio of 0.4 and HAD at 50°C for hybrid drying).

4.3.1.3 Ash/inorganic residues

The ash/inorganic residues are due to the presence of mineral elements in aloe vera gel. Ash/inorganic residues remained almost unaffected for different drying processes as expected. The average value of ash/inorganic residues was around 14% by weight. Gulia et al. (2010) reported a similar value of 15.5% ash content in aloe vera gel.

4.3.1.4 Functional properties of dried aloe vera gel

Functional properties, namely, swelling, WRC and FAC are measured to account for the changes which occur in the matrix structure during dehydration of vegetables and foodstuffs. Functional properties are associated with the chemical structure of the high molecular weight polysaccharides in aloe vera gel. In the drying processes, the spatial arrangement of the molecules might be inherently effected depending on the drying

conditions. The tissue integrity and dense structure of collapse also may be lost which is associated with the reduction of hydrophilic and rehydration properties. The study of functional properties reveals the modification in the solid gel matrix under various drying processes. The obstacle to the movement of water in dried gel matrix during rehydration is reflected by its swelling property. The swelling values for different drying treatments are highly significant (p<0.005). ANOVA summary table for statistical analysis for swelling is shown in Appendix (Table A1). In HAD, the highest swelling value (75 mL/g d.m.) was observed at 50°C (Figure 4.5). It reduced to 68 and 66 mL/g d.m. at 70 and 90°C, respectively. High swelling values indicated that a vast internal pressure was produced in the matrix tissues which promoted the dried aloe vera gel to expand and puff. In MWAD, the swelling was less sensitive towards the microwave power. MWAD showed a swelling value of 66±2 mL/g d.m., whereas, the freeze dried sample showed a swelling value of 90 mL/g d.m. (Figure 4.5). CFFD, MWFFD, CFHAD, and MWFHAD also exhibited good swelling properties of 84, 75, 80 and 65 mL/g d.m., respectively.

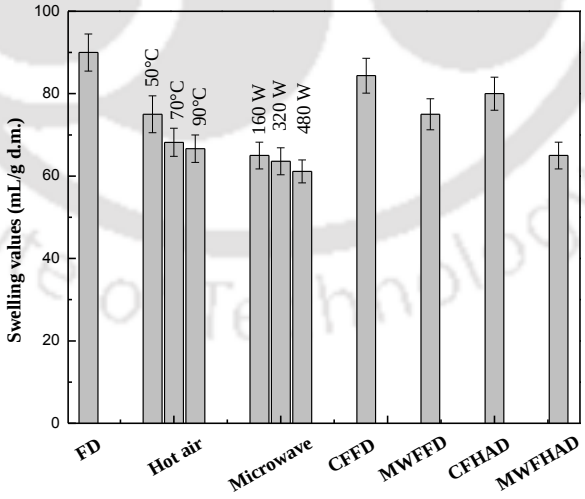

Figure 4.5: Performance of FD, HAD, MWAD, CFFD, MWFFD, CFHAD and MWFHAD on swelling of aloe vera gel (Conditions: Centrifugation at 3940g for 30 min; MWAD at 160 W up to moisture ratio of 0.4 and HAD at 50°C for hybrid drying).

Figure 4.6a shows the WRC of dried aloe vera gel. A gradual decrease in WRC was observed in HAD with increasing temperatures. WRC was reduced from 35.2 to 24.8 g/g d.m. within the temperature range of 50 to 90°C. WRC was determined as 24, 23 and 22.7 g/g d.m. at 160, 320 and 480 W, respectively, in MWAD. It implies that the microwave power practically did not have any impact on the WRC (p<0.001).

CFFD showed about 20.1% more WRC than MWFFD dried gel. CFHAD and MWFHAD showed WRC of 38.7 and 28.5 g/g d.m., i.e., 4.9 and 12.3% less as compared to that of CFFD and MWFFD. The rupture of the cellular structure caused a lower diffusion of water through the surface during rehydration. HAD affected the fibrous matrix of aloe vera gel. The rehydration process was based on the fiber processing, as shrinkage and rupture occur in the matrix-structure and tissues during drying of food materials (Kaymak-Ertekin, 2002).

The high value of FAC implies the higher hydrophobic interaction between added oil and fat present in the dried aloe vera gel. Generally, dehydration promotes a drop in FAC (Garau et al., 2007). HAD at 70 and 90°C showed a significant fall in FAC in comparison to 50°C. FAC was independent of the input powers (160–480 W) of microwave irradiation. Thibault et al. (1992) reported that lignin is responsible for fat adsorption. The amount of lignin in fresh aloe gel was found to be less than 3% by weight (Femenia et al., 2003). The value of FAC was around 4.42 g/g d.m., whereas, for freeze dried sample, it was 8.84 g/g d.m. CFFD and MWFFD, and CFHAD and MWFHAD showed almost a similar FAC of freeze dried gel (Figure 4.6b).

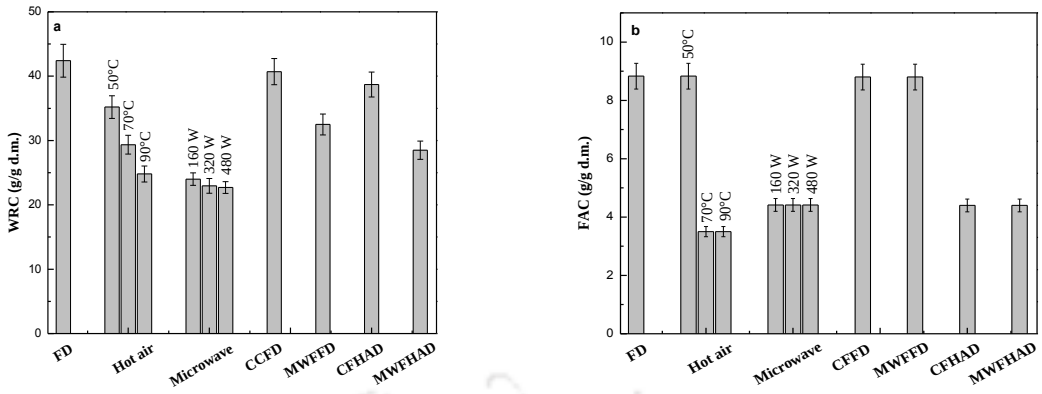

Figure 4.6: Performance of FD, HAD, MWAD, CFFD, MWFFD, CFHAD and MWFHAD on (a) WRC and, (b) FAC of aloe vera gel (Conditions: Centrifugation at 3940g for 30 min; MWAD at 160 W up to moisture ratio of 0.4 and HAD at 50°C for hybrid drying).

4.3.1.5 Influence of HAD, MWAD and hybrid drying techniques on functional groups

Functionalization of the bio-active component is straightforwardly related to the presence of specific functional groups. In aloe vera gel, the main bio-active component is mannose which synergistically functions with other components present in the aloe vera gel. The modification of functional groups in polysaccharides under various drying processes could be ascertained using FT-IR analysis. These changes in functional groups were reflected in the carbohydrate and protein contents which in turn could affect the bio-activity. The presence of functional groups associated with carbohydrate and protein molecules was confirmed by the FT-IR spectra of the dehydrated aloe vera gel. An IR spectrum of freeze and hot air dried gels at different temperatures is illustrated in Figure 4.7a. A broad peak around 3460 cm^{-1} was observed in the freeze dried gel. It represents -OH group in the carbohydrate units. The bands at 1597 and 1320 cm^{-1} were corresponding to -RNH_2 and -COOH stretches. The peak at 1066 cm^{-1} in aloe vera gel signified the mannopyranose

component (Kacurakova et al., 2000). The weak peaks between the wavelengths of 800 and 1400 cm^{-1} were associated with the various units of polysaccharides. The peak at 1031 cm^{-1} was due to the glucan units. The pyranoside and mannose were detected in aloe vera gel at band 876 and 806 cm^{-1}, respectively (Yan et al., 2003). The peaks at 1732 and 1250 cm^{-1} confirmed the presence of o-acetyl ester which is suggested as the necessary component for biological activation (Reynolds and Dweck, 1999). On the other hand, the peak at 3460 cm^{-1} was absent in hot air-dried gel. The decrease in intensity was due to deacetylation of polysaccharide and denaturation of proteins (Femenia et al., 2003).The peak at 3460 cm^{-1} corresponding to -OH was missing in MWAD. FT-IT spectra displayed a significant decrease of the bands at 1732, 1597 and 1320 cm^{-1} which could be assigned to o-acetyl ester, $-RNH_2$ and -COOH stretches, respectively (Figure 4.7b).

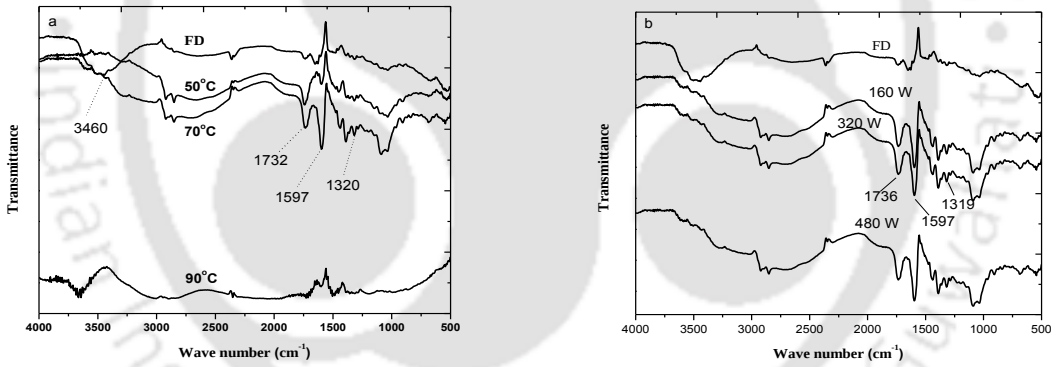

Figure 4.7: FT-IR spectra of dried aloe vera gel. (a) hot air drying and, (b) microwave-assisted drying.

Figures 4.8a and 4.8b show the infrared spectra of freeze dried, CFFD, MWFFD, CFHAD and MWFHAD aloe vera gels. -OH group in sugar units was absorbed around 3394 and 3448 cm^{-1}. The peaks between 1576 and 1539 and 1400 and 1369 cm^{-1}, corresponding to $-RNH_2$ and –COOH groups, were observed in the hybrid drying processes. The other major peaks around 1625-1740, 1066, 1031 and 806 cm^{-1} attributed to o-acetyl ester,

mannopyranose, glucan and mannose respectively in CFFD and MWFFD. The decrease in intensity of IR peaks in MWFFD denotes the possible modification of polysaccharide and protein molecules due to the microwave treatment.

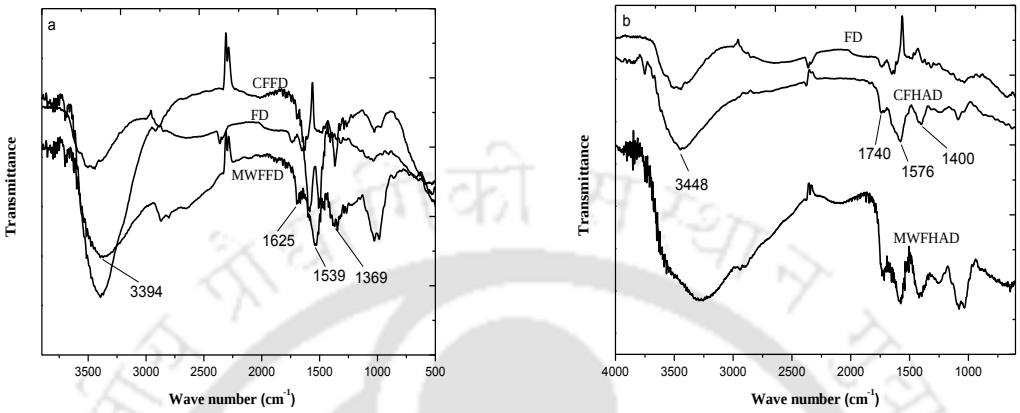

Figure 4.8: FT-IR spectra of dried aloe vera gel in hybrid drying processes. (a) CFFD and MWFFD and, (b) CFHAD and MWFHAD (Conditions: Centrifugation at 3940g for 30 min; MWAD at 160 W up to moisture ratio of 0.4 and HAD at 50°C for hybrid drying).

4.3.2 Prediction of drying kinetics and moisture diffusivity in MWAD

In this study, the drying kinetics of aloe vera gel using microwave radiation at various input powers was investigated. The kinetic models, namely, Newton, Page, Modified Page, Henderson and Pabis, Logarithmic, Wang and Singh, Two term and Midilli were tested to predict the drop of moisture content with the irradiation time. The effectiveness of the models was verified in terms of regression coefficient (R^2), root mean square error (*RMSE*) and chi-square (χ^2). Further, the influence of microwave power on the diffusivity of moisture is evaluated along with the activation energy and the drying efficiency of microwave-assisted drying of aloe vera gel.

4.3.2.1 Effect of microwave power on drying kinetics of aloe vera gel

The change of moisture ratio of aloe vera gel with drying time is presented in Figure 4.9. It shows the typical diffusion-controlled characteristics under all test conditions. The entire drying kinetics of aloe vera gel lied in the falling rate period. The microwave power had a profound effect on the residual moisture content and, the drying curves became steeper at a higher input power which clearly indicates the faster removal of moisture. The time required to decrease the moisture content from the initial value of 65.7% to 1.5 % was 21, 11 and 6 min for 160, 320 and 480 W, respectively.

The model parameters determined by fitting to the experimental results using non-linear regression analysis are presented in Table 4.4. The values of R^2, *RMSE* and χ^2 ranged from 0.793 to 0.999, 0.00086 to 0.12678 and 0.018×10^{-4} to 0.019, respectively. The best fitted kinetic model was selected on the basis of the highest value of R^2 and the lowest values of *RMSE* and χ^2. Among all the models, the 'Two term' model provided the best fit to the variation of *MR* with drying time. It can be seen that the value of rate constants was increased

with microwave powers. In MWAD, the moisture transport within gel occurs mainly owing to diffusion. The model was derived from the Fick's second law of diffusion and, likewise, it showed the best fit to the drying kinetics (Figure 4.9).

Table 4.4: Results of regression analyses and values of model constants for microwave-assisted drying of aloe vera gel.

Model	Power (W)	Model constants×10^2				R^2	*RMSE*×10^2	$\chi^2 \times 10^4$
Newton	160	k = 23.2				0.994	2.13	4.76
	320	k = 62.7				0.993	2.40	6.30
	480	k = 100.7				0.999	1.20	1.68
Page	160	k = 20.8	n = 106.9			0.995	1.95	4.16
	320	k = 72.2	n = 80.4			0.998	1.30	2.01
	480	k = 105.4	n = 87.2			0.999	0.55	0.43
Modified Page	160	k = 22.9	n = 106.9			0.995	1.95	4.16
	320	k = 66.7	n = 80.4			0.998	1.30	2.01
	480	k = 106.2	n = 87.2			0.999	0.55	0.43
Henderson and Pabis	160	k = 24.0	a = 103.4			0.995	1.92	4.06
	320	k = 61.7	a = 98.5			0.993	2.36	6.70
	480	k = 100.4	a = 99.7			0.999	1.20	1.10
Wang and Singh	160	a = -14.1	b = 0.5			0.925	0.77	65.51
	320	a = -29.0	b = 1.9			0.793	12.7	192.9
	480	a = -50.9	b = 6.0			0.905	10.25	147.2
Logarithmic	160	k = 25.1	a = 102.8	c = 1.3		0.996	1.78	3.65
	320	k = 69.2	a = 96.4	c = 3.2		0.999	0.96	1.22
	480	k = 106.6	a = 98.1	c = 1.8		0.999	0.34	0.20
Two term	160	k_0 = 22.7	k_1 = 22.9	a = -645.3	b = 748.4	0.998	1.37	2.23
	320	k_0 = 18.4	k_1 = 80.8	a = 14.5	b = 85.6	0.999	0.39	0.23
	480	k_0 = 30.3	k_1 = 114.8	a = 8.2	b =91.8	0.999	0.09	0.02
Midilli et al.	160	k = 20.3	n = 111.9	a = 101.6	b = 0.1	0.995	1.93	4.53
	320	k = 70.7	n = 87.1	a = 100.1	b = 0.2	0.999	0.84	1.05
	480	k = 105.3	n = 92.3	a = 1	b = 0.2	0.999	0.17	0.07

Figure 4.10 summarizes the parity plot for experimental and 'Two term' model predicted values of *MR*. The predicted data banded surrounding the best fitted straight line, with a value of R^2 of 0.998. Abbaszadeh et al. (2011) also showed that HAD kinetics of a thin layer of *Elaeagnus angustifolia* can be successfully predicted using the Two term model.

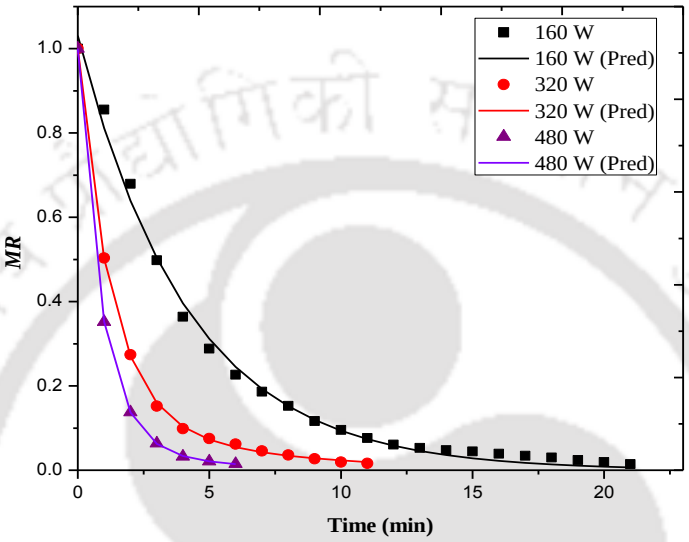

Figure 4.9: Experimental and 'Two term' model predicted (—) values of *MR* at 160 W (■), 320 W (●) and 480 W (▲) for microwave-assisted drying of aloe vera gel.

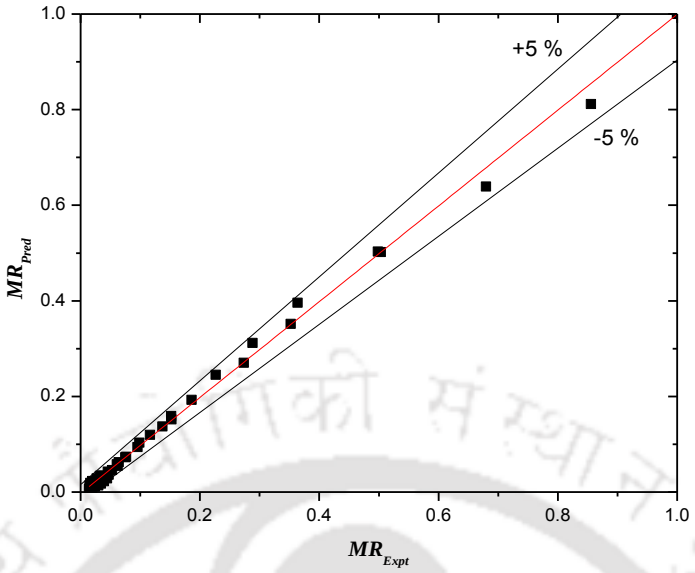

Figure 4.10: Parity plots of experimental and 'Two term' model predicted values of moisture ratio.

4.3.2.2 Effective moisture diffusivity and activation energy

The effective moisture diffusivity of aloe vera gel in MWAD was determined graphically by the method of slope. The logarithm of *MR* was plotted against the drying time '*t*' (Eq. 4.8) under various experimental conditions which produced a straight line having a slope of $\frac{-D_{eff}\pi^2}{4L^2}$ and a constant intercept of $ln(8/\pi^2)$ (Figure 4.11). The values of D_{eff} were calculated as 2.025×10^{-6}, 5.062×10^{-6} and 7.087×10^{-6} m^2 s^{-1} at 160, 320 and 480 W, respectively, with well accordance with the literature. It generally varies in the range from 10^{-6} to 10^{-11} m^2 s^{-1} for foodstuffs (Zarein et al., 2015). D_{eff} in MWAD is immensely influenced by the input power. Higher microwave energy facilitates a quick energy absorption, rapid heat penetration and forced expulsion of vapor from the inside of the drying substances which is resulted as higher D_{eff} (Prabhanjan et al., 1995). The observed values of D_{eff} for microwave drying of apple vary from 1.0465×10^{-8} to 3.6854×10^{-8} m^2 s^{-1} for 150 to 600 W (Wang et al.,

2007), and from 3.93×10^{-8} to 2.27×10^{-7} m^2 s^{-1} for 200 to 600 W (Zarein et al., 2015). It is reported to be between 3.982×10^{-11} and 2.073×10^{-10} m^2 s^{-1} in the case of mint leaves for 180 to 900 W (Ozbek and Dadali, 2007). On the other hand, D_{eff} varied from 5.30×10^{-10} to 17.73×10^{-10} m^2 s^{-1} with the increase of temperature from 50 to 90°C (Vega et al., 2007) for HAD, and from 0.19×10^{-8} to 1.98×10^{-8} m^2 s^{-1} for the osmotic dehydration (Garcia-Segovia et al., 2010) of aloe vera gel which were much lower than the values of D_{eff} obtained in the present work.

The dependency of D_{eff} on microwave power and the activation energy were estimated from Eq. 4.9. $ln(D_{eff})$ versus gel amount to power ratio (m/P) yielded a straight line (R^2=0.99), indicating the process would follow the Arrhenius type dependency (Figure 4.12). The relation between D_{eff} of aloe vera gel and microwave input power is presented as in Eq. (4.13) where the activation energy is 49.82 W g^{-1}.

$$D_{eff} = 1.31\times10^{-5}\exp\left(-49.82\frac{m}{P}\right) \quad (4.13)$$

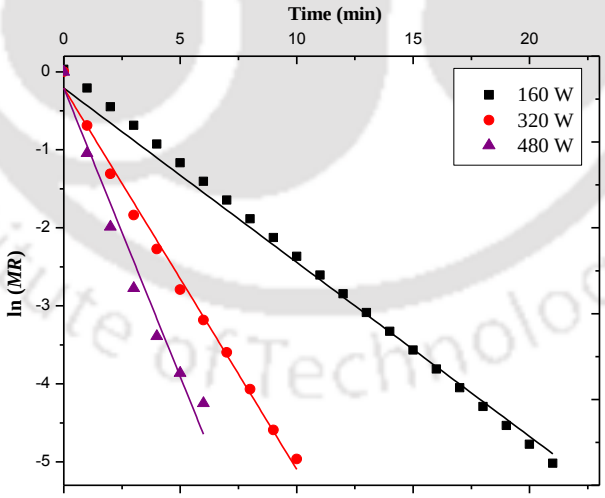

Figure 4.11: Plot of *ln(MR)* versus drying time at different microwave powers ((■) 160 W, (●) 320 W, (▲) 480 W and (—) linear fitting).

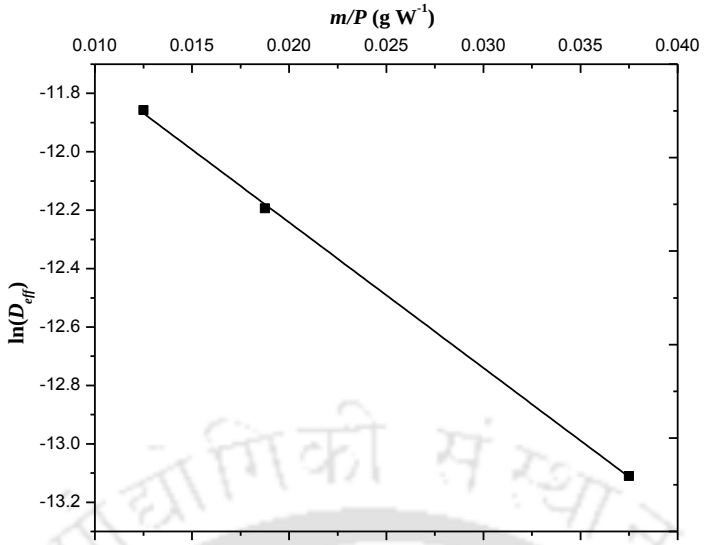

Figure 4.12: Linear relationship between $ln(D_{eff})$ and (m/P) using Arrhenius-type relationship.

4.3.2.3 Drying efficiency of aloe vera gel

The variation of microwave drying efficiency (η_d) with the irradiation time for the dehydration of aloe vera gel is presented in Figure 4.13. The drying efficiency was higher in the initial stages of drying. The energy consumption in MWAD is proportional to the residual water content. For this reason, the absorption of microwave energy decreased with the irradiation time which was resulted in a drastic reduction of drying efficiency. The highest drying efficiency was found to be 68.7 % for 320 W appeared in 1 min. At 160 and 480 W, it was 50.8 and 60.5 % found at 3 and 1 min, respectively. Zarein et al. (2015) reported that the drying efficiency varied from 17.4 to 54.3 % for the microwave dehydration of apple slice in between 200 and 600 W.

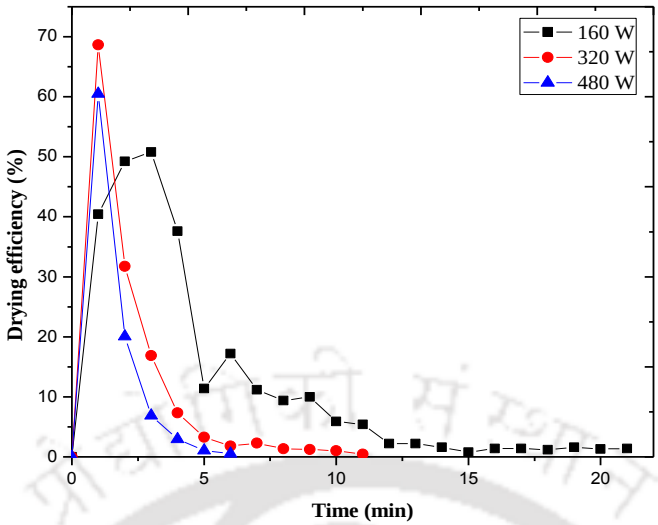

Figure 4.13: Variation of microwave drying efficiency (η_d) with drying time at different operating powers.

4.3.3 Optimality in microwave-assisted drying of aloe vera

In this section, the characteristics of aloe vera gel in MWAD and the process optimization were investigated including the influence of microwave-power, gel quantity, and drying time on the moisture content. The face-centered central composite design (FCCD) developed a regression model to evaluate their effects on the moisture content. An ANN model was generated for the mapping between the process variables and the desired response.

4.3.3.1 Drying dynamics

The influence of microwave power and amount of aloe vera sample on moisture ratio is shown in Figure 4.14. The drying curves showed the typical smooth diffusion-controlled characteristics for all the test conditions. The time needed to decrease the moisture ratio to a particular extent depended on the microwave power, which was the maximum at 160 W and minimum at 480 W. For a sample mass of 6±0.3 g, the drying time was 6, 11 and 21 min for 480, 320 and 160 W, respectively, to reduce *MR* from the initial to 0.015. The respective drying time was 16 and 7 min for 4 and 8 g samples at 320 W. The drying time was reduced with the increase in the sample quantity. This probably occurred due to a higher surface area of the sample exposed to microwave radiation. It built up a high internal pressure inside the sample resulting in an enhanced evaporation which in turn improved the diffusivity of moisture (Maskan, 2000). A faster heat generation and forced removal of vapor from the inside of aloe gel caused a rapid drying in MWAD (Prabhanjan et al., 1995). The drying curves fell sharply at a higher power which indicates a quicker expulsion of moisture from the aloe vera gel. The half-drying time (time required to reach *MR* by one-half) were 0.7, 1 and 3 min at 480, 320 and 160 W, respectively, for 6±0.3 g aloe gel.

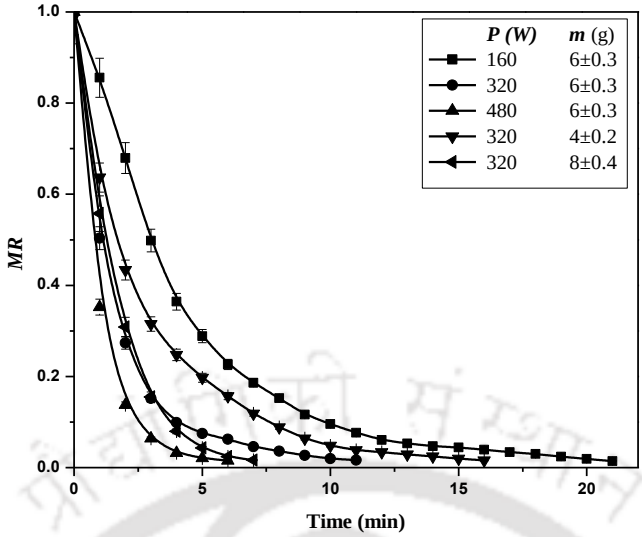

Figure 4.14: Drying curves of fresh aloe vera gel at various microwave powers and sample quantities.

The changes in the drying rate associated with moisture content are illustrated in Figure 4.15. All the drying curves started from the initial moisture content of 65.6 g water per g of dry matter. A proportional relationship was observed between the drying rate and residual moisture content. In case of microwave power of 160 W, an acceleration of drying rate was observed up to 2.5 min followed by the falling rate period. Such drying dynamic is also reported for the drying of apple pulp in MWAD (Wang et al., 2007). For the high moisture content stuff like aloe vera, it was expected to have a constant rate drying. However, it was absent in all the experimental conditions as a lower rate of diffusional transportation than the evaporating rate governing the dehydration rate (Bhandari, 2006). The progressive dehydration shrinks the vascular tissues in aloe gel which in turn ruptured the transport channels, increases the roughness and, hinders the vapor diffusion. The increase in solid concentration also builds up the resistance to transport of vapor. Similar results were also found in MWAD of food products (Diamante and Munro, 1991; Doymaz and Pala 2003;

Wang et al. 2007). The drying curves overlapped with each other at the lower moisture content (< 10 g water per g of dry matter).

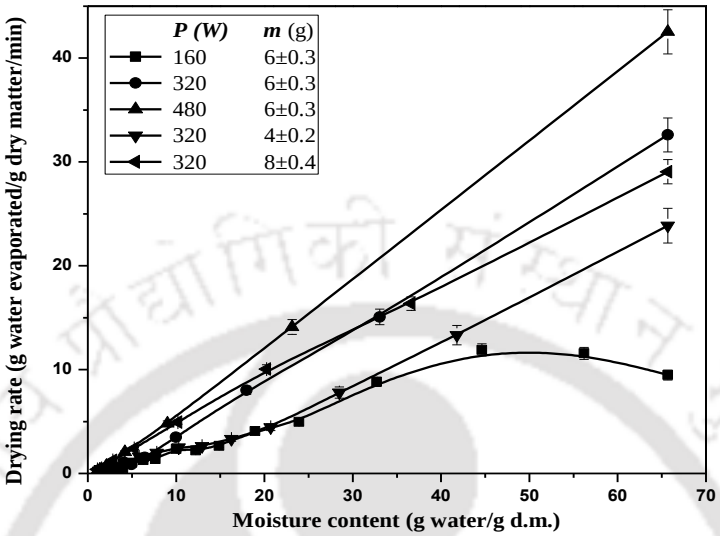

Figure 4.15: Drying rate of fresh aloe vera gel at different microwave powers and sample quantities.

4.3.3.2 RSM and optimization of drying parameters

Analysis of variance (ANOVA)

The interaction between the independent drying parameters (*P*, *m*, and *t*) and the desired response (*MR*) are represented graphically by the three-dimensional response surface as shown in Figure 4.16. It is apparent from the figures that the independent factors involved in drying process were in a nonlinear relationship with *MR*. The combined effect of sample quantity and microwave power is shown in Figure 4.16a keeping the drying time at the central point. The microwave power had a profound effect on *MR*. It was observed that the reduction in *MR* was facilitated with the higher power levels. The rate of *MR* gradually decreased at the higher input power levels since the dehydration rate was proportional to the residual moisture content. The quantity of sample showed a little effect on *MR* (Figures 4.16a

and 4.16c). A slight decrease in *MR* occurred with the increase in the sample quantity.

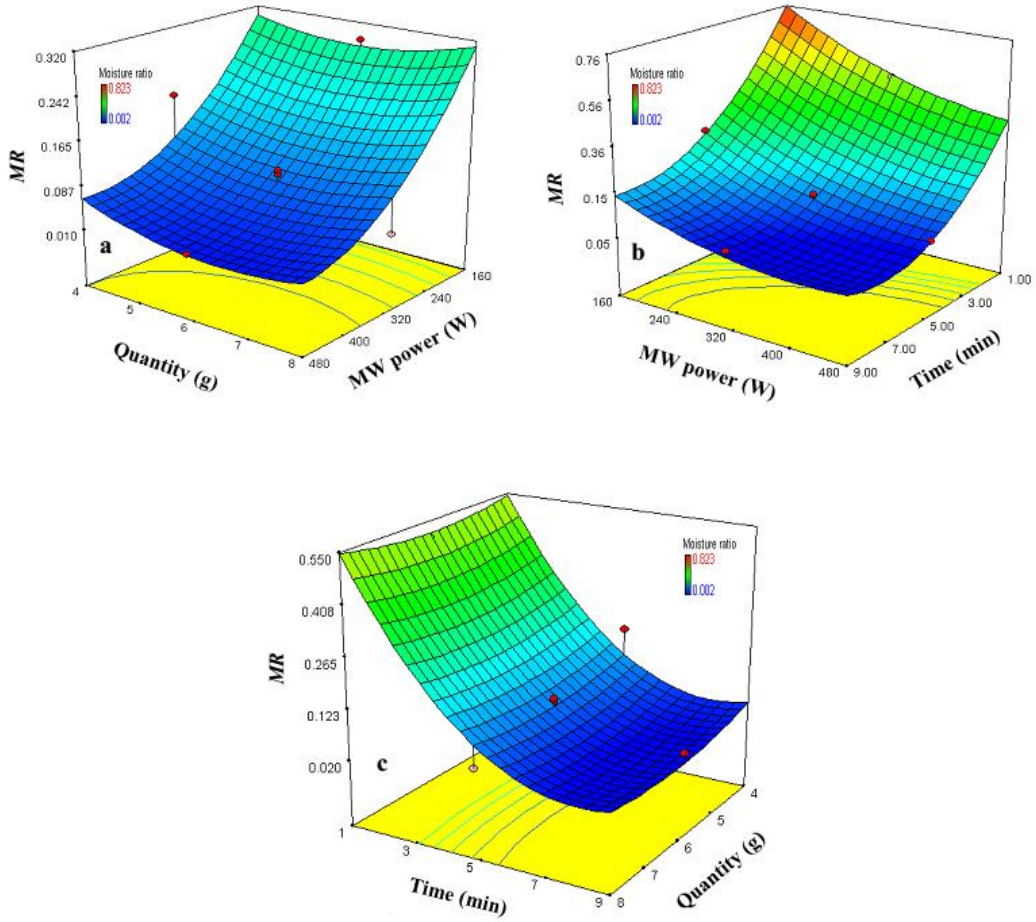

Figure 4.16: Response surface plots showing the combined effect of (a) microwave power and sample amount, (b) drying time and microwave power and, (c) sample amount and drying time.

Various types of mathematical models were checked by FCCD to fit the experimental results with the design layout (Table 4.2) for a better prediction on the statistical basis. In the present study, FCCD proposed the best fit quadratic empirical model correlating all the independent variables with the desired response, *MR*, as shown in Eq. 4.14.

$$MR = 1.502 - 2.587\times10^{-3}P - 7.532\times10^{-2}m - 0.191t - 3.32\times10^{-5}\,Pm + 7.441\times10^{-5}\,Pt - 1.078\times10^{-3}\,mt + 2.509\times10^{-6}\,P^2 + 7.307\times10^{-3}\,m^2 + 1.089\times10^{-2}\,t^2 \quad (4.14)$$

Table 4.5 represents the analysis of variance and model regression. The statistical analysis of the quadratic model was evaluated by the F-test and p-value. High F-value (75.47) with low p-value (<0.0001) was considered as a significant model fitting (Atkinson and Donev, 1992). It signifies that there was only 0.01 % probability for 'Model F-value' to occur due to the noise. Regression coefficient (R^2) signifies how well the data fits a statistical model and, it was found to be 0.986. It implies that 98.6 % variation of *MR* could be explained by the variation of *P*, *m*, *t* and, the model could not interpret only 1.4 % of the total variance. The predicted regression coefficient (R^2_{Pred}) (0.903) showed a reasonable agreement with adjusted regression coefficient (R^2_{Adj}) (0.972). Hence, the proposed model can be employed to formulate the design space. The values of 'Prob>F' less than 0.050 indicate the significant model terms including *P*, *t*, *Pt*, P^2 and t^2. High F-value and low 'Prob>F' values (<0.0001) of the model terms, *i.e.*, *P* and *t*, predominantly influenced the *MR*. The corresponding F-values were 99.68 and 397.18, respectively. The p-value (0.0592) of 'lack of fit' of the model suggests that it was insignificant and, the quadratic model indeed can be employed for an optimization of MWAD of aloe gel.

Table 4.5: ANOVA of proposed quadratic model.

Source	**Sum of square**	**Degree of freedom**	**Mean square**	**F-value**	**p-value Prob >F**
Model	1.14	9	0.13	75.47	<0.0001
P	0.17	1	0.17	99.68	<0.0001
m	0.0005	1	0.0005	0.32	0.0585
t	0.67	1	0.67	397.18	<0.0001
Pm	0.0009	1	0.0009	0.54	0.4799
Pt	0.018	1	0.018	10.82	0.0082
mt	0.0006	1	0.0006	0.35	0.5646
P^2	0.011	1	0.011	6.76	0.0265
m^2	0.0023	1	0.0023	1.40	0.2640
t^2	0.083	1	0.083	49.77	< 0.0001
Residual	0.017	10	0.0016		
Lack of fit	0.014	5	0.0027	4.62	0.0592
Model statistics					
Std. Dev.	0.041		R-Squared	0.986	
Mean	0.22		Adj. R-Squared	0.972	
C.V. %	8.79		Predicted R-Squared	0.903	

Statistical diagnostic and model verification

The interactive effects of the independent parameters can be investigated using RSM. The combined effect of independent parameters was analyzed by the model calculation. Figure 4.17 shows the binary interaction of independent variables. The non-parallel curvature between the independent variables, microwave power and drying time (Figure 4.17a), signifies a comparatively strong interaction between them (Bose and Das, 2014). As a result of this, '*Pt'* appeared as a significant term in Eq. 4.14. The parallel curvatures denote that there was no such strong interaction between the microwave power and sample amount (*P-m*) (Figure 4.17b) and, the sample amount and drying time (*m-t*) (Figure 4.17c) although an individual effect of these parameters exists on the *MR*.

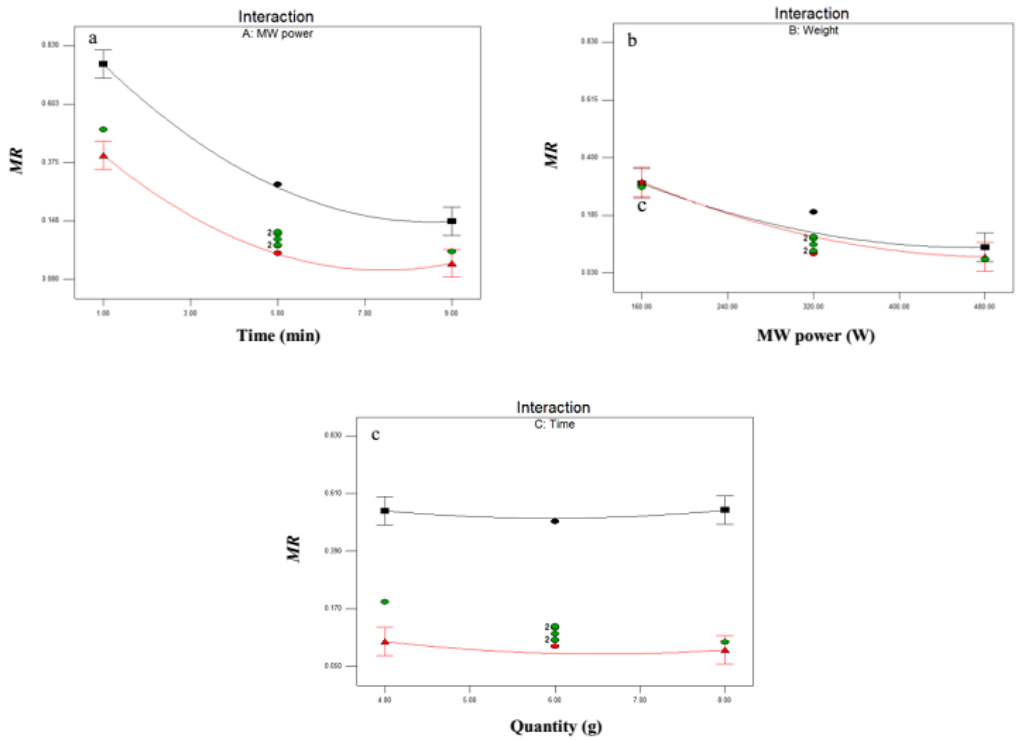

Figure 4.17: Interaction of binary combinations of microwave power, amount of sample and drying time on moisture ratio (■: lower factorial value, ▲: higher factorial value).

Figures 4.18 and 4.19 represent the major diagnostic plots to study the residual analysis of RSM design to ensure data fitted according to the statistical assumption and, to check whether the standard deviation between the experimental and predicted responses distributes in a normal way (Lee and Gilmore, 2005). The residual points fall near the straight line showing no sign of non-normality of the experimental points (Figure 4.18). Figure 4.19 represents the residual versus predicted response plot for *MR*. All the experimental points are randomly scattered within ±3 % (Bose and Das, 2014) which implies that the proposed model is adequate and, the assumption of constant variation is established.

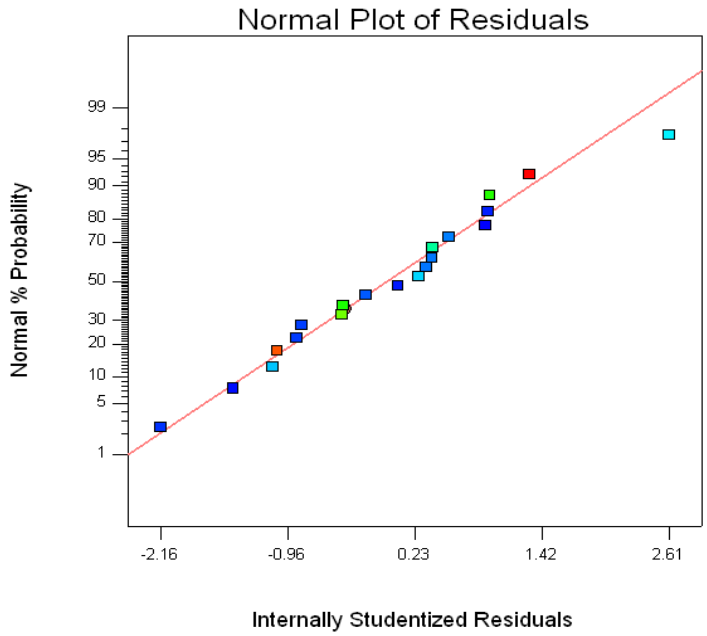

Figure 4.18: Normal probability plot of residual for moisture ratio.

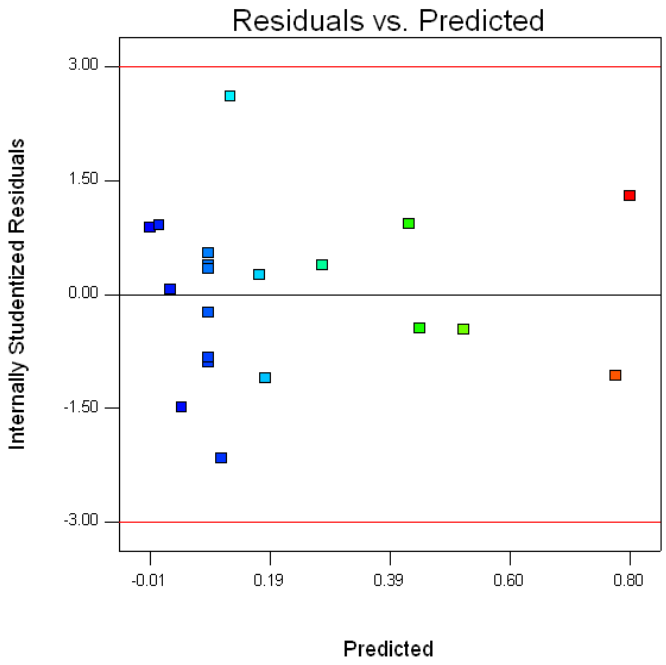

Figure 4.19: Plot of residuals versus predicted responses of moisture ratio.

The predicted responses from the empirical model were compared with the experimental values to ensure the reliability and adequacy of the empirical model (Figure 4.20). The goodness of model fitting was assured by the value of high regression coefficient (R^2), which was 0.986 for the proposed empirical model. The points above the diagonal line are over-estimated and, below the line are under-estimated. The points are well distributed along the diagonal line in the parity plot. The predicted responses from the empirical model are well-fitted with an acceptable variance when compared with the experimental results.

In the numerical optimization of MWAD of aloe gel, the desired goal was to reduce *MR* as low as 0.15 (moisture content 10 % d.b.) since charring and case hardening were observed beyond that. So, the target *MR* was minimized to 0.15. All the independent variables were kept within the ranges, *i.e.*, *P* (160-480 W), *m* (4-8 g) and *t* (1-9 min) to find the 'best' local minima within the response surface (Amini and Younesi, 2009). The optimum condition for the target response was found as the sample quantity of 4.47 g and drying time

of 5.78 min at microwave power of 227.94 W with desirability 1.

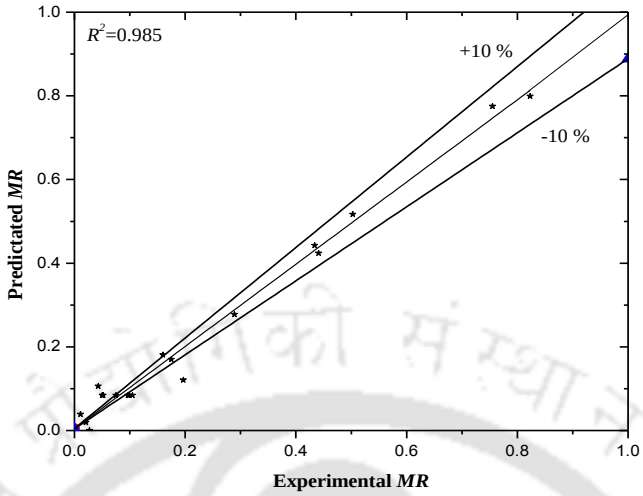

Figure 4.20: Comparison of moisture ratio with experimental and RSM model.

4.3.3.3 Artificial neural network modeling

The experimental outcomes of FCCD layout of MWAD of aloe vera (Table 4.2) were used to find the optimal ANN architecture. 'Levenberg-Marquardt backpropagation' (trainlm) algorithm was employed to train the neural network. Table 4.6 shows how *MSE* and R^2 vary with the hidden layer neurons in the training period. The best performance was observed with 3-5-1 topology at the lowest *MSE* of 0.0273×10^{-4} and the highest R^2 of 0.999 which signify the neural network as a robust tool for modeling.

A comparison among the different training algorithms for the hidden layer with 3-5-1 topology and Tansig-Purelin functions is shown in Table 4.7. 'Levenberg-Marquardt backpropagation (trainlm)' algorithm performed most satisfactorily as compared to that of 'Resilient backpropagation (trainrp)', 'Conjugate gradient backpropagation with Polak-Ribiere updates (traincgp)', 'Scaled conjugate gradient backpropagation (trainscg)' and "Gradient descent backpropagation (traingdm, traingda and traingdx)'. The same algorithm is also executed adequately for the prediction of dye concentration from pomegranate

comprising of three neurons in the input layer (Sinha et al., 2012). A comparison between FCCD and ANN models predicted responses with the experimental outcomes is presented in Figure 4.21. The performance of both the models was statistically compared in terms of *MSE*, R^2, and *AAD* (Figure 4.21). Both the models fitted well to the experimental data, but ANN showed a better prediction over FCCD.

Table 4.6: Summary of performance of ANN model with varying number of hidden layer neurons trained with the Levenberg-Marquardt algorithm.

No. of hidden layer neuron	R^2	*MSE*
1	0.937	8.469×10^{-3}
2	0.998	1.393×10^{-4}
3	0.997	1.544×10^{-4}
4	0.999	0.598×10^{-4}
5	0.999	0.027×10^{-4}
6	0.999	1.099×10^{-4}
7	0.999	0.369×10^{-4}
8	0.999	0.235×10^{-4}
9	0.999	1.544×10^{-4}
10	0.979	8.687×10^{-4}

Table 4.7: Summary of performance of various training algorithms in ANN prediction (Topology: 3-5-1, transfer functions: Tansig-Purelin).

Training algorithm	Function	R^2
Levenberg-Marquardt backpropagation	trainlm	0.999
Gradient descent with momentum backpropagation	traingdm	0.967
Gradient descent with adaptive learning rate backpropagation	traingda	0.939
Gradient descent with momentum and adaptive learning rate backpropagation	traingdx	0.802
Resilient backpropagation	trainrp	0.998
Conjugate gradient backpropagation with Polak-Ribiere updates	traincgp	0.986
Scaled conjugate gradient backpropagation	trainscg	0.998

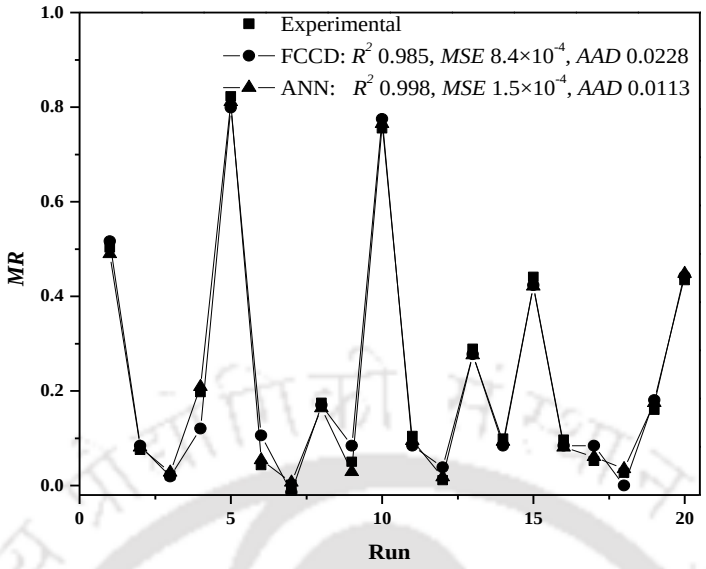

Figure 4.21: Comparison between ANN and RSM models predicted moisture ratio with observed values. Each run number represents the drying conditions as designed by FCCD.

4.4 Summary

The performance of HAD, MWAD and hybrid drying processes, such as, CFFD, MWFFD, CFHAD and MWFHAD for the dehydration of aloe vera gel were studied for the better retentivity of carbohydrate, protein and functional properties. The proposed hybrid drying processes could speed up the drying rates without much affecting the physico-chemical and functional properties of dry product and, it can be a potential drying technique for the bioactive materials. There was a reduction in carbohydrate and protein contents at higher temperature and microwave power. All the physico-chemical properties decreased significantly (p<0.05) for HAD at higher temperature and, for MWAD at higher input power. The hybrid drying processes showed a lower degradation of carbohydrate and protein due to the reduction in drying time as compared to the individual drying process where the dehydrated gel was relatively more concentrated. CFFD retained the highest carbohydrate content followed by CFHAD. The retentivity of both carbohydrate and protein followed the order as FD>CFFD>CFHAD> MWFFD>MWFHAD > HAD (50°C) > MWAD (160 W). The change in inorganic residues was almost insignificant (around 14%) (p<0.01) in all the drying processes. The dried gel obtained in different processes couldn't regain the initial moisture content and, the lowered the rehydration values as compared to FD due to shrinkage and rupture of the gel matrix. CFFD and CFHAD regained 89 to 94 and 91 to 96% swelling, and WRC of the freeze dried gel, respectively, which could be established as a potential drying technique for heat sensitive materials.

The drying curves obtained in MWAD showed a smooth diffusion controlled characteristics. 'Two term' model showed the best fit to the experimental outcomes for all the drying conditions as it was based on the Fick's second law of diffusion which indeed related to the diffusion-controlled drying behavior of aloe vera gel. The effective moisture diffusivity of aloe vera gel varied from 2.025×10^{-6} to 7.087×10^{-6} m^2 s^{-1} and, the activation energy was

found to be 49.82 W g^{-1}. The drying efficiency was dependent on the absorption of energy by the moisture in gel which was proportional to the residual moisture content and, it ranged between 50.8 and 68.7 % at the initial stage of drying.

MWAD became a faster and efficient process due to its internal heat generation and rapid expulsion of vapor. The typical diffusion-controlled drying curves without constant drying rate period were observed. Whereas, drying rate was found to be proportional to the residual moisture content. The drying time and microwave power had greater effects on the moisture content of aloe gel than the sample quantity. Both RSM and ANN models well predicted the moisture ratio with the variation of microwave power, sample amount, and drying time. RSM predicted optimum condition was found to be 9.5 W/g microwave power at 5.78 min corresponding to the moisture ratio of 0.15. A three layered feed-forward backpropagation neural network with 3-5-1 topology using Tansig-Purelin functions successfully mapped the target response from input parameters. ANN predicted responses showed a bit better agreement with the observed responses in MWAD.

References

Abbaszadeh, A., Motevali, A., Khoshtaghaza, M. H. and Kazemi, M., "Evaluation of thin-layer drying models and neural network for describing drying kinetics of *Lasagnas angustifolia* L.", *International Food Research Journal*, **18**, 1321-1328 (2011).

Akgun, N. A. and Doymaz, I., "Modelling of olive cake thin-layer drying process", *Journal of Food Engineering*, **68**, 455-461 (2005).

Amini, M. and Younesi, H., "Biosorption of Cd(II), Ni(II) and Pb(II) from aqueous solution by dried biomass of Aspergillus niger: application of response surface methodology to the optimization of process parameters", *Clean-Soil Air Water*, **37**, 776-786 (2009).

Atkinson, A. C. and Donev, A. N., *Optimum Experimental Designs*, vol. 8, Oxford Statistical Science Series, Clarendon Press, Oxford, 1992.0

Bose, S. and Das, C., "Role of binder and preparation pressure in tubular ceramic membrane processing: Design and optimization study using response surface methodology (RSM)", *Industrial and Engineering Chemistry Research*, **53**, 12319-12329 (2014).

Brooker, D. B., Bakker-Arkema, F. W. and Hall, C. W., *Drying and storage of grains and oilseeds*, Van Nostrand Reinhold, New York (1992), p. 212-213.

Cohen, J. S. and Yang, T. C. S., "Progress in food dehydration", *Trends in Food Science and Technology*, **6**, 20-25 (1995).

Crank, J., *The Mathematics of Diffusion*, Oxford University Press, London (1975).

Dadali, G., Apar, D. K. and Ozbek, B., "Microwave drying kinetics of okra", Drying Technol., (2007).

Diamante, L. M. and Munro, P.A., "Mathematical modeling of hot air drying of sweet potato slices", *International Journal of Food Science and Technology*, **26**, 99 (1991).

Diamente, L. M. and Munro, P. A., "Mathematical modeling of the thin layer solar drying of sweet potato slices", *Solar Energy*, **51**, 271-276 (1993).

Doymaz, I. and Pala, M., "The thin-layer drying characteristics of corn", *Journal of Food Engineering*, **60**, 125-130 (2003).

Femenia, A., Garcia-Pascual, P., Simal, S. and Rossello, C., "Effects of heat treatment and dehydration on bioactive polysaccharide acemannan and cell wall polymers from Aloe barbadensis Miller", *Carbohydr. Polym.*, **51,** 397-405 (2003).

Fennema, O., "Chemical changes in food during processing" in *Chemical changes in food during processing* (Edited by Richardson, T. and Finley, J. W.), pp. 10, Springer science & business media (1985).

Garau, M. C., Simal, S., Rossello, C. and Femenia, A., "Effect of air-drying temperature on physico-chemical properties of dietary fibre and antioxidant capacity of orange (Citrus aurantium v. Canoneta) by-products", *Food Chem.*, **104**, 1014-1024 (2007).

Garcia-Pascual, P., Sanjuan, N., Melis, R. and Mulet, A., Morchella esculenta (morel) rehydration process modeling, *Journal of Food Engineering*, **72**, 346-353(2006).

Garcia-Segovia, P., Mognetti, C., Andres-Bello, A. and Martinez-Monzo, J., "Osmotic dehydration of aloe vera (Aloe barbadensis Miller)", *J. Food Eng.*, **97**, 154-160 (2010).

Gulia, A., Sharma, H. K., Sarkar, B. C., Upadhyay, A. and Shitandi, A., "Changes in physico-chemical and functional properties during convective drying of aloe vera (Aloe barbadensis) leaves", *Food Bioprod. Process.*, **88**, 161-164 (2010).

Henderson, S. M., "Progress in developing the thin layer drying equation", *Transactions of the American Society of Agricultural and Biological Engineers*, **17**, 1167-1168, 1172 (1974).

Kaya, A., Aydin, O., Demirtas, C. and Akgun, M., "An experimental study on the drying kinetics of quince, Desalination", **212**, 328–343 (2007).

Kaymak-Ertekin, F., "Drying and rehydrating kinetics of green and red peppers", *J. Food Sci.*, **67**, 168-175 (2002).

Lee, K-M. and Gilmore, D. F., "Formulation and process modeling of biopolymer (polyhydroxyalkanoates: PHAs) production from industrial wastes by novel crossed experimental design", *Process Biochemistry*, **40**, 229-246 (2005).

Magnin, D. and Dumitriu, S., "Interactions between polysaccharides and polypeptides" in *Polysaccharides: Structural diversity and functional versatility* (Edited by Dumitriu, S.) pp. 309-310, CRC press (2010).

Marini, F., "Artificial neural networks in foodstuff analyses: trends and perspectives, a review", *Analytical Chimica Acta*, **635**, 121-131(2009).

Maskan, M., "Microwave/air and microwave finish drying of banana", *Journal of Food Engineering*, **44**, 71-78 (2000).

Midilli, A., Kucuk, H. and Yapar, Z., "A new model for single layer drying", *Drying Technology*, **20**, 1503-1513 (2002).

Nourbakhsh, H., Emam-Djomeh, Z., Omid, M., Mirsaeedghazi, H. and Moini, S., "Prediction of red plum juice permeate flux during membrane processing with ANN optimized using RSM", *Computers and Electronics in Agriculture*, **102**, 1-9 (2014).

Okos, M. R., Narsimhan, G., Singh, R. K. and Weitnauer, A. C., "Food dehydration" In: Hand book of food engineering, (D.R. Heldman, D.B. Lund and C. Sabliov, eds.), CRC Press., (1982).

Ozbek, B. and Dadali, G., "Thin-layer drying characteristics and modelling of mint leaves undergoing microwave treatment", *J. Food Eng*., **83**, 541-549 (2007).

Ozdemir, M. and Devres, Y. O., "The thin layer drying characteristics of hazelnuts during roasting", *Journal of Food Engineering*, **42**, 225-233 (1999).

Phoungchandang, S. and Woods, J. L., "Moisture diffusion and desorption isotherms for banana", *Journal of Food Science*, **65**, 651-657 (2000).

Prabhanjan, D. G., Ramaswamy, H. S. and Raghavan, G. S. V., "Microwave-assisted convective air drying of thin layer carrots", *J. Food Eng*., **25**, 283-293 (1995).

Radhika, G. B., Satyanarayana, S. V. and Rao, D. G., "Mathematical model on thin layer drying of finger millet (*Eluesine coracana*)", *Advance Journal of Food Science and Technology*, **3**, 127-131 (2011).

Razavi, M. A., Mortazavi, A. and Mousavi, M., "Application of neural networks for cross-flow milk ultrafiltration simulation", *International Dairy Journal*, **14**, 69-80 (2004).

Severini, C., Baiano, A., Pilli, T. D., Carbone, B.F. and Derossi, A., "Combined treatments of blanching and dehydration: study on potato cubes", *Journal of Food Engineering*, **68**, 289-296(2005).

Sinha, K., Chowdhury, S., Das Saha, P. and Datta, S., "Modeling of microwave-assisted extraction of natural dye from seeds of Bixa orellana (Annatto) using response surface methodology (RSM) and artificial neural network (ANN)", *Industrial Crops and Products*, **41**, 165-171 (2013).

Sinha, K., Das Saha, P. and Datta, S., "Response surface optimization and artificial neural network modeling of microwave assisted natural dye extraction from pomegranate rind", *Industrial Crops and Products*, **37**, 408-414 (2012).

Soysal, Y., Oztekin, S. and Eren, O., "Microwave Drying of Parsley: Modelling, Kinetics, and Energy Aspects", *Biosystems Engineering*, **93**, 403-413 (2006).

Thibault, J. F., Lahaye, M.and Guillon, F., "Physico-chemical properties of food plant cell walls" in *Dietary fibre - a component of food* (Edited by Schweizer, T. F. and Edwards, C. A.), London, Springer, pp. 21-39 (1992)

Thomsen, S. and Pearce, J. A., "Thermal damage and rate processes in biological tissues", in *Optical-thermal response of laser irradiated tissue* (Edited by Welch, A. J. and Gemert, M. J. C. van.), Springer, pp. 500-501 (2011).

Torrecilla, J. S., Otero, L. and Sanz, P. D., "A neural network approach for thermal/pressure food processing", *Journal of Food Engineering*, **62**, 89-95 (2004).

Vega, A., Uribe, E., Roberto, L. and Margarita, M., "Hot-air drying characteristics of aloe vera (*Aloe barbadensis* Miller) and influence of temperature on kinetic parameters", *LWT-Food Science and Technology*, **40**, 1698-1707 (2007).

Vega-Galvez, A., Miranda, M., Aranda, M., Henriquez, K., Vergara, J., Tabilo-Munizaga, G. and Perez-Won, M., "Effect of high hydrostatic pressure on functional properties and quality characteristics of Aloe vera gel (Aloe barbadensis Miller)", *Food Chem.*, **129**, 1060-1065 (2011a).

Vega-Galvez, A., Notte-Cuello, E., Lemus-Mondaca, R., Zura, L. and Miranda, M., "Mathematical modelling of mass transfer during rehydration process of Aloe vera (Aloe barbadensis Miller)", *Food Bioprod. process*., **87**, 254-260 (2009).

Vega-galvez, A., Uribe, E., Perez, M., Tabilo-Munizaga, G., Vergara, J., Garcia-Segovia, P., Lara, E. and Scala, K. D., "Effect of high hydrostatic pressure pretreatment on drying kinetics, antioxidant activity, firmness and microstructure of aloe vera (Aloe barbadensis Miller) gel", *Food Sci. Technol*., **44**, 384-391 (2011b).

Wang, C. Y. and Singh, R. P., "A single layer drying equation for rough rice", *American Society of Agricultural Engineers*, Paper No. **3001** (1978).

Wang, R., Zhang, M., Mujumdar, A. S. and Sun, J. C., "Microwave freeze-drying characteristics and sensory quality of instant vegetable soup", *Drying Technology*, **27**, 962-968 (2009).

Wang, Z., Sun, J., Chen, F., Liao, X. and Hu, X., "Mathematical modelling on thin layer microwave drying of apple pomace with and without hot air pre-drying", *J. Food Eng*., **80**, 536-544 (2007).

Whith, G. M., Brldges, T. C., Loewer, O. J. and Ross, I. J., "Seed coat damage in thin layer drying of soybeans as affected by drying conditions", *American Society of Agricultural Engineers*, Paper no. **3052** (1978).

Xanthopoulos, G., Oikonomou, N. and Lambrinos, G., "Applicability of a single-layer drying model to predict the drying rate of whole figs", *Journal of Food Engineering*, **81**, 553-559 (2007).

Yaldiz, O. and Ertekin, C., "Thin-layer solar drying of some vegetables", *Drying Technology*, **19**, 583-596 (2002).

Yucel, U., Alpas, H. and Bayindirli, A., "Evaluation of high pressure pretreatment for enhancing the drying rates of carrot, apple, and green bean", *J. Food Eng.*, **98**, 266-272 (2010).

Zarein, M., Samadi, S. H. and Ghobadian, B., "Investigation of microwave dryer effect on energy efficiency during drying of apple slices", *Journal of the Saudi Society of Agricultural Sciences*, **14**, 41-47 (2015).

Zhang, Q. and Litchfield, J. B., "An optimization of intermittent corn drying in a laboratory scale thin-layer dryer", *Drying Technology*, **9**, 383-395 (1991).

CHAPTER 5

Conclusions and Future Work Directions

This chapter summarizes the inferences drawn from the present study and, provides some directions towards future scope of research.

CHAPTER 5

Conclusions and Future Work Directions

5.1 Overall Conclusions

- Water, a green solvent, played an important role in the extraction of Reb-A from stevia leaves. In the hot water extraction process, Reb-A recovery was found to be the highest at 60°C; beyond that, the change in recovery became insignificant. The excess recovery of Reb-A above 60°C might have compensated by the decomposition of Reb-A. The rate of extraction increased linearly up to 45 min irrespective of the leaves to water ratio. At a higher leaves concentration, the overall rate of Reb-A recovery was low since the cumulative accumulation of Reb-A hindered the overall extraction. At 60°C, the maximum recovery of Reb-A of 77 and 67.1 % at 60 min and 68.7 % at 45 min were obtained with the leaves to water ratio 2, 5 and 3 %, respectively.
- Statistical analysis of Reb-A extraction using CCD reveals that the effects of extraction time, temperature, and leaves to water ratio were significant on the recovery of Reb-A. CCD suggests that the maximum 73.1 % recovery of Reb-A could be achieved in 51 min for leaves to water ratio of 2.36 % at 71°C. A three layer feed forward back propagation neural network with 3-8-1 topology, and Logsig-Purelin transfer functions exhibited the best prediction of Reb-A recovery.
- 30 kDa MWCO membrane gave the highest permeate flux and Reb-A yield in permeate compared to 10, 20 and 50 kDa membranes. Higher MWCO membranes did not necessarily produce a higher flux due to the severe pore blocking and concentration polarization. Clarification of stevia extract was performed in a cross-

flow module using 30 kDa MWCO membrane. TMP drop played a significant role on the steady state permeate flux. The maximum recovery of 31 % and selectivity of 0.45 for Reb-A were obtained at *Re* number 1667 and 414 kPa TMP drop. The corresponding steady state permeate flux was 5.86×10^{-6} m^3 m^{-2} s^{-1}.

- The modified Hermia's model, namely, complete pore blocking, standard pore blocking, intermediate pore blocking, and cake filtration well described the fouling mechanism for the ultrafiltration of stevia extract in the cross-flow module for both the transient and steady state regimes. The membrane resumed almost of its initial permeability after cleaning using SDS solution (2 %) and distilled water.
- Chemical alteration of carbohydrate and protein molecules in aloe vera gel was susceptible at the higher temperature for HAD and microwave power for MWAD. The tissue integrity and dense structure of solid gel matrix collapsed at higher temperature and microwave power. The irreversible modification of gel matrix caused the inferior rehydration properties of dry aloe gel. Hybrid drying processes retained the acceptable physico-chemical properties of dry aloe vera gel. The retentivity of physico-chemical properties followed the order as FD>CFFD>CFHAD>MWFFD>MWFHAD >HAD (50°C)>MWAD (160 W).
- 'Two term' drying model exhibited the best fit to drying kinetics of aloe vera gel in MWAD. The proposed 'Two term' model predicted the moisture ratio with ±5 % proximity of the experimental values. The effective moisture diffusivity of aloe vera gel in MWAD was found to be much higher compared to HAD. The activation energy was estimated using the modified Arrhenius equation. The drying efficiency was proportional to the residual moisture content.
- MWAD of aloe vera gel followed the typical smooth diffusion-controlled characteristics. MWAD of aloe vera gel predominately occurred in the falling drying

rate period due to a lower rate of diffusional transport than the evaporation rate. FCCD predicted optimum conditions for MWAD of aloe vera gel were found to be 9.5 W/g power density and microwave irradiation time of 5.78 min corresponding to the moisture ratio of 0.15. A three layered feed-forward back propagation neural network with 3-5-1 topology using Tansig-Purelin functions successfully mapped the corresponding moisture ratio from input MWAD parameters.

5.2 Scope of Future Work

The present study can be extended in the following directions:

- Extraction of Reb-A can be studied using selective enzymatic treatment for a better yield.
- Clarification of stevia extract may be studied using a ceramic membrane to lessen the extent of membrane fouling.
- Thermal degradation mechanism of aloe vera gel in the drying process is also a prudent area of future research.
- The biological activity of dried aloe vera gel can be investigated *in vivo*.

Appendix

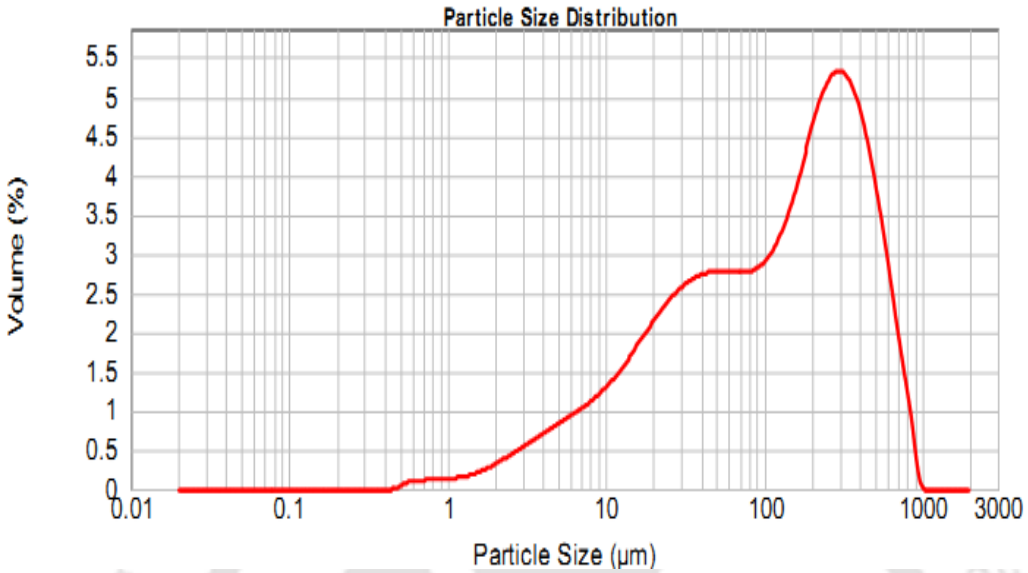

Figure A1: Particle size distribution of ground stevia leaves.

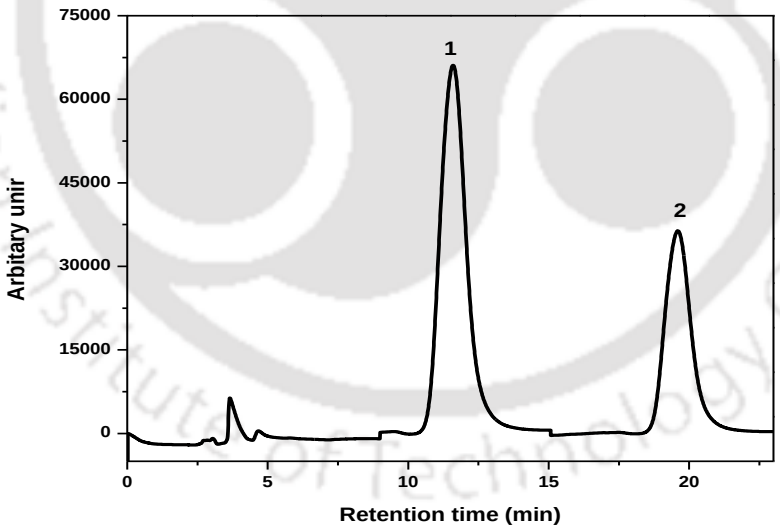

Figure A2: HPLC chromatogram of stevioside (1) and, rebaudioside A (2). Separation was carried out on an NH_2 column (4.6 mm i.d. × 250 mm, 5 µm) at a column temperature of 40˚C using an 80:20 (v/v) mixture of acetonitrile and water adjusted to a pH of 3.0 with phosphoric acid as the mobile phase at a flow rate of 1.0 mL/min. The eluted compounds were monitored at 210 nm.

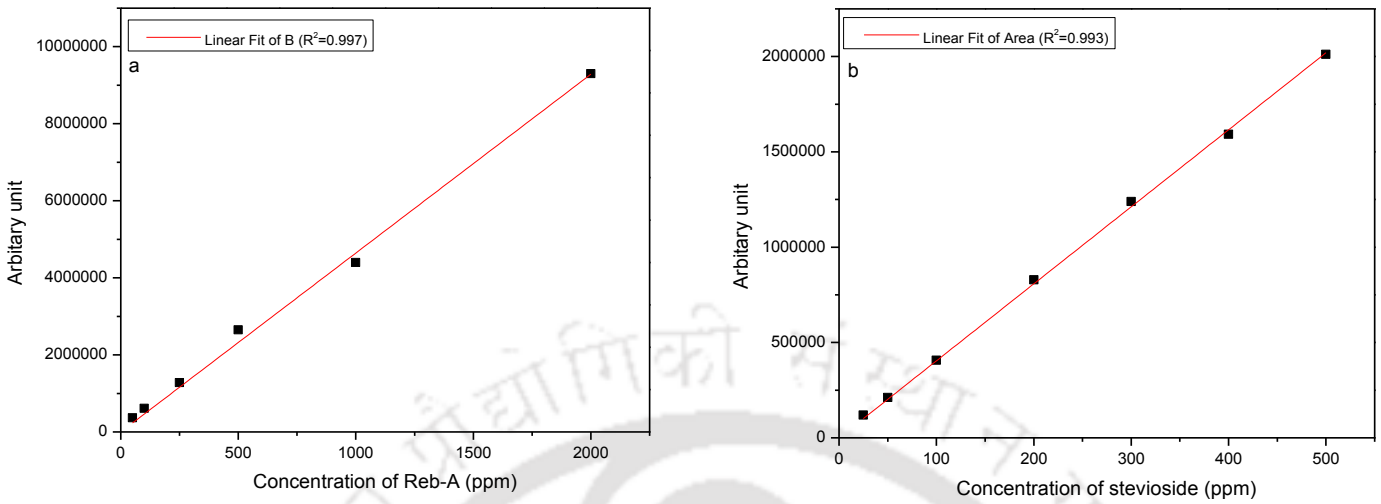

Figure A3: Calibration curves of (a) Reb-A and, (b) stevioside. Separation was carried out on an NH2 column (4.6 mm i.d. × 250 mm, 5 µm) at a column temperature of 40˚C using an 80:20 (v/v) mixture of acetonitrile and water adjusted to a pH of 3.0 with phosphoric acid as the mobile phase at a flow rate of 1.0 mL/min. The eluted compounds were monitored at 210 nm.

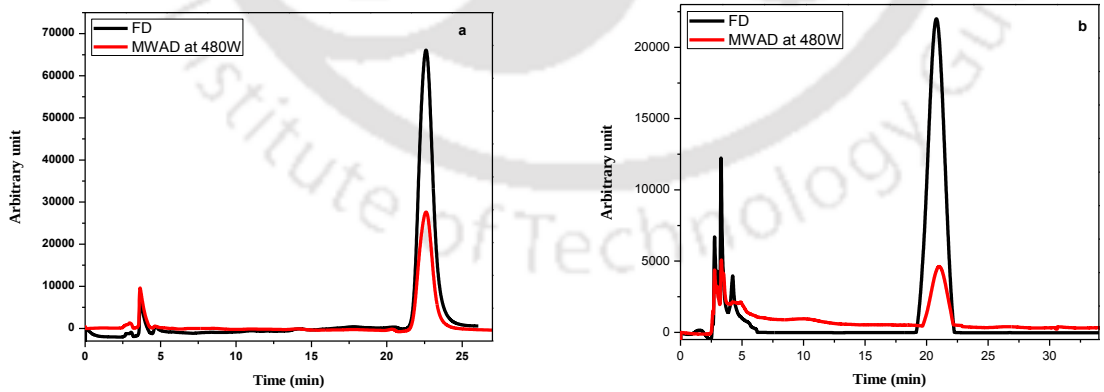

Figure A4: HPLC spectra of (a) carbohydrate and, (b) protein in dried aloe vera gel.

Table A1: ANOVA summary table for the data of swelling values.

	HAD 50°C	MWAD 160W	CFFD	MWFFD	CFHAD	MWFHAD
	75	68.25	88.20	75	84	68.25
	70.5	65	84	78.75	80	65
	79.5	61.75	79.80	71.25	76	61.75
	3	3	3	3	3	3
Mean	75.000	65.000	84.000	75.000	80.000	65.000
Std dev.	4.500	3.250	4.200	3.750	4.000	3.250
$Mean_{avg}$	74.000					

Source	df	SS	MS	F	*p*-value
Between groups	5	900.000	180.000	12.1243	0.0002
Within groups (error)	12	178.155	14.846		
Total	17	1078.155			

Research Publications

Journal Publications

A. Das, A. K. Golder and C. Das, "Enhanced extraction of rebaudioside-A: Experimental, response surface optimization and prediction using artificial neural network", *Industrial Crops and Products*, 65(c), 415-421, (2015).

A. Das, D. Paul, A. K. Golder and C. Das, "Separation of rebaudioside-A from stevia extract: Membrane selection, assessment of permeate quality and fouling behavior in laminar flow regime", *Separation and Purification Technology*, 144, 8-15, (2015).

C. Das, **A. Das** and A. K. Golder "Optimality in microwave-assisted drying of aloe vera (*Aloe Barbadensis* Miller) gel using response surface methodology and artificial neural network modeling", *Journal of the Institution of Engineers (India): Series E*, (2016) (DOI: 10.1007/s40034-016-0083-7).

A. Das, A. K. Golder and C. Das, "Evaluation of physico-chemical and functional properties of dried aloe vera gel: Comparison among hot air, microwave-assisted and hybrid drying processes", *The Natural Products Journal* 6, 1-8, (2016).

A. Das, A. K. Golder and C. Das, "Prediction of drying kinetics and moisture diffusivity during microwave-assisted drying of thin layer Aloe vera (*Aloe barbadensis* Miller) gel" (Submitted).

International Conferences

A. Das, A.K. Golder and C. Das, "Effect of Microwave Power on Drying Rate of Aloe Vera Gel", Indian Chemical Engineering Congress (CHEMCON-2013), 27-30th December, 2013, Institute of Chemical Technology, Mumbai, India.

A. Das, A.K. Golder and C. Das, "Comparison of extraction efficiency of stevioside using water and methanol", International Conference on Frontiers in Chemical Engineering (ICFCE-2013), 9-11th December, 2013, NIT Rourkela, Odisha, India.

A. Das, A.K. Golder and C. Das, "Reduction of Moisture Content of Aloe Vera gel using Microwave", International Conference on Advances in Chemical Engineering (ICACE 2013), 5-6th April, 2013, NIT Raipur, India.

A. Das, A.K. Golder and C. Das, "Comparative study of stevioside extraction using different solvents and their cost analysis", Indian Chemical Engineering Congress (CHEMCON-2012), 27-29th December, 2012, NIT Jalandhar, Punjab, India.

A. Das, A.K. Golder and C. Das, "Comparison of microwave assisted drying of Aloe Vera with direct hot air drying", Indian Chemical Engineering Congress (CHEMCON-2011), 27-29th December, 2011, M.S. Ramaiah Institute of Technology, Bangalore, India.

A. Das and C. Das, "Extraction and purification of stevioside with water as a solvent using ultrafiltration", Indian Chemical Engineering Congress (CHEMCON-2010), 27-29th December, 2010, Annamalai University, Tamil Nadu, India.

Other Publication

V. Singh, **A. Das**, C. Das, G Pugazhenthi, M. Srinivas and S. Senthilmurugan, "Fouling and Cleaning Characteristics of Reverse Osmosis (RO) Membranes", *Journal of Chemical Engineering and Process Technology*, 6, 244, (2015).

Dr. Arijit Das

Lecturer
Department of Chemical Engineering
National Institute of Technology Hamirpur (H.P)
E-mail: arichem.iitg@gmail.com
Mobile: 98828 78191

EDUCATION

2016	PhD in Chemical Engineering Thesis title: "Studies on Extraction and Purification of Rebaudioside-A and Dehydration of Aloe Vera Gel"	IIT Guwahati
2010	M. Tech in Chemical Engineering Specialization: "Petroleum Refinery Engineering" Thesis title: "Preparation of low cost stevioside by ultrafiltration" CPI obtained: 8.10	IIT Guwahati
2008	B. E in Chemical Engineering % obtained: 66.40	Jadavpur University, Kolkata

SUPPLEMENTARY EDUCATION/TRAINING

2014 KIC-TEQIP workshop on "Membrane Technology and Application", IIT Guwahati

2013 QIP workshop on "Advanced Chemical Process Design", IIT Guwahati

2012 QIP workshop on "Engineering Optimization using Matlab and Excel", IIT Guwahati

PUBLICATIONS

Journal papers

Arijit Das, Animes Kumar Golder, Chandan Das, "Enhanced extraction of rebaudioside-A: Experimental, response surface optimization and prediction using artificial neural network", Industrial Crops and Products. 65 (c), 415-421, (2015).

Arijit Das, Diptadeep Paul, Animes Kumar Golder, Chandan Das, "Separation of rebaudioside-A from stevia extract: Membrane selection, assessment of permeate quality and fouling behavior in laminar flow regime", Separation and Purification Technology. 144, 8-15, (2015).

Bio data

Chandan Das, **Arijit Das**, Animes Kumar Golder, "Optimality in microwave-assisted drying of aloe vera (*Aloe Barbadensis* Miller) gel using response surface methodology and artificial neural network modeling", Journal of the Institution of Engineers (India): Series E., (DOI: 10.1007/s40034-016-0083-7).

Arijit Das, Animes Kumar Golder, Chandan Das, "Evaluation of physico-chemical and functional properties of dried aloe vera gel: Comparison among hot air, microwave-assisted and hybrid drying processes", The Natural Products Journal 6, 1-8, (2016).

V. Singh, **A. Das**, C. Das, G Pugazhenthi, M. Srinivas and S. Senthilmurugan, "Fouling and Cleaning Characteristics of Reverse Osmosis (RO) Membranes" Journal of Chemical Engineering and Process Technology, 6, 244, (2015).

Arijit Das, Animes Kumar Golder, Chandan Das, "Prediction of drying kinetics and moisture diffusivity during microwave-assisted drying of thin layer Aloe vera (*Aloe barbadensis* Miller) gel" (communicated).

Conference papers

Arijit Das, Animes Kumar Golder, Chandan Das, "Effect of Microwave Power on Drying Rate of Aloe Vera Gel", Indian Chemical Engineering Congress (CHEMCON-2013), 27-30th December, 2013, Institute of Chemical Technology, Mumbai, India.

Arijit Das, Animes Kumar Golder and Chandan Das "Comparison of extraction efficiency of stevioside using water and methanol", International Conference on Frontiers in Chemical Engineering (ICFCE-2013), 9-11th December, 2013, NIT Rourkela, Odisha, India.

Arijit Das, Animes Kumar Golder and Chandan Das, "Reduction of Moisture Content of Aloe Vera gel using Microwave", International Conference on Advances in Chemical Engineering (ICACE 2013), 5-6th April, 2013, NIT Raipur, India.

Arijit Das, Animes Kumar Golder and Chandan Das, "Comparative study of stevioside extraction using different solvents and their cost analysis", Indian Chemical Engineering Congress (CHEMCON-2012), 27-29th December, 2012, NIT Jalandhar, Punjab, India.

Arijit Das, Animes Kumar Golder and Chandan Das, "Comparison of microwave assisted drying of Aloe Vera with direct hot air drying", Indian Chemical Engineering Congress (CHEMCON-2011), 27-29th December, 2011, M.S. Ramaiah Institute of Technology, Bangalore, India.

Arijit Das and Chandan Das, "Extraction and purification of stevioside with water as a solvent using ultrafiltration", Indian Chemical Engineering Congress (CHEMCON-2010), 27-29th December, 2010, Annamalai University, Tamilnadu, India.

AWARDS AND ACHEIVEMENTS

Awarded national scholarship (MHRD, Govt. of India) for the period of 2010-2014

Awarded national scholarship (MHRD, Govt. of India) for the period of 2008-2010

Qualified in GATE 2008

PROFESSIONAL MEMBERSHIP

Associate member, Indian Institute of Chemical Engineers (IIChE) (AM-41309)

POSITION OF RESPONSIBILITY

Student representative of departmental disciplinary committee of Chemical Engineering Department of IIT Guwahati for the period of 2012-2014

Active member of executive committee of Indian Institute of Chemical Engineers Guwahati Regional Centre (IIChE GRC) for the period of 2012-2013

EXTRACURRICULAR ACTIVITIES AND HOBBIES

Diploma in Hawaiian guitar

Attached with social welfare organizations

Like to travel, listening to music, reading story books, playing chess

PERSONAL DETAILS

DOB	11-06-1979
Sex	Male
Parents	Tapan Kumar Das and Kabita Das
Marital Status	Single
Language	Bengali, English, Hindi
Permanent Address	13/1 Siddheswari Tala Lane Howrah, West Bengal, PIN-711 101, India